Hindawi Publishing Corporation
ISRN Optics
Volume 2013, Article ID 783865, 51 pages
http://dx.doi.org/10.1155/2013/783865

Review Article

Universal Dynamical Control of Open Quantum Systems

Gershon Kurizki

Weizmann Institute of Science, 76100 Rehovot, Israel

Correspondence should be addressed to Gershon Kurizki; gershon.kurizki@weizmann.ac.il

Received 25 March 2013; Accepted 24 April 2013

Academic Editors: M. D. Hoogerland, D. Kouznetsov, A. Miroshnichenko, and S. R. Restaino

Due to increasing demands on speed and security of data processing, along with requirements on measurement precision in fundamental research, quantum phenomena are expected to play an increasing role in future technologies. Special attention must hence be paid to omnipresent decoherence effects, which hamper quantumness. Their consequence is always a deviation of the quantum state evolution (error) with respect to the expected unitary evolution if these effects are absent. In operational tasks such as the preparation, transformation, transmission, and detection of quantum states, these effects are detrimental and must be suppressed by strategies known as dynamical decoupling, or the more general dynamical control by modulation developed by us. The underlying dynamics must be Zeno-like, yielding suppressed coupling to the bath. There are, however, tasks which cannot be implemented by unitary evolution, in particular those involving a change of the system's state entropy. Such tasks necessitate efficient coupling to a bath for their implementation. Examples include the use of measurements to cool (purify) a system, to equilibrate it, or to harvest and convert energy from the environment. If the underlying dynamics is anti-*Zeno like*, enhancement of this coupling to the bath will occur and thereby facilitate the task, as discovered by us. A general task may also require state and energy transfer, or entanglement of noninteracting parties via shared modes of the bath which call for maximizing the shared (two-partite) couplings with the bath, but suppressing the single-partite couplings. For such tasks, a more subtle interplay of Zeno and anti-Zeno dynamics may be optimal. We have therefore constructed a general framework for optimizing the way a system interacts with its environment to achieve a desired task. This optimization consists in adjusting a given "score" that quantifies the success of the task, such as the targeted fidelity, purity, entropy, entanglement, or energy by dynamical modification of the system-bath coupling spectrum on demand.

1. Introduction

Due to the ongoing trends of device miniaturization, increasing demands on speed and security of data processing, along with requirements on measurement precision in fundamental research, quantum phenomena are expected to play an increasing role in future technologies. Special attention must hence be paid to omnipresent decoherence effects, which hamper quantumness [1–70]. These may have different physical origins, such as coupling of the system to an external environment (bath), noise in the classical fields controlling the system, or population leakage out of a relevant system subspace. Their consequence is always a deviation of the quantum state evolution (error) with respect to the expected unitary evolution if these effects are absent. In operational tasks such as the preparation, transformation, transmission, and detection of quantum states, these effects are detrimental and must be suppressed by dynamical control. The underlying dynamics must be *Zeno-like* yielding suppressed coupling to the bath.

Environmental effects generally hamper or completely destroy the "quantumness" of any complex device. Particularly fragile against environment effects is quantum entanglement (QE) in multipartite systems. This fragility may disable quantum information processing and other forthcoming quantum technologies: interferometry, metrology, and lithography. Commonly, the fragility of QE rapidly mounts with the number of entangled particles and the temperature of the environment (thermal "bath"). This QE fragility has been the standard resolution of the Schrödinger-cat paradox: the environment has been assumed to preclude macrosystem entanglement.

In-depth study of the mechanisms of decoherence and their prevention is therefore an essential prerequisite for

applications involving quantum information processing or communications [3]. The present paper aimed at furthering our understanding of these formidable issues. It is based on progress by our group, as well as others, towards a unified approach to the dynamical control of decoherence and disentanglement. This unified approach culminates in universal formulae allowing design of the required control fields.

Most theoretical and experimental methods that aimed at assessing and controlling (suppressing) decoherence of qubits (two-level systems that are the quantum mechanical counterparts of classical bits) have focused on one of two particular situations: (a) single qubits decohering *independently*, or (b) many qubits *collectively* perturbed by the same environment. Thus, quantum communication protocols based on entangled two-photon states have been studied under collective depolarization conditions, namely, *identical* random fluctuations of the polarization for both photons [71, 72]. Entangled qubits that reside at the same site or at equivalent sites of the system, for example, atoms in optical lattices, have likewise been assumed to undergo identical decoherence.

By contrast, more general problems of decay of *nonlocal* mutual entanglement of two or more small systems are less well understood. This decoherence process may occur on a time scale much shorter than the time for either body to undergo local decoherence, but much longer than the time each takes to become disentangled from its environment. The disentanglement of individual particles from their environment is dynamically controlled by interactions on non-Markovian time-scales, as discussed below. Their disentanglement from each other, however, may be purely Markovian [73–75], in which case the present non-Markovian approach to dynamical control/prevention is insufficient.

1.1. Dynamical Control of Single-Particle Decay and Decoherence on Non-Markovian Time Scales. Quantum-state decay to a continuum or changes in its population via coupling to a thermal bath is known as amplitude noise (AN). It characterizes decoherence processes in many quantum systems, for example, spontaneous emission of photons by excited atoms [76], vibrational and collisional relaxation of trapped ions [1], and the relaxation of current-biased Josephson junctions [77]. Another source of decoherence in the same systems is proper dephasing or phase noise (PN) [78], which does not affect the populations of quantum states but randomizes their energies or phases.

For independently decohering qubits, a powerful approach for the suppression of decoherence appears to be the "dynamical decoupling" (DD) of the system from the bath [79–92]. The standard "bang-bang" DD, that is, π-phase flips of the coupling via strong and sufficiently frequent resonant pulses driving the qubit [82–84], has been proposed for the suppression of proper dephasing [93].

This approach is based on the assumption that during these strong and short pulses there is no free evolution; that is, the coupling to the bath is intermittent with control fields. These π-pulses hence serve as a complete phase reversal, meaning that the evolution after the pulse negates the deleterious effects of dephasing prior to the pulse, similar to spin-echo technique [94]. However, some residual decoherence remains and increases with the interpulse time interval, and thus in order to combat decoherence effectively, the pulses should be very frequent. While standard DD has been developed for combating first-order dephasing, several extensions have been suggested to further optimize DD under proper dephasing, such as multipulse control [89], continuous DD [88], concatenated DD [90], and optimal DD [95, 96]. DD has also been adapted to suppress other types of decoherence couplings such as internal state coupling [91] and heating [84].

Our group has proposed a universal strategy of approximate DD [97–103] for both decay and proper dephasing, by either pulsed or continuous wave (CW) modulation of the system-bath coupling. This strategy allows us to optimally tailor the strength and rate of the modulating pulses to the spectrum of the bath (or continuum) by means of a simple universal formula. In many cases, the standard π-phase "bang-bang" (BB) is then found to be inadequate or nonoptimal compared to dynamic control based on the optimization of the universal formula [104].

Our group has purported to substantially expand the arsenal of decay and decoherence control. We have presented a *universal form of the decay rate* of unstable states into *any* reservoir (continuum), dynamically modified by perturbations with arbitrary time dependence, focusing on non-Markovian time-scales [97, 99, 100, 102, 105]. An analogous form has been obtained by us for the dynamically modified rate of proper dephasing [100, 101, 105]. Our unified, optimized approach reduces to the BB method in the particular case of proper dephasing or decay via coupling to *spectrally symmetric* (e.g., Lorentzian or Gaussian) noise baths with limited spectral width (see below). The type of phase modulation advocated for the suppression of coupling to phonon or photon baths with frequency cutoff [103] is, however, drastically different from the BB method. Other situations to which our approach applies, but not the BB method, include *amplitude modulation* of the coupling to the continuum, as in the case of decay from quasibound states of a periodically tilted washboard potential [99]: such modulation has been experimentally shown [106] to give rise to either slowdown of the decay (Zeno-like behavior) or its speedup (anti-Zeno-like behavior), depending on the modulation rate.

The theory has been generalized by us to finite temperatures and to qubits driven by an *arbitrary* time-dependent field, which may cause the failure of the rotating-wave approximation [100]. It has also been extended to the analysis of *multilevel systems*, where quantum interference between the levels may either inhibit or accelerate the decay [107].

Our general approach [99] to dynamical control of states coupled to an arbitrary "bath" or continuum has reaffirmed the intuitive anticipation that, in order to suppress their decay, we must modulate the system-bath coupling at a rate exceeding the spectral interval over which the coupling is significant. Yet our analysis can serve as a general recipe for

optimized design of the modulation aimed at an effective use of the fields for decay and decoherence suppression or enhancement.

1.2. Control of Symmetry-Breaking Multipartite Decoherence. Control of multiqubit or, more generally, multipartite decoherence is of even greater interest, because it can help protect the entanglement of such systems, which is the cornerstone of many quantum information processing applications. However, it is very susceptible to decoherence, decays faster than single-qubit coherence, and can even completely disappear in finite time, an effect dubbed entanglement sudden death (ESD) [73, 74, 108–113]. Entanglement is effectively protected in the collective decoherence situation, by singling out decoherence-free subspaces (DFS) [114], wherein symmetrically degenerate many-qubit states, also known as "dark" or "trapping" states [78], are decoupled from the bath [87, 115–117].

Symmetry is a powerful means of protecting entangled quantum states against decoherence, since it allows the existence of a decoherence-free subspace or a decoherence-free subsystem [77, 78, 80–87, 102, 114–120]. In multipartite systems, this requires that all particles be perturbed by the *same* environment. In keeping with this requirement, quantum communication protocols based on entangled two-photon states have been studied under *collective* depolarization conditions, namely, *identical* random fluctuations of the polarization for both photons [71].

Entangled states of two or more particles, wherein each particle travels along a different channel or is stored at a different site in the system, may present more challenging problems insofar as combating and controlling decoherence effects are concerned: if their channels or sites are differently coupled to the environment, their entanglement is expected to be more fragile and harder to protect.

To address these fundamental challenges, we have developed a very general treatment. Our treatment does not assume the perturbations to be stroboscopic, that is, strong or fast enough, but rather to act concurrently with the particle-bath interactions. This treatment extends our earlier single-qubit universal strategy [97, 99, 100, 104, 121, 122] to *multiple entangled systems (particles)* which are either coupled to partly correlated (or uncorrelated) finite-temperature baths or undergo locally varying random dephasing [107, 123–126]. Furthermore, it applies *to any difference* between the couplings of individual particles to the environment. This difference may range from the large-difference limit of completely independent couplings, which can be treated by the single-particle dynamical control of decoherence via modulation of the system-bath coupling, to the opposite zero-difference limit of completely identical couplings, allowing for multiparticle collective behavior and decoherence-free variables [86, 87, 115–117, 127–130]. The general treatment presented here is valid anywhere between these two limits and allows us to pose and answer the key question: under what conditions, if any, is *local control* by modulation, addressing each particle individually, preferable to *global control*, which does not discriminate between the particles?

We show that in the realistic scenario, where the particles are differently coupled to the bath, it is *advantageous to locally control each particle by individual modulation, even if such modulation is suboptimal* for suppressing the decoherence of a single particle. This local modulation allows synchronizing the phase-relation between the different modulations and eliminates the cross coupling between the different systems. As a result, it allows us to preserve the multipartite entanglement and reduces the multipartite decoherence problem to the single particle decoherence problem. We show the advantages of local modulation, over global modulation (i.e., identical modulation for all systems and levels), as regards the preservation of arbitrary initial states, preservation of entanglement, and the intriguing possibility of entanglement increase compared to its initial value.

The experimental realization of a universal quantum computer is widely recognized to be difficult due to decoherence effects, particularly dephasing [1, 131–133], whose deleterious effects on entanglement of qubits via two-qubit gates [134–136] are crucial. To help overcome this problem, we put forth a universal dynamical control approach to the dephasing problem during *all the stages of quantum computations* [125, 137], namely, (i) storage, wherein the quantum information is preserved in between gate operations, (ii) single-qubit gates, wherein individual qubits are manipulated, without changing their mutual entanglement, and (iii) two-qubit gates, that introduce controlled entanglement. We show that in terms of reducing the effects of dephasing, it is advantageous to concurrently and specifically control all the qubits of the system, whether they undergo quantum gate operations or not. Our approach consists in specifically tailoring each dynamical quantum gate, with the aim of suppressing the dephasing, thereby greatly increasing the gate fidelity. In the course of two-qubit entangling gates, we show that cross dephasing can be completely eliminated by introducing additional control fields. Most significantly, we show that one can increase the gate duration, while simultaneously reducing the effects of dephasing, resulting in a total increase in gate fidelity. This is at odds with the conventional approaches, whereby one tries to either reduce the gate duration, or increase the coherence time.

A general task may also require state and energy transfer [138], or entanglement [139] of noninteracting parties via *shared* modes of the bath [123, 140] which call for maximizing the shared (two-partite) couplings with the bath, but suppressing the single-partite couplings.

It is therefore desirable to have a general framework for optimizing the way a system interacts with its environment to achieve a desired task. This optimization consists in adjusting a given "score" that quantifies the success of the task, such as the targeted fidelity, purity, entropy, entanglement, or energy by dynamical modification of the system-bath coupling spectrum on demand. The goal of this work is to develop such a framework.

1.3. Dynamical Protection from Spontaneous Emission. Schemes of quantum information processing that are based on *optically manipulated atoms* face the challenge of protecting the quantum states of the system from decoherence, or fidelity

loss, due to atomic spontaneous emission (SE) [1, 141, 142]. SE becomes the dominant source of decoherence at low temperatures, as nonradiative (phonon) relaxation becomes weak [4, 5]. SE suppression *cannot be achieved* by frequent modulations or perturbations of the decaying state, because of the extremely broad spectrum of the radiative continuum ("bath") [76, 97]. A promising means of protection from SE is to embed the atoms in photonic crystals (three-dimensionally periodic dielectrics) that possess spectrally wide, omnidirectional photonic bandgaps (PBGs) [6]: atomic SE would then be blocked at frequencies within the PBG [6–8]. Thus far, studies of coherent optical processes in a PBG have assumed *fixed* values of the atomic transition frequency [9]. However, in order to operate quantum logic gates, based on pairwise entanglement of atoms by field-induced dipole-dipole interactions [10, 143, 144], one should be able to switch the interaction on and off, most conveniently by AC Stark-shifts of the transition frequency of one atom relative to the other, thereby changing its detuning from the PBG edge. The question then arises: should such frequency shifts be performed adiabatically, in order to minimize the decoherence and maximize the quantum-gate fidelity? The answer is expected to be affirmative, based on the existing treatments of adiabatic entanglement and protection from decoherence [11, 12, 129] and on the tendency of nonadiabatic evolution to spoil fidelity and promote transitions to the continuum [13]. Surprisingly, our analysis (Section 6) demonstrates that only an *appropriately phased sequence of "sudden"* (strongly nonadiabatic) *changes* of the detuning from the PBG edge may yield *higher fidelity* of qubit and quantum gate operations than their adiabatic counterparts. This unconventional nonadiabatic protection from decoherence is valid for qubits that are *strongly coupled to the continuum edge* [14, 145], as opposed to the weak coupling approach in Sections 2–5.

1.4. Outline. In this paper we develop, step by step, the framework for universal dynamical control by modulating fields of multilevel systems or qubits, aimed at suppressing or preventing their noise, decoherence, or relaxation in the presence of a thermal bath. Its crux is the general master equation (ME) of a multilevel, multipartite system, weakly coupled to an arbitrary bath and subject to arbitrary temporal driving or modulation. The present ME, derived by the technique [146, 147], is more general than the ones obtained previously in that it does not invoke the rotating wave approximation and therefore applies at arbitrarily short times or for arbitrarily fast modulations.

Remarkably, when our general ME is applied to either AN or PN, the resulting dynamically controlled relaxation or decoherence rates obey *analogous formulae* provided that the corresponding density-matrix (generalized Bloch) equations are written in the appropriate basis. This underscores the universality of our treatment. It allows us to present a PN treatment that does not describe noise phenomenologically, but rather dynamically starting from the ubiquitous spin-boson Hamiltonian.

In Sections 2 and 3, we present a universal formula for the control of single-qubit zero-temperature relaxation and discuss several limits of this formula. In Sections 4 and 5, we extend this formula to multipartite or multilevel systems. In Section 6 dynamical control in the strong coupling regime is considered. In Section 7, the treatment is extended to the control of finite-temperature relaxation and decoherence and culminates in single-particle Bloch equations with dynamically modified decoherence rates that essentially obey the universal formula of Section 3. We then discuss in Section 7.4 the possible modulation arsenal for either AN or PN control. In Section 8, we discuss the extensions of the universal control formula to entangled multipartite systems. The formalism is applicable in a natural and straightforward manner to such systems [123]. It allows us to focus on the ability of symmetries to overcome multipartite decoherence [87, 114–117]. In Section 8, we discuss the implementations of the universal formula to multipartite quantum computation. Section 9 discusses some general aspects of multipartite dynamical control. We develop a general optimization strategy for performing a chosen unitary or nonunitary task on an open quantum system. The goal is to design a controlled time-dependent system Hamiltonian by variationally minimizing or maximizing a chosen function of the system state, which quantifies the task success (score), such as fidelity, purity, or entanglement. If the time dependence of the system Hamiltonian is fast enough to be comparable to or shorter than the response time of the bath, then the resulting non-Markovian dynamics is shown to optimize the chosen task score to second order in the coupling to the bath. This strategy can not only protect a desired unitary system evolution from bath-induced decoherence but also take advantage of the system-bath coupling so as to realize a desired nonunitary effect on the system. Section 10 summarizes our conclusions whereby this universal control can effectively protect complex systems from a variety of decoherence sources.

2. Modulation-Affected Control of Decay into Continua and Zero-Temperature Baths: Weak-Coupling Theory

2.1. Framework. Consider the decay of a state $|e\rangle$ via its coupling to a bath, described by the orthonormal basis $\{|j\rangle\}$, which forms either a discrete or a continuous spectrum (or a mixture thereof). The total Hamiltonian is

$$H = H_S(t) + H_B(t) + H_I(t). \tag{1}$$

Here

$$H_S(t) = \hbar\left(\omega_a + \delta_a(t)\right)|e\rangle\langle e| \tag{2}$$

is the dynamically modulated Hamiltonian of the system, with $\hbar\omega_a$ being the energy of $|e\rangle$. The time-dependent frequency $\delta_a(t)$ can be attributed to the controllable dynamically imposed Stark shift, or to proper dephasing (uncontrolled, random fluctuation). The term

$$H_B(t) = \hbar\sum_j \left(\omega_j + \delta_f(t)\right)|j\rangle\langle j| \tag{3}$$

is the time-dependent Hamiltonian of the bath, with $\hbar\omega_j$ being the energies of $|j\rangle$. The time-dependent frequencies

$\delta_f(t)$, like $\delta_a(t)$, may arise from proper dephasing or dynamical Stark shifts. Finally

$$H_I(t) = \epsilon(t)\,\mu_{je}\,|e\rangle\,\langle j| + \text{h.c.}, \tag{4}$$

denotes the off-diagonal coupling of $|e\rangle$ with the continuum/bath, with $\widetilde{\epsilon}(t)$ being the dynamical modulation function and μ_{je} the system-bath coupling matrix elements.

We write the wave function of the system as

$$\begin{aligned}|\Psi(t)\rangle = {} & \alpha(t)\,e^{-i\omega_a t - i\int_0^t \delta_a(t')dt'}\,|e\rangle \\ & + \sum_j \beta_j(t)\,e^{-i\omega_j t - i\int_0^t \delta_f(t')dt'}\,|j\rangle,\end{aligned} \tag{5}$$

with the initial condition being

$$|\Psi(0)\rangle = |e\rangle. \tag{6}$$

A one-level system $|e\rangle$ which can exchange its population with the bath states $\{|j\rangle\}$ represents the case of autoionization or photoionization. However, the above Hamiltonian describes also a qubit, which can undergo transitions between the excited and ground states $|e\rangle$ and $|g\rangle$, respectively, due to its off-diagonal coupling to the bath. The bath may consist of quantum oscillators (modes) or two-level systems (spins) with different eigenfrequencies. Typical examples are spontaneous emission into photon or phonon continua. In the rotating-wave approximation (RWA), which is alleviated in Section 7, the present formalism applies to a relaxing qubit, under the substitutions

$$|e\rangle \longrightarrow |e\rangle\,|\text{vac}\rangle, \qquad |j\rangle \longrightarrow |g\rangle\,|j\rangle. \tag{7}$$

3. Single-Qubit Zero-Temperature Relaxation

To gain insight into the requirements of decoherence control, consider first the simplest case of a qubit with states $|e\rangle, |g\rangle$ and energy separation $\hbar\omega_a$ relaxing into a zero-temperature bath via off-diagonal (σ_x) coupling, Figure 1(a). The Hamiltonian is given by

$$\begin{aligned}H &= H_S + H_B + H_I, \\ H_S &= \hbar\omega_a\,|e\rangle\langle e|, \\ H_B &= \hbar\sum_j \omega_j a_j^\dagger a_j, \\ H_I &= \sum_j \mu_{ej}\,|e,0\rangle\langle g,1_j| + \text{H.c.},\end{aligned} \tag{8}$$

the sum extending over all bath modes, where $a_j, a_j^\dagger$ are the annihilation and creation operators of mode j, respectively, with $|\{0\}\rangle$ and $|1_j\rangle$ denoting the bath vacuum and jth-mode single excitation, respectively, and μ_{ej} being the corresponding transition matrix element and H.C. being Hermitian conjugate. We have also taken the rotating wave approximation (RWA). The general time-dependent state can be written as

$$\Psi(t) = \widetilde{\alpha}_e(t)\,|e,0\rangle + \sum_j \widetilde{\beta}_j(t)\,|g,1_j\rangle. \tag{9}$$

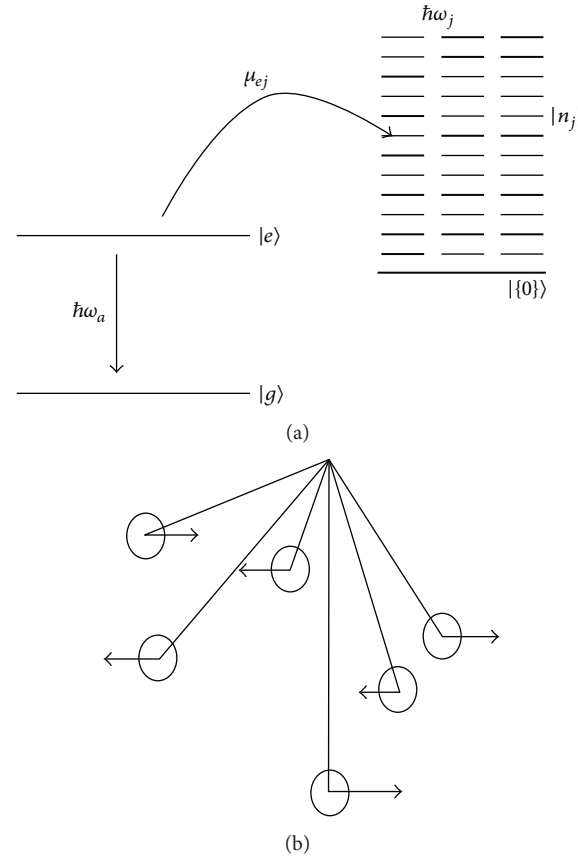

Figure 1: (a) Schematic drawing of a two-level system with off-diagonal coupling to a continuum or a bath. (b) Schematic drawing of a bath comprised of many harmonic oscillators with different frequencies, whose temporal dephasing after correlation time t_c renders the system-bath interaction practically irreversible.

The Schrödinger equation results in the following coupled equations [83]:

$$\begin{aligned}\partial_t\widetilde{\alpha}_e(t) &= -i\omega_a\widetilde{\alpha}_e - i\hbar^{-1}\sum_j \mu_{ej}\widetilde{\beta}_j, \\ \partial_t\widetilde{\beta}_j(t) &= -i\omega_j\widetilde{\beta}_j - i\hbar^{-1}\mu_{ej}^*\widetilde{\alpha}_e.\end{aligned} \tag{10}$$

One can go to the rotating frame, define $\alpha_e(t) = \widetilde{\alpha}_e(t)e^{i\omega_a t}$, $\beta_j(t) = \widetilde{\beta}_j(t)e^{i\omega_j t}$, and get:

$$\beta_j(t) = -i\hbar^{-1}\int_0^t dt'\,e^{i\omega_j t'}\mu_{ej}^* e^{-i\omega_a t'}\alpha_e(t'), \tag{11}$$

$$\partial_t\alpha_e = -\int_0^t dt'\,\Phi(t-t')\,e^{i\omega_a(t-t')}\alpha_e(t'), \tag{12}$$

where

$$\begin{aligned}\Phi &= \hbar^{-2}\,\langle e,0|\,H_I e^{-(iH_0 t/\hbar)}H_I\,|e,0\rangle \\ &= \hbar^{-2}\sum_j |\mu_{ej}|^2 e^{-i\omega_j t},\end{aligned} \tag{13}$$

is the bath response/correlation function, expressible in terms of a sum over all transition matrix elements squared oscillating at the respective mode frequencies ω_j.

It is the spread of oscillation frequencies ω_j that causes the environment response to decohere after a (typically short) *correlation time* t_c (Figure 1(b)). Hence, the Markovian assumption that the correlation function decays to 0 instantaneously, $\Phi(t) \approx \delta(t)$, is widely used: it is in particular the basis for the venerated Lindblad's master equation describing decoherence [148]. It leads to exponential decay of α_e at the Golden Rule (GR) rate [76, 78] as

$$R_{\mathrm{GR}} = 2\pi \sum_j \left|\mu_{ej}\right|^2 \delta\left(\omega_a - \omega_j\right). \tag{14}$$

We, however, are interested in the extremely non-Markovian time scales, much shorter than t_c, on which all bath modes excitations oscillate in unison and the system-bath exchange is *fully reversible*. How does one probe, or, better still, maintain the system in a state corresponding to such time scales?

To this end, we assume modulations of $H_S(t)$ and $H_I(t)$,

$$\begin{aligned} H_S(t) &= \hbar\left(\omega_a + \delta_a(t)\right)|e\rangle\langle e|, \\ H_I(t) &= \sum_j \widetilde{\epsilon}(t)\,\mu_{ej}\,|e,0\rangle\left\langle g,1_j\right| + \mathrm{H.c.}, \\ \epsilon(t) &= \widetilde{\epsilon}(t)\,e^{i\int_0^t d\tau \delta_a(\tau)}, \end{aligned} \tag{15}$$

that result in the time-dependent modulation function $\epsilon(t)$, which has two components, namely, an amplitude modulation $\widetilde{\epsilon}(t)$ and phase modulation $\delta_a(t)$. The modulation function $\epsilon(t)$ is related to $\epsilon(t)$ in 3 via

$$\epsilon(t) = \widetilde{\epsilon}(t)\exp\left[-i\int_0^t \delta_{af}\left(t_1\right)dt_1\right], \tag{16}$$

with

$$\delta_{af}(t) = \delta_a(t) - \delta_f(t). \tag{17}$$

This modulation may pertain to *any intervention* in the system-bath dynamics: (i) measurements that effectively interrupt and completely dephase the evolution, describable by stochastic $\epsilon(t)$ [149], (ii) coherent perturbations that describe *phase modulations* of the system-bath interactions [99, 124].

For any $\epsilon(t)$, the *exact* equation (12) is then rewritten as

$$\partial_t \alpha_e = -\int_0^t dt' \Phi\left(t - t'\right)\epsilon(t)\,\epsilon^*\left(t'\right)e^{i\omega_a(t-t')}\alpha_e\left(t'\right). \tag{18}$$

We now resort to the *crucial* approximation that $\alpha_e(t)$ *varies slower* than either $\epsilon(t)$ or $\Phi(t)$. This approximation is justifiable in the *weak-coupling regime* (to second order in H_I), as discussed below. Under this approximation, (18) is transformed into a differential equation describing relaxation at a time-dependent rate as

$$\begin{aligned} \partial_t \alpha_e &= -q(t)\,\alpha_e, \\ q(t) &= \int_0^t dt' \Phi\left(t - t'\right)\epsilon(t)\,\epsilon^*\left(t'\right)e^{i\omega_a(t-t')} \\ &\equiv \frac{r(t)}{2} + i\Delta_a(t), \end{aligned} \tag{19}$$

where $r(t)$ is the instantaneous time-dependent relaxation rate and $\Delta_a(t)$ is the Lamb shift due to the coupling to the bath. One can separate the spectral representation of $\Phi(t)$ into the real and imaginary parts

$$\Phi(\omega) = \int_0^\infty dt \Phi(t)\,e^{i\omega t} = \pi G(\omega) - i\chi(\omega), \tag{20}$$

which satisfy the Kramers-Kronig relations

$$\chi(\omega) = \mathscr{P}\int \frac{G\left(\omega'\right)d\omega'}{\omega' - \omega}, \tag{21}$$

with $\mathscr{P}$ denoting the principal value. Henceforth, we shall concentrate on the relaxation rate, as it determines the excited state population,

$$P(t) = |\epsilon(t)|^2 = e^{-R(t)t}, \tag{22}$$

where

$$R(t) = \frac{1}{t}\int_0^t dt' r(t) \tag{23}$$

is the average relaxation rate.

It is advantageous to consider the frequency domain, as it gives more insight into the mechanisms of decoherence. For this purpose, we define the finite-time Fourier transform of the modulation function as

$$\epsilon_t(\omega) = \frac{1}{\sqrt{2\pi}}\int_0^t dt' \epsilon\left(t'\right)e^{i\omega t'}. \tag{24}$$

The average time-dependent relaxation rate can be rewritten, by using the Fourier transforms of $\Phi(t)$ and $\epsilon(t)$, in the following form:

$$R(t) = 2\pi\int_{-\infty}^{\infty} d\omega G\left(\omega + \omega_a\right)F_t(\omega), \tag{25}$$

where

$$G(\omega) = \pi^{-1}\,\mathrm{Re}\int_0^\infty dt e^{i\omega t}\Phi(t) \tag{26}$$

is the spectral-response function of the bath, and

$$F_t(\omega) = \frac{\left|\epsilon_t(\omega)\right|^2}{t} \tag{27}$$

is the finite-time spectral intensity of the (random or coherent) intervention/modulation function, where the $1/t$ factor

comes about from the definition of the decoherence rate *averaged* over the $(0, t)$ interval.

The relaxation rate $R(t)$ described by (25)–(27) embodies our *universal recipe for dynamically controlled relaxation* [99, 124], which has the following merits: (a) it holds for any bath and any type of interventions, that is, coherent modulations and incoherent interruptions/measurements alike; (b) it shows that in order to suppress relaxation we need to *minimize the spectral overlap* of $G(\omega)$, given to us by nature, and $F_t(\omega)$, which we may design to some extent; (c) most importantly, it shows that in the short-time domain, only broad (coarse-grained) spectral features of $G(\omega)$ and $F_t(\omega)$ are important. The latter implies that, in contrast to the claim that correlations of the system with each individual bath mode must be accounted for, if we are to preserve coherence in the system, we actually only need to characterize and suppress (by means of $F_t(\omega)$) the *broad spectral features* of $G(\omega)$, the bath response function. The universality of (25)–(27) will be elucidated in what follows, by focusing on several limits.

3.1. The Limit of Slow Modulation Rate. If $\epsilon(t)$ corresponds to sufficiently slow rates of interruption/modulation ν_t, the spectrum of $F_t(\omega)$ is much narrower than the interval of change of $G(\omega)$ around ω_a, the resonance frequency of the system. Then $F_t(\omega)$ can be replaced by $\delta(\omega)$, so that the spectral width of G plays no role in determining R, and we may as well replace $G(\omega+\omega_a)$ by a spectrally finite, flat (*white-noise*) reservoir; that is, we may take the *Markovian limit*. The result is that (25) coincides with the Golden Rule (GR) rate, (14) (Figure 2(a)) as

$$R \approx R_{\mathrm{GR}} = 2\pi \int_{-\infty}^{\infty} d\omega \delta(\omega) G(\omega + \omega_a) = 2\pi G(\omega_a). \quad (28)$$

Namely, slow interventions do not affect the onset and rate of exponential decay.

3.2. The Limit of Frequent Modulation. Frequent interruptions, intermittent with free evolution, are represented by a repetition of the free-evolution modulation spectrum

$$\begin{aligned} F_{t=n\tau}(\omega) &= n\frac{\left|\epsilon_\tau(\omega)\right|^2}{t} = \frac{n}{2\pi t}\left|\int_0^\tau dt' e^{i\omega t'}\right|^2, \\ &= \frac{n}{2\pi t}\tau^2 \mathrm{sinc}^2\left(\frac{\omega\tau}{2}\right) = \frac{\tau}{2\pi}\mathrm{sinc}^2\left(\frac{\omega\tau}{2}\right), \end{aligned} \quad (29)$$

where $\tau = 1/\nu_t$ being the time-interval between consecutive interruptions. If $\epsilon(t)$ describes *extremely* frequent interruptions or measurements $\nu_t \gg 1/t_c$, $F_t(\omega)$ is much broader than $G(\omega + \omega_a)$. We may then pull $F_t(\omega)$ out of the integral, whereupon (25) yields

$$R(t) \approx \tau \int_{-\infty}^{\infty} G(\omega + \omega_a) d\omega. \quad (30)$$

This limit is that of the quantum Zeno effect (QZE), namely, the suppression of relaxation as the interval between interruptions decreases [150–152]. In this limit, the system-bath exchange is reversible and the system coherence is fully maintained (Figure 2(b)). Namely, the essence of the QZE is that sufficiently rapid interventions prevent the excitation escape to the continuum, by *reversing* the exchange with the bath.

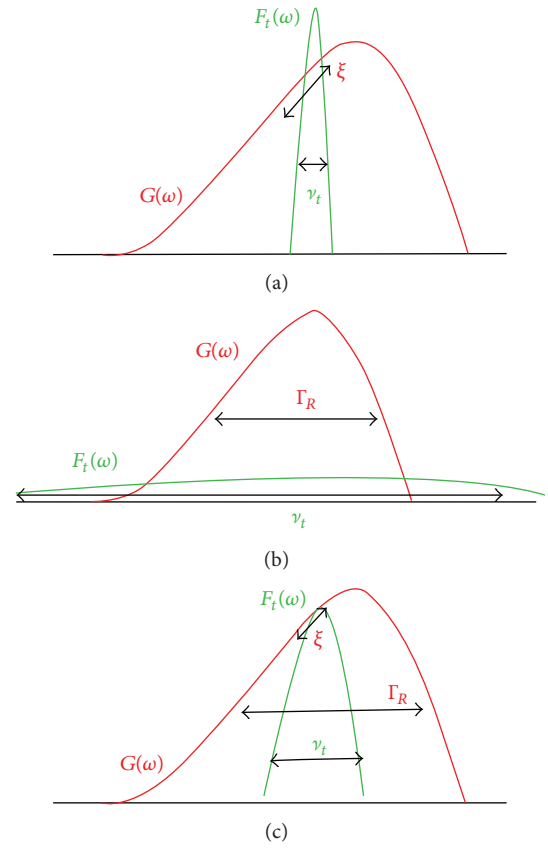

Figure 2: Frequency-domain representation of the dynamically controlled decoherence rate in various limits (Section 7). (a) Golden Rule limit. (b) Quantum Zeno effect (QZE) limit. (c) Anti-Zeno effect (AZE) limit. Here, $F_t(\omega)$ and $G(\omega)$ are the modulation and bath spectra, respectively, ξ and Γ_R are the interval of change and width of $G(\omega)$, respectively, and ν_t is the interruption rate.

3.3. Intermediate Modulation Rate. In the intermediate time-scale of interventions, where the width of $F_t(\omega)$ is broader than the width of ξ_a (so that the Golden Rule is violated) but narrower than the width of $G(\omega)$ (so that the QZE does not hold), the overlap of $F_t(\omega)$ and $G(\omega)$ *grows* as the rate of interruptions, or modulations, increases. This brings about the *increase of relaxation rates $R(t)$ with the rate of interruptions*, marking the anti-Zeno effect (AZE) [85, 102, 153] (Figure 2(c)). On such time-scales, more frequent interventions (in particular, interrupting measurements) *enhance the departure of the evolution from reversibility*. Namely, the essence of the AZE is that if you do not *intervene in time* to prevent the excitation escape to the continuum, then any intervention only drives the system further from its initial state.

We note that the AZE can only come about when the peaks of $F_t(\omega)$ and $G(\omega)$ *do not* overlap, that is, the resonant

coupling is shifted from the maximum of $G(\omega)$. If, by contrast, the peaks of $F_t(\omega)$ and $G(\omega)$ do coincide, any rate of interruptions would result in QZE (Figure 2(b)). This can be understood by viewing $F_t(\omega)$ as an averaging kernel of $G(\omega)$ around ω_a. If $G(\omega_a)$ is the maximum of the spectrum, any averaging can only be *lower* than this maximum, which is the Golden Rule decay rate. Hence, any rate of interruptions can only decrease the decay rate with respect to the Golden Rule rate, that is, cause the QZE.

3.4. Quasiperiodic Amplitude and Phase Modulation (APM). The modulation function $\epsilon(t)$ can be either random or regular (coherent) in time, as detailed below. Consider first the most general coherent *amplitude and phase* modulation (APM) of the quasiperiodic form,

$$\epsilon(t) = \sum_k \epsilon_k e^{-i\omega_k t}. \tag{31}$$

Here ω_k ($k = 0, \pm 1, \ldots$) are arbitrary discrete frequencies with the minimum spectral distance Ω. If $\epsilon(t)$ is periodic with the period Ω, then $\omega_k = k\Omega$ and ϵ_k become the Fourier components of $\epsilon(t)$. For a general quasiperiodic $\epsilon(t)$, one obtains

$$\begin{aligned} \left|\epsilon_t(\omega)\right|^2 &= \epsilon_c^2 t \sum_k \left|\lambda_k\right|^2 S(\eta_k, t) \\ &\quad + \epsilon_c^2 \sum_{k \neq l} \lambda_k \lambda_l^* \frac{1 + e^{i(\eta_k - \eta_l)t} - e^{i\eta_k t} - e^{-i\eta_l t}}{2\pi \eta_k \eta_l}. \end{aligned} \tag{32}$$

Here

$$\epsilon_c^2 = \sum_k \left|\epsilon_k\right|^2 \tag{33}$$

equals the average of $|\epsilon(t)|^2$ over a period of the order of $1/\Omega$, $\lambda_k = \epsilon_k/\epsilon_c$, and $\eta_k = \omega - \omega_k$, whereas

$$S(\eta_k, t) = \frac{2\sin^2(\eta_k t/2)}{\pi t \eta_k^2} \tag{34}$$

is a bell-like function of η_k normalized to 1.

For a sufficiently long time, the function $S(\eta_k, t)$ becomes narrower than the respective characteristic width $\xi(\omega_a + \omega_k)$ of $G(\omega)$ around $\omega_a + \omega_k$, and one can set

$$S(\eta_k, t) \approx \delta(\eta_k). \tag{35}$$

Thus, when

$$t \gg t_c \equiv \max_k \left\{ \frac{1}{\xi(\omega_a + \omega_k)} \right\}, \tag{36}$$

where t_c is the effective *correlation (memory) time* of the reservoir, (25) is reduced to

$$R = 2\pi \sum_k \left|\lambda_k\right|^2 G(\omega_a + \omega_k). \tag{37}$$

For the validity of (37), it is also necessary that

$$\epsilon_c^2 R t_c \ll 1. \tag{38}$$

This condition is well satisfied in the regime of interest, that is, weak coupling to essentially any reservoir, unless (for some harmonic k) $\omega_a + \omega_k$ is extremely close to a sharp feature in $G(\omega)$, for example, a band edge [145], a case covered by Section 6. Otherwise, the long-time limit of the general decay rate (25) under the APM is a sum of the GR rates, corresponding to the resonant frequencies shifted by ω_k, with the weights $|\lambda_k|^2$.

Formula (37) provides a *simple general recipe* for manipulating the decay rate by APM. Its powerful generality allows for the *optimized* control of decay, not only for a single level but also for a *band* characterized by a spectral distribution $P(\omega_a)$ (e.g., inhomogeneous or vibrational spectrum). We can then choose λ_k and ω_k in (37) so as to minimize the decay convoluted with $P(\omega_a)$. In what follows, various limits of (37) will be analyzed.

3.5. Coherent Phase Modulation (PM)

3.5.1. Monochromatic Perturbation. Let

$$\epsilon(t) = \epsilon_0 e^{-i\delta_{af} t}. \tag{39}$$

Then

$$R = 2\pi G(\omega_a + \Delta), \tag{40}$$

where $\Delta = \delta_{af} = \text{const}$ is a frequency shift, induced by the ac Stark effect (in the case, e.g., of atoms) or by the Zeeman effect (in the case of spins). In principle, such a shift may drastically enhance or suppress R relative to R_{GR}. It provides the *maximal variation* of R achievable by an external perturbation, since it does not involve any averaging (smoothing) of $G(\omega)$ incurred by the width of $F_t(\omega)$: the modified R can even *vanish*, if the shifted frequency $\omega_a + \Delta$ is beyond the cut-off frequency of the coupling, where $G(\omega) = 0$. Conversely, the increase of R due to a shift can be much greater than that achievable by repeated measurements, that is, the anti-Zeno effect [97, 98, 101, 102]. In practice, however, ac Stark shifts are usually small for (cw) monochromatic perturbations, whence pulsed perturbations should often be used.

3.5.2. Impulsive Phase Modulation. Let the phase of the modulation function periodically jump by an amount ϕ at times $\tau, 2\tau, \ldots$. Such modulation can be achieved by a train of n identical, equidistant, narrow pulses of nonresonant radiation, which produce pulsed frequency shifts $\delta_{af}(t)$. Now

$$\epsilon(t) = e^{i[t/\tau]\phi}, \tag{41}$$

where $[\cdots]$ is the integer part. One then obtains that

$$\begin{aligned} \epsilon_c &= 1, \\ F_{n\tau}(\omega) &= \frac{2\sin^2(\omega\tau/2)\sin^2\left[n(\phi + \omega\tau)/2\right]}{\pi n \tau \omega^2 \sin^2\left[(\phi + \omega\tau)/2\right]}. \end{aligned} \tag{42}$$

The decay, according to (22), has then the form (at $t = n\tau$)

$$P(n\tau) = \exp\left[-R(n\tau)\, n\tau\right], \tag{43}$$

where $R(n\tau)$ is defined by (25).

For sufficiently long times

$$\omega_k = \frac{2k\pi}{\tau} - \frac{\phi}{\tau}, \qquad \left|\lambda_k\right|^2 = \frac{4\sin^2(\phi/2)}{(2k\pi - \phi)^2}. \tag{44}$$

For *small phase shifts*, $\phi \ll 1$, the $k = 0$ peak dominates,

$$\left|\lambda_0\right|^2 \approx 1 - \frac{\phi^2}{12}, \tag{45}$$

whereas

$$\left|\lambda_k\right|^2 \approx \frac{\phi^2}{4\pi^2 k^2} \quad (k \neq 0). \tag{46}$$

In this case, one can retain only the $k = 0$ term in (37) (unless $G(\omega)$ is changing very fast). Then the modulation acts as a constant shift

$$\Delta = -\frac{\phi}{\tau}. \tag{47}$$

With the increase of $|\phi|$, the difference between the $k = 0$ and $k = 1$ peak heights diminishes, *vanishing* for $\phi = \pm\pi$. Then

$$\left|\lambda_0\right|^2 = \left|\lambda_1\right|^2 = \frac{4}{\pi^2}, \tag{48}$$

that is, $F_t(\omega)$ for $\phi = \pm\pi$ contains *two identical peaks symmetrically shifted in opposite directions* (the other peaks $|\lambda_k|^2$ decrease with k as $(2k-1)^{-2}$, totaling 0.19).

The above features allow one to adjust the modulation parameters for a given scenario to obtain an optimal decrease or increase of R. The phase-modulation (PM) scheme with a small ϕ is preferable near the continuum edge, since it yields a spectral shift in the required direction (positive or negative). The adverse effect of $k \neq 0$ peaks in $F_t(\omega)$ then scales as ϕ^2 and hence can be significantly reduced by decreasing $|\phi|$. On the other hand, if ω_a is near a *symmetric* peak of $G(\omega)$, R is reduced more effectively for $\phi \simeq \pi$, as in [80, 81], since the main peaks of $F_t(\omega)$ at ω_0 and ω_1 then shift stronger with τ^{-1} than the peak at $\omega_0 = -\phi/\tau$ for $\phi \ll 1$.

3.6. Amplitude Modulation (AM). Amplitude modulation (AM) of the coupling arises, for example, for radiative-decay modulation due to atomic motion through a high-Q cavity or a photonic crystal [154, 155] or for atomic tunneling in optical lattices with time-varying lattice acceleration [106, 156]. Let the coupling be turned on and off periodically, for the time τ_1 and $\tau_0 - \tau_1$, respectively, that is,

$$\epsilon(t) = \begin{cases} 1 & \text{for } n\tau_0 < t < n\tau_0 + \tau_1, \\ 0 & \text{for } n\tau_0 + \tau_1 < t < (n+1)\,\tau_0, \end{cases} \tag{49}$$

($n = 0, 1, \ldots$). Now [157]

$$F_{n\tau_0}(\omega) = \frac{2\sin^2(\omega\tau_1/2)\sin^2(n\omega\tau_0/2)}{\pi n\tau_1\omega^2\sin^2(\omega\tau_0/2)}, \tag{50}$$

so that (see (43))

$$P(n\tau_0) = \exp\left[-R(n\tau_0)\, n\tau_1\right], \tag{51}$$

where $R(n\tau_0)$ is given by (25) and (50).

This case is also covered by (37) and (38), where the parameters are now found to be

$$\epsilon_c^2 = \frac{\tau_1}{\tau_0}, \qquad \omega_k = \frac{2k\pi}{\tau_0}, \qquad \left|\lambda_k\right|^2 = \frac{\tau_1}{\tau_0}\,\mathrm{sinc}^2\left(\frac{k\pi\tau_1}{\tau_0}\right), \tag{52}$$

with

$$\mathrm{sinc}(x) = \frac{\sin x}{x}, \quad \mathrm{sinc}(0) = 1. \tag{53}$$

It is instructive to consider the limit wherein $\tau_1 \ll \tau_0$ and τ_0 is much greater than the correlation time of the continuum; that is, $G(\omega)$ does not change significantly over the spectral intervals $(2\pi k/\tau_0, 2\pi(k+1)/\tau_0)$. In this case, one can approximate the sum (37) by the integral (25) with

$$F_t(\omega) \approx \left(\frac{\tau_1}{2\pi}\right)\mathrm{sinc}^2\left(\frac{\omega\tau_1}{2}\right), \tag{54}$$

characterized by the spectral broadening $\sim 1/\tau_1$. Then (25) for R reduces to that obtained when ideal projective measurements are performed at intervals τ_1 [97]. Thus the AM scheme *can imitate measurement-induced (dephasing) effects* on quantum dynamics, if the interruption intervals τ_0 exceed the *correlation time of the continuum*.

The decay probability $P(t)$, calculated for parameters similar to [106], *completely coincides* with that obtained for ideal impulsive measurements at intervals τ_1 [97, 98, 101] and demonstrates either the quantum Zeno effect (QZE) or the anti-Zeno effect (AZE) behavior, depending on the rate of modulation.

Since the Hamiltonian for atoms in accelerated optical lattices is similar to the Legett Hamiltonian for *current-biased Josephson junctions* [77], the present theory has been extended to describe effects of current modulations on the rate of macroscopic quantum tunneling in Josephson junctions in [100].

Projective measurements at an effective rate ν, whether impulsive or continuous, usually result in a broadened (to a width ν) modulation function $F(\omega)$, without a shift of its center of gravity [97, 98, 101, 158, 159],

$$\Delta = \int d\omega\omega F(\omega) \approx 0. \tag{55}$$

This feature was shown in [97] to be responsible for either the standard quantum Zeno effect whereby R scales as

$$R \propto \frac{1}{\nu}, \tag{56}$$

or the anti-Zeno effect whereby R grows with ν. In contrast, a weak and broadband chaotic field, such that

$$|\chi_a|\,\bar{I} \ll \nu_B, \tag{57}$$

where $\bar{I}$ is the mean intensity, ν_B is the bandwidth, and χ_a is the effective polarizability (electric or magnetic, depending on the system), would give rise to a Lorentzian dephasing function $F(\omega)$ with a substantial shift

$$\Delta = \chi_a \bar{I}. \tag{58}$$

This shift would have a much stronger effect on R than the QZE or AZE, which are associated with the rate ν, since

$$\nu \sim \frac{\chi_a^2 \bar{I}^2}{\nu_B} \ll |\Delta|. \tag{59}$$

4. Multipartite Decay Control

4.1. Multipartite PN Control by Resonant Modulation. One can describe phase noise, or proper dephasing, by a stochastic fluctuation of the excited-state energy, $\omega_a \rightarrow \omega_a + \delta_r(t)$, where $\delta_r(t)$ is a stochastic variable with zero mean, $\langle \delta(t) \rangle = 0$ and $\langle \delta(t)\delta(t') \rangle = \Phi^P(t - t')$ is the second moment. For multipartite systems, where each qubit can undergo different proper dephasing, $\delta_j(t)$, one has an additional second moment for the cross dephasing, $\langle \delta_j(t)\delta_{j'}(t') \rangle = \Phi^P_{jj'}(t - t')$. A general treatment of multipartite systems undergoing this type of proper dephasing is given in [107]. Here we give the main results for the case of two qubits.

Let us take two TLS, or qubits, which are initially prepared in a Bell state. We wish to obtain the conditions that will preserve it. In order to do that, we change to the Bell basis, which is given by

$$\begin{aligned} |B_{1,2}\rangle &= \frac{1}{\sqrt{2}e^{i\omega_a t}\left(|e\rangle_1|g\rangle_2 \pm |g\rangle_1|e\rangle_2\right)}, \\ |B_{3,4}\rangle &= \frac{1}{\sqrt{2}\left(e^{i2\omega_a t}|e\rangle_1|e\rangle_2 \pm |g\rangle_1|g\rangle_2\right)}. \end{aligned} \tag{60}$$

For an initial Bell-state $\bar{\rho}_l(0) = |B_l\rangle\langle B_l|$, where $l = 1, \ldots, 4$, one can then obtain the fidelity, $F_l(t) = \langle B_l|\, \bar{\rho}_l(t)\, |B_l\rangle$, as

$$F_l(t) = \cos\left(\phi_\pm(t)\right) \mathrm{Re}\left[e^{i\phi_\pm(t)} \left(1 - \frac{1}{2} \sum_{jj'} J^P_{jj',l}(t) \right) \right], \tag{61}$$

where

$$\phi_j(t) = 2\int_0^t d\tau V_{0,j}(\tau), \tag{62}$$

$$J^P_{jj',l}(t) = 2\pi \int_{-\infty}^{\infty} d\omega G^P_{jj'}(\omega)\, F_{t,jj',l}(\omega), \tag{63}$$

$$G^P_{jj'}(\omega) = \int_{-\infty}^{\infty} dt \Phi^P_{jj'}(t)\, e^{i\omega t}, \tag{64}$$

$$F_{t,jj,l}(\omega) = \left|\epsilon_{t,j}(\omega)\right|^2, \tag{65}$$

$$F_{t,jj',3}(\omega) = -F_{t,jj',1}(\omega) = \epsilon^*_{t,j}(\omega)\, \epsilon^*_{t,j'}(\omega), \tag{66}$$

$$F_{t,jj',4}(\omega) = -F_{t,jj',2}(\omega) = \epsilon_{t,j}(\omega)\, \epsilon^*_{t,j'}(\omega), \tag{67}$$

where $V_{0,j}(t)$ is the amplitude of the resonant field applied on qubit j, $\phi_\pm(t) = (\phi_1(t) \pm \phi_2(t))/2$, and the ϕ_+ corresponds to $k = 1, 3$ and ϕ_- to $k = 2, 4$. Expressions (61)–(67) provide our recipe for minimizing the Bell-state fidelity losses. They hold for *any* dephasing time-correlations and *arbitrary* modulation.

One can choose between two modulation schemes, depending on our goals. When one wishes to preserve and initial quantum state, one can equate the modified dephasing and cross dephasing rates of all qubits, $J_{jj',l}(t) = J(t)$. This results in complete preservation of the singlet only, that is, $F_2(t) = 1$, for all t, but reduces the fidelity of the triplet state. On the other hand, if one wishes to equate the fidelity for all initial states, one can eliminate the cross dephasing terms, by applying different modulations to each qubit (Figure 3), causing $F_{t,jj',l}(\omega) = 0$ for all $j \neq j'$. This requirement can be important for quantum communication schemes.

5. Dynamical Control of Zero-Temperature Decay in Multilevel Systems

5.1. General Formalism. Here we discuss in detail a model for dynamical decay modifications in a multilevel system. The system with energies $\hbar\omega_n$, $1 \leq n \leq N$, is coupled to a zero-temperature bath of harmonic oscillators with frequencies ω_j. Using the factorized coupling defined in Section 2.1, the corresponding Hamiltonian is found to be as in 1, where

$$H_S(t) = \hbar \sum_n \omega_n\ |n\rangle\langle n| + \sum_{nn'} O_{nn'}(t)\, |n\rangle\langle n'|, \tag{68}$$

$$H_B(t) = \hbar \sum_j \omega_j\, |j\rangle\langle j|, \tag{69}$$

$$H_I(t) = \sum_{n,j} \epsilon_n(t)\, \mu_{jn}\, |n\rangle\langle j| + \text{h.c.}, \tag{70}$$

where now each level has a different modulation $\epsilon_n(t)$ and a *different coupling to the bath* μ_{jn} and $O_{nn'}(t)$ denotes a gate operation.

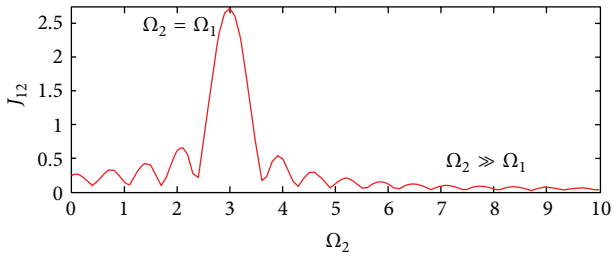

FIGURE 3: Cross decoherence as a function of local modulation. Here two qubits are modulated by continuous resonant fields, with amplitudes $\Omega_{1,2}$. The cross decoherence decays as the two qubits' modulations become increasingly different. The bath parameters are $\Phi_T(t) = e^{-t/t_c}$, where $t_c = 0.5$ is the correlation time, and $\Omega_1 = 3$.

The system evolution is divided into two phases, one of storage without gate operations and a gate operation of finite duration

$$O_{nn'}(t) = \begin{cases} g_{nn'}, & t' \le t \le t' + \tau, \\ 0, & \text{elsewhere.} \end{cases} \tag{71}$$

The full wave function is given by

$$|\Psi(t)\rangle = \sum_n \alpha_n(t)\, e^{-i\omega_n t} |n\rangle + \sum_j \beta_j(t)\, e^{-i\omega_j t} |j\rangle. \tag{72}$$

Similarly to what was said in Section 2.1, one can consider two types of situations. The above equations (68)–(72) were written for an N-level system which can exchange its population with the reservoir. In addition, one can consider an $(N+1)$-level system, where transitions are possible between any level $\langle n|$ and a lower level $\langle g|$, the reservoir consisting of quantum systems, as described in Section 2.1. The theory in Section 5 holds for both situations, with the minor difference that one should substitute as

$$|n\rangle \longrightarrow |n\rangle |\text{vac}\rangle, \qquad |j\rangle \longrightarrow |g\rangle |j\rangle \tag{73}$$

in (70) and (72) and perform a similar substitution in (76) below.

In order to find the solution, one has to diagonalize the system hamiltonian by introducing a matrix that rotates the amplitudes $\alpha(t) = \{\alpha_n(t)\}$ as

$$\alpha(t) = \Theta(t)\, \tilde{\alpha}(t), \tag{74}$$

such that, by defining $\Omega_{nn'}(t) = \omega_n \delta_{nn'} + O_{nn'}(t)$, one gets

$$\widetilde{\Omega}_{nn'}(t) = \left(\Theta^{-1}(t)\, \Omega \Theta(t)\right)_{nn'} = \tilde{\omega}_n(t)\, \delta_{nn'}, \tag{75}$$

where $\omega_n(t)$ are the eigenvalues of the new rotated system. Thus the transformed wave function becomes

$$|\Psi(t)\rangle = \sum_{\tilde{n}} \tilde{\alpha}_n(t)\, e^{-i\int_0^t \tilde{\omega}_n(\tau)d\tau} |\tilde{n}\rangle + \sum_j \beta_j(t)\, e^{-i\omega_j t} |j\rangle. \tag{76}$$

Using these rotated state amplitudes, a procedure similar to that used for one level, one finds that they obey the following integrodifferential equations, assuming slowly varying $\alpha_n(t)$ as

$$\dot{\tilde{\alpha}}(t) = -\left[f(t) + q(t)\right] \tilde{\alpha}. \tag{77}$$

Here, the $f(t)$ and $q(t)$ matrices are given by

$$\begin{aligned} f_{nn''}(t) &= it\dot{\tilde{\omega}}_n(t)\, \delta_{nn''} + \\ &\quad + \sum_{n'} \left[\Theta^{-1}(t)\right]_{nn'} \dot{\Theta}_{n'n''}(t)\, e^{i\int_0^t [\tilde{\omega}_n(\tau) - \tilde{\omega}_{n''}(\tau)]d\tau}, \\ q_{nn''}(t) &= \sum_{n'} \int_0^t dt' K_{nn'}(t, t')\, \Phi_{nn'}(t - t') \times \\ &\quad \times e^{i\int_0^t \tilde{\omega}_n(\tau)d\tau - i\int_0^{t'} \tilde{\omega}_{n''}(\tau)d\tau} \Theta_{n'n''}(t'), \end{aligned} \tag{78}$$

with $K(t, t')$ and $\Phi(t)$ being the modulation and reservoir-response matrices, respectively, given by

$$\begin{aligned} K_{nn'}(t, t') &= \epsilon_n^*(t)\, \epsilon_{n'}(t'), \\ \Phi_{nn'}(t) &= \int d\omega G_{nn'}(\omega)\, e^{-i\omega t}, \end{aligned} \tag{79}$$

where

$$G_{nn'}(\omega) = \hbar^{-2} \sum_j \mu_{nj}^* \mu_{n'j} \delta(\omega - \omega_j). \tag{80}$$

During the storage phase, one has $\Theta_{nn'}(t) = \delta_{nn'}$, $\tilde{\omega}_n(t) = \omega_n$ and $\tilde{g}_{nn''}(t) = \delta_{nn''}$, and during the gate-operation phase, $\Theta_{nn'}(t) = \Theta_{nn'}$, $\tilde{\omega}_n(t) = \tilde{\omega}_n$, and $\tilde{g}_{nn''}(t) = g_{nn''}$.

The solution to (77) is of the form

$$\tilde{\alpha}(t) = T_+ e^{-\int_0^t [f(t') + q(t')]dt'} \tilde{\alpha}(0). \tag{81}$$

To simplify the analysis, one can define the fluence and the modulation spectral matrices as

$$\begin{aligned} Q_{nn'}(t) &= \int_0^t d\tau \epsilon_n^*(\tau)\, \epsilon_{n'}(\tau), \\ F_{nn',t}(\omega) &= \frac{\epsilon_{t,n}^*(\omega - \omega_n)\, \epsilon_{t,n'}(\omega - \omega_{n'})}{Q_{nn'}(t)}. \end{aligned} \tag{82}$$

The relevant imaginary parts of the spectral response of the reservoir can be expressed, analogously to (20) and (21), by the Kramers-Kronig relations

$$\begin{aligned} \widetilde{\Phi}_{nn'}(\omega) &= \pi G_{nn'}(\omega) - i\chi_{nn'}(\omega), \\ \chi_{nn'}(\omega) &= \mathcal{P} \int \frac{G_{nn'}(\omega')\, d\omega'}{\omega' - \omega}. \end{aligned} \tag{83}$$

Defining

$$J(t) = \int_0^t dt' q(t'), \tag{84}$$

we shall now represent $J_{nn'}(t)$ in different regimes (phases).

(i) As a reference, it is important to consider the decoherence effects with no modulations at all, that is, $F_{nn',t}(\omega) = \delta(\omega - \omega_n)\delta(\omega_n - \omega_{n'})$. In this case, one obtains a *diagonal* decoherence matrix

$$J_{nn'}(t) = t\delta_{nn'}\widetilde{\Phi}_{nn'}(\omega_n). \quad (85)$$

This means that interference of decaying levels n and n' cancels out in the long time limit, and the decoherence is without cross relaxation.

(ii) During the storage phase, (84) results in

$$J_{nn'}(t) = Q_{nn'}(t)\int_{-\infty}^{\infty} d\omega F_{nn',t}(\omega)\widetilde{\Phi}_{nn'}(\omega). \quad (86)$$

One can easily see that for the off-diagonal terms, a *simple separation into decay rates and energy shifts is inapplicable* in this formulation.

(iii) During gate operations, (84) assumes the form

$$J_{nn'}(t) = \sum_{n''} Q_{nn''}(t)\Theta_{n''n'}\int_{-\infty}^{\infty} d\omega F_{nn'',t}(\omega)\widetilde{\Phi}_{nn''}(\omega). \quad (87)$$

In a more compact and enlightening form, one can rewrite this equation as $J^{\text{gate}} = J^{\text{storage}} \times \Theta$, where J^{storage} is given in (86).

6. The Strong-Coupling Regime: Decay Control Near Continuum Edge by Nonadiabatic Interference

The analysis expounded thus far has been based on a *perturbative* treatment of the system-bath coupling. Here, we address the regime of *strong system-bath coupling*, as in the case of a resonance frequency very near to the continuum edge, a situation that may be encountered in atomic excitation near the ionization energy, vibrational excitation frequency in a solid near the Debye cutoff, or an atomic excitation in a photonic crystal near a photonic bandgap. In the strong-coupling regime, it is advantageous to work in the combined basis of the system (qubit) and field (bath) states that incorporate the system-bath interaction. Dynamical control of the decay can then be analysed by exact solution of the Schrödinger equation in this basis. Analytical expressions are obtainable for alternating static evolutions with different parameters (e.g., resonant frequency), the dynamical control resulting from their *interference*. Specifically, we shall consider optical manipulations of atoms embedded in photonic crystals with atomic transition frequencies near a photonic bandgap (PBG), that is, near the edge of the photonic mode continuum, where the qubit *is strongly coupled* to the continuum, and spontaneous emission (SE) is only partially blocked, because an initially excited atom then evolves into a *superposition of decaying and stable states*, the stable state representing photon-atom binding [14, 145]. In what follows we shall demonstrate the ability of appropriately alternating sudden changes of the detuning to *augment the interference* of the emitted and back-scattered photon amplitudes, thereby increasing the probability amplitude of the stable (photon-atom bound) state. As a result, phase-gate operations affected by dipole-dipole interactions can be performed with higher fidelity than in the case of adiabatic frequency change.

6.1. Hamiltonian and Equations of Motion. We consider a two-level atom with excited and ground states $|e\rangle$ and $|g\rangle$ coupled to the field of a discrete (or defect) mode and to the photonic band structure (PBS) in a photonic crystal. The hamiltonian of the system in the rotating-wave approximation assumes the form [145]

$$\begin{aligned} H = {} & \hbar\omega_{at}|e\rangle\langle e| + \hbar\int_0^{+\infty}\omega a_\omega^\dagger a_\omega \rho(\omega)\, d\omega \\ & + \hbar\left(\kappa_d^\star a_d^\dagger |g\rangle\langle e| + \text{h.c.}\right) \\ & + \hbar\int_0^{+\infty}\left[\kappa^\star(\omega)\, a_\omega^\dagger |g\rangle\langle e| + \text{h.c.}\right]\rho(\omega)\, d\omega. \end{aligned} \quad (88)$$

Here, $\hbar\omega_{at}$ is the energy of the atomic transition frequency, $a_\omega^\dagger$ and a_ω are, respectively, the creation and annihilation operators of the field mode at frequency ω, $\rho(\omega)$ is the mode density of the PBS, and $\kappa(\omega)$ and κ_d are the coupling rates to the atomic dipole of a mode from the continuum and the discrete mode, respectively.

Let us first consider the initial state obtained by absorbing a photon from the discrete mode as

$$|\Psi(0)\rangle = |e, \{0_\omega\}\rangle, \quad (89)$$

where $|\{0_\omega\}\rangle$ is the vacuum state of the field. Then the evolution of the wavefunction $|\Psi(t)\rangle$ has the general form

$$\begin{aligned} |\Psi(t)\rangle = {} & \alpha(t)|e, \{0_\omega\}\rangle + \beta_d(t)|g, 1_d\rangle \\ & + \int_0^{+\infty}\beta_\omega(t)|g, 1_\omega\rangle\rho(\omega)\, d\omega, \end{aligned} \quad (90)$$

where we have denoted by $|1_\omega\rangle$ and $|1_d\rangle$ the single-photon state of the relevant modes. The Schrödinger equation $i\dot{\Psi}(t) = H\Psi(t)$ then leads to the set of coupled differential equations

$$\begin{aligned} \dot{\alpha}(t) = {} & -i\omega_{at}\alpha(t) - i\kappa_d\beta_d(t) \\ & - i\int_0^{+\infty}\kappa(\omega)\beta_\omega(t)\rho(\omega)\, d\omega, \\ \dot{\beta}_d(t) = {} & -i\omega_d\beta_d(t) - i\kappa_d^\star\alpha(t), \\ \dot{\beta}_\omega(t) = {} & -i\omega\beta_\omega(t) - i\kappa^\star(\omega)\alpha(t). \end{aligned} \quad (91)$$

This evolution reflects the interplay between the off-resonant Rabi oscillations of $|e, \{0_\omega\}\rangle$ and $|g, 1_d\rangle$, at the driving rate κ_d, and the *partly inhibited oscillatory decay* from $|e, \{0_\omega\}\rangle$ to $|g, \{1_\omega\}\rangle$ via coupling to the continuum $\rho(\omega)$. This decay depends on the detuning of ω_{at} from the continuum edge at ω_U (the upper cutoff of the PBG). For a spectrally steep edge (see below), we are in the regime of *strong coupling* to the mode continuum (as in a high-Q cavity [8]) which allows for the existence of an oscillatory, nondecaying, component of $\alpha(t)$, associated with a photon-atom bound state [7, 145].

6.2. Periodic Sudden Changes of the Detuning. Let us now introduce abrupt changes of ω_{at}, that is, of the detuning $\Delta_{at} = \omega_U - \omega_{at}$ from the upper cutoff, ω_U, of the PBG (by fast AC-Stark modulations as discussed below), at intervals τ. In the sudden-change approximation for ω_{at}, the amplitudes $(\alpha_{\mathrm{dyn}}(t), \beta_{d\,\mathrm{dyn}}, \{\beta_{\omega\,\mathrm{dyn}}(t)\})$ of the excited state, the discrete mode and the continuum still evolve according to (91), except that from $t = 0$ to $t = \tau$ the atomic transition frequency is $\omega_{at} = \omega_A$, that is, the detuning $\Delta_{at} = \omega_U - \omega_A = \Delta_A$, while for $t > \tau$, we have $\omega_{at} = \omega_B$, that is, $\Delta_{at} = \Delta_B$. This dynamics leads to the relation

$$\begin{aligned} \alpha_{\mathrm{dyn}}(t) &= \alpha_A(t), \qquad \beta_{d\,\mathrm{dyn}}(t) = \beta_{d,A}(t), \\ \beta_{\omega\,\mathrm{dyn}}(t) &= \beta_{\omega,A}(t), \quad (t \le \tau); \\ \alpha_{\mathrm{dyn}}(t) &= \alpha_B^{(s)}(t), \qquad \beta_{d\,\mathrm{dyn}}(t) = \beta_{d,B}^{(s)}(t), \\ \beta_{\omega\,\mathrm{dyn}}(t) &= \beta_{\omega,B}^{(s)}(t), \quad (t > \tau). \end{aligned} \tag{92}$$

Here, $(\alpha_A(t), \beta_{d,A}(t), \{\beta_{\omega,A}(t)\})$ and $(\alpha_B^{(s)}(t), \beta_{d,B}^{(s)}(t), \{\beta_{\omega,B}^{(s)}(t)\})$ are solutions of (91) with a static (fixed) atomic transition frequency, ω_A or ω_B. However, the initial condition at the instant $t = \tau$ of the frequency change from Δ_A to Δ_B is no longer the excited state (89) but the superposition

$$\begin{aligned} |\Psi(\tau)\rangle = \alpha_A(\tau)\,|e, \{0_\omega\}\rangle + \beta_{d,A}(\tau)\,|g, 1_d\rangle \\ + \int_0^{+\infty} \beta_{\omega,A}(\tau)\,|g, 1_\omega\rangle\,\rho(\omega)\,d\omega. \end{aligned} \tag{93}$$

In other words, the dynamics is equivalent to two successive static evolutions, the second one starting from initial conditions $(\alpha_A(\tau), \beta_{d,A}(\tau), \{\beta_{\omega,A}(\tau)\})$.

Using the Laplace transform of the system (91) with the initial condition (93), it is possible to express the dynamic amplitude of the excited state after the sudden change as

$$\begin{aligned} \alpha_{\mathrm{dyn}}(t) = \alpha_A(\tau)\,\alpha_B(t-\tau) + \beta_{d,A}(\tau)\,\beta_{d,B}(t-\tau) \\ + \int_0^{+\infty} \beta_{\omega,A}(\tau)\,\beta_{\omega,B}(t-\tau)\,\rho(\omega)\,d\omega, \quad (t > \tau), \end{aligned} \tag{94}$$

where we have used the initial conditions $(\alpha_A(\tau), \beta_{d,A}(\tau), \{\beta_{\omega,A}(\tau)\})$ and the solution $(\alpha_B(t), \beta_{d,B}(t), \{\beta_{\omega,B}(t)\})$ of (91) for the initial condition (89).

There is an advantageous feature to the sudden change: since the time dependence of $\alpha_{\mathrm{dyn}}(t)$ in (92) arises from the static amplitudes α_B, $\beta_{d,B}$, and $\beta_{\omega,B}$ at the *shifted* time $t - \tau$, a consequence of the sudden change is to revive the excited-state population oscillations, which tend to disappear at long times in the static case. Hence, by applying several *successive* sudden changes, we should be able to maintain large-amplitude oscillations of the *coherence* between $|e\rangle$ and $|g\rangle$. The scenario leading to the largest amplitude consists in *periodic* shifts of the energy detuning from Δ_A to Δ_B. When the initial detuning Δ_A is large and we first reduce it to Δ_B before it increases to Δ_A, the *dynamic population and the* $|e\rangle - |g\rangle$ *coherence*, thanks to the revival of oscillations, are *periodically larger* than the static ones. This remarkable result occurs unexpectedly: it implies that successive abrupt changes can *reverse* the decay to the continuum, even though they *cannot be associated with the Zeno effect*: they occur at intervals much longer than the correlation (Zeno) time of the radiative continuum, which is utterly negligible (10^{-18} s) [97], or even longer than the static-oscillation half period. The fact that this happens only for the rather "counter-intuitive" ordering of detuning values (from large to small then back again) is a manifestation of interference between successive static evolutions: their relative phases determine the beating between the emitted and reabsorbed (back-scattered) photon amplitudes and thereby the oscillation of $\alpha_{\mathrm{dyn}}(t)$.

Let us now consider the initial superposition

$$|\Psi(0)\rangle = \alpha(0)\,|e, \{0_\omega\}\rangle + \beta_d(0)\,|g, 1_{\omega_d}\rangle \tag{95}$$

and a nonnegligible coupling constant κ_d. In this case, the periodic dynamic population of the excited state also strongly exceeds the static one. Most importantly, the *instantaneous dynamic fidelity* $|\langle\Psi(0)|\Psi(t)\rangle|^2$ is periodically enhanced as compared to the static one, as demonstrated numerically.

In order to use these results for quantum logic gates, let us consider the example of the dipole-dipole induced control-phase gate, which consists in shifting the phase of the target-qubit excited state by π via interaction with the control qubit [10, 143, 144]. The phase shift must be accumulated gradually, to preserve the coherence of the system. We have found that ten or twenty sudden shifts of $\pi/10$ or $\pi/20$, respectively, alternating with appropriate detuning changes, can keep the fidelity high, with little decoherence. The system begins to evolve following the "counter-intuitive" detuning sequence discussed above (not to be confused with the adiabatic STIRAP method [11, 12, 129]). As soon as two sudden changes of the detuning have been performed, the conditional phase shift of $\pi/10$ or $\pi/20$ takes place and the process is further repeated. The total gate operation is completed within the time interval of maximum fidelity. The fidelity of the system relative to its initial state during the realization of a control phase gate, with alternating detunings, is perhaps our most impressive finding. We find that the fidelity is increased using the "counterintuitive" sequence of detunings (solid line) as compared to the static (fixed) choice of maximal detuning (long-dashed line), or compared to the dynamically enhanced fidelity $|\langle\Psi(0)|\Psi(t)\rangle|^2$ obtained without gate operations (dot-dashed line).

6.3. Comparison with the Weak-Coupling Regime. We have compared the results of this method, which allows for *possibly strong coupling* of $|e\rangle$ with the continuum edge, with those of the universal formula of Section 2 (25), which expresses the decay rate of $\alpha(t)$ by the convolution of the modulation spectrum and the PBS coupling spectrum. We find good agreement with this formula only in the regime of *weak coupling* to the PBG edge, when the dimensionless detuning parameter $\Delta_{at}/\gamma_c > 5$, as expected from the limitations of the theory in Section 2.

6.4. Experimental Scenario. The following experimental scenario may be envisioned for demonstrating the proposed effect: pairs of qubits are realizable by two species of active rare-earth dopants [17, 18] or quantum dots in a photonic crystal. The transition frequency of one species is initially detuned by $\Delta_{at} \sim 1$ MHz from the PBG edge with coupling constant $\gamma_c \sim 10$ MHz and by ~3 MHz from the resonance of the other species. This Δ_{at} is abruptly modulated by $f$sec nonresonant laser pulses which exert ~3 MHz AC Stark shifts. Between successive shifts, the qubits are near resonant with their neighbours and therefore become dipole-dipole coupled, thus affecting the high-fidelity phase-control gate operation [10, 143, 144]. The required pulse rate is $\gamma_c/10 \sim 1$ MHz, much lower than the pulse rate stipulated under similar conditions by previously proposed strategies [81, 99, 118].

7. Finite-Temperature Relaxation and Decoherence Control

So far we have treated the case of an empty (zero-temperature) bath. In order to account for finite-temperature situations, where the bath state is *close* to a thermal (Gibbs) state, we resort to a master equation (ME) for any dynamically controlled reduced density matrix of the system [100, 124] that we have derived using the Nakajima-Zwanzig formalism [70, 146, 147, 160]. This ME becomes manageable and transparent under the following assumptions. (i) The weak-coupling limit of the system-bath interaction H_I prevails, corresponding to the neglect of $O(H_I^3)$ terms. This is equivalent to the Born approximation, whereby the back effect of the system on the bath and their resulting entanglement are ignored. (ii) The system and the bath states are initially factorisable. (iii) The initial mean value of H_I vanishes.

We present the general form of the Nakajima-Zwanzig formalism and resort to the aforementioned assumptions only when necessary. Hence, the formalism may seem cumbersome, yet it can be simplified greatly if the assumptions are made from the outset (see [70]).

7.1. Explicit Equations for Factorisable Interaction Hamiltonians. We now wish to write the ME explicitly for time-dependent Hamiltonians of the following form [100]:

$$\begin{aligned} H(t) &= H_S(t) + H_B + H_I(t), \\ H_I(t) &= S(t)\, B, \end{aligned} \tag{96}$$

where H_S and H_B are the system and bath Hamiltonians, respectively, and H_I, the interaction Hamiltonian, is the product of operators S and B which act on the system and bath, respectively.

Finally, defining the correlation function for the bath,

$$\Phi_T(t) = \left\langle B\widetilde{B}(t) \right\rangle_B, \tag{97}$$

we obtain the ME for ρ in the Born approximation as

$$\begin{aligned} \dot{\rho}(t) = & -i\left[H_S, \rho(t)\right] \\ & + \int_0^t d\tau \left\{ \Phi_T(t-\tau) \left[\widetilde{S}(t,\tau)\, \rho(t), S(t) \right] + \text{H.c.} \right\}. \end{aligned} \tag{98}$$

We focus on two regimes: a two-level system coupled to either an amplitude- or phase-noise (AN or PN) thermal bath. The bath Hamiltonian (in either regime) will be explicitly taken to consist of harmonic oscillators and be linearly coupled to the system

$$\begin{aligned} H_B &= \sum_\lambda \omega_\lambda a_\lambda^\dagger a_\lambda, \\ B &= \sum_\lambda \left(\kappa_\lambda a_\lambda + \kappa_\lambda^* a_\lambda^\dagger \right). \end{aligned} \tag{99}$$

Here $a_\lambda, a_\lambda^\dagger$ are the annihilation and creation operators of mode λ, respectively, and κ_λ is the coupling amplitude to mode λ.

7.1.1. Amplitude-Noise Regime. We first consider the AN regime of a two-level system coupled to a thermal bath. We will use off-resonant dynamic modulations, resulting in AC-Stark shifts. The Hamiltonians then assume the following form:

$$H_S(t) = \left(\omega_a + \delta_a(t)\right) |e\rangle\langle e|, \tag{100}$$

$$S(t) = \widetilde{\epsilon}(t)\, \sigma_x, \tag{101}$$

where $\delta_a(t)$ is the dynamical AC-Stark shifts, $\widetilde{\epsilon}(t)$ is the time-dependent modulation of the interaction strength, and the Pauli matrix $\sigma_x = |e\rangle\langle g| + |g\rangle\langle e|$.

7.1.2. Phase-Noise Regime. Next, we consider the PN regime of a two-level system coupled to a thermal bath via σ_z operator. To combat it, we will use near-resonant fields with time-varying amplitude as our control. The Hamiltonians then assume the following forms:

$$H_S(t) = \omega_a |e\rangle\langle e| + V(t)\, \sigma_x, \tag{102}$$

$$S(t) = \widetilde{\epsilon}(t)\, \sigma_z, \tag{103}$$

where $V(t) = \Omega(t) e^{-i\omega_a t} + c.c$ is the time-dependent resonant field, with real envelope $\Omega(t)$, $\widetilde{\epsilon}(t)$ is the time-dependent modulation of the interaction strength, and $\sigma_z = |e\rangle\langle e| - |g\rangle\langle g|$.

Since we are interested in dephasing, phases due to the (unperturbed) energy difference between the levels are immaterial.

7.2. Universal Master Equation. To derive a universal ME for both amplitude- and phase-noise scenarios, we move to the interaction picture and rotate to the appropriate

diagonalizing basis, where the appropriate basis for the AN case of (100) is

$$|\uparrow,\downarrow\rangle = |e,g\rangle\,, \tag{104}$$

while for the PN case of (102) the basis is

$$|\uparrow,\downarrow\rangle = \frac{1}{\sqrt{2}}\left(e^{-i\omega_a t}\,|e\rangle \pm |g\rangle\right). \tag{105}$$

In this rotated and tilted frame,

$$\begin{aligned} U_S(t,\tau) &= U_S(t,0)\,U_S^{\dagger}(\tau,0)\,,\\ U_S(t,0) &= e^{-i\phi(t)}\,|\uparrow\rangle\langle\uparrow| + e^{i\phi(t)}\,|\downarrow\rangle\langle\downarrow|\,, \end{aligned} \tag{106}$$

where

$$\phi(t) = \begin{cases} \omega_a t + \displaystyle\int_0^t dt'\delta_a\left(t'\right) & \text{for AN,}\\ \displaystyle\int_0^t dt'\,\frac{\Omega\left(t'\right)}{2} & \text{for PN} \end{cases} \tag{107}$$

is the phase-modulation due to the time-dependent control in the system Hamiltonian.

Allowance for *arbitrary* time-dependent intervention in the system and interaction dynamics $H_S(t)$, $H_I(t)$, respectively, yields the following *universal* ME for a dynamically controlled decohering system [100, 124]:

$$\dot{\widetilde{\rho}}(t) = \int_0^t dt'\left\{\Phi\left(t-t'\right)\left[\widetilde{S}\left(t'\right)\widetilde{\rho}(t),\widetilde{S}(t)\right] + \text{H.c.}\right\}. \tag{108}$$

Here $\widetilde{S}(t) = \epsilon(t)\widetilde{\sigma}_x$ is the modulated interaction operator, where $\widetilde{\ }$ denotes the rotated and tilted frame, and $\widetilde{\sigma}_x = |\uparrow\rangle\langle\downarrow| + |\downarrow\rangle\langle\uparrow|$. The modulation function is given by

$$\epsilon(t) = \widetilde{\epsilon}(t)\,e^{i\phi(t)} \tag{109}$$

for both AN and PN. It is important to note that $\widetilde{\rho}$ is a function of t only (*not of* t'): this *convolutionless* form of the ME is *fully non-Markovian* to second order in H_I, as proven exactly in [124].

7.3. Universal Modified Bloch Equations. The resulting modified Bloch equations, in the appropriate diagonalizing basis (see (104) for AN and (105) for PN), are given by

$$\dot{\rho}_{\uparrow\uparrow} = -\dot{\rho}_{\downarrow\downarrow} = -r_{\uparrow}(t)\,\rho_{\uparrow\uparrow} + r_{\downarrow}(t)\,\rho_{\downarrow\downarrow}, \tag{110}$$

$$r_{\uparrow(\downarrow)} = 2\,\text{Re}\int_0^t dt'\Phi\left(t-t'\right)K_{\pm}\left(t,t'\right), \tag{111}$$

$$K_{+}\left(t,t'\right) = K_{-}^{*}\left(t,t'\right) = \epsilon(t)\,\epsilon^{*}\left(t'\right). \tag{112}$$

The time-dependent relaxation rates are real, and the only difference between them is the complex conjugate of the combined modulation function, $K_{\pm}(t,t')$. They can be very different for a complex correlation function.

One can derive the corresponding time-averaged relaxation rates of the upper and lower states as

$$\begin{aligned} R_{\uparrow} &= \int_{-\infty}^{\infty} d\omega G(+\omega)\,F_t(\omega)\,,\\ R_{\downarrow} &= \int_{-\infty}^{\infty} d\omega G(-\omega)\,F_t(\omega)\,. \end{aligned} \tag{113}$$

For both AN (see (100)) and PN (see (102)),

$$G(\omega) = G_0(\omega)\left(n_T(\omega)+1\right) + G_0(-\omega)\,n_T(-\omega)\,, \tag{114}$$

$$G_0(\omega) = \rho(\omega)\left|\mu_{eg}\right|^2(\omega)\,\Theta(\omega)\,, \tag{115}$$

where $G_0(\omega)$ is the zero-temperature bath spectrum, $\rho(\omega)$ and $\mu_{eg}(\omega)$ are the frequency-dependent density of bath modes and the $e \leftrightarrow g$ transition matrix element, respectively, $n_T(\omega) = (e^{\beta\omega}-1)^{-1}$ is the temperature-dependent bath mode population, and $\beta = \hbar/k_B T$ is the inverse temperature. Also, $\Theta(\omega)$ is the Heaviside function, that is, the zero-temperature bath spectrum is defined only for positive frequencies $G_0(\omega < 0) = 0$. Hence, the first right-hand side of (114) is nonzero for positive frequencies and the second right-hand side is nonzero for negative frequencies.

For either AN or PN, we may control the decoherence by either off-resonant or near-resonant modulations, respectively. The modulation spectrum has the *same form* for both (see Section 7.4) as

$$F_t(\omega) = \frac{1}{t}\left|\int_0^t dt' e^{i\omega t'}\,\epsilon\left(t'\right)\right|^2, \tag{116}$$

where the modulation function is given in (107) and (109). The time-dependent modulation phase factor is obtained for AN in the form of an AC-Stark shift, time-integrated over

$$\delta_a(t) = \int_0^t dt'\,\frac{\left|\Omega\left(t'\right)\right|^2}{\Delta\left(t'\right)}, \tag{117}$$

where $\Omega(t)$ is the Rabi frequency of the control field and $\Delta(t')$ is the detuning. The corresponding phase factor for PN is the integral of the Rabi frequency $\Omega(t)$, that is, the pulse area of the resonant control field, (107) (Figure 4).

Hence, upon making the appropriate substitutions, the Bloch equations (110) have the *same universal* form for either AN or PN. An arbitrary combination of AN and PN requires a more detailed treatment, yet the universal form is maintained.

7.3.1. Dynamically Modified Decay Rates. Since we are interested here in dynamical control of relaxation, we shall concentrate on the transition rates $R_{e(g)}(t)$ rather than the level shifts. The average rate of the $|e\rangle \rightarrow |g\rangle$ transition $R_e(t)$ and its $|g\rangle \rightarrow |e\rangle$ counterpart $R_g(t)$ are given by

$$R_{e(g)}(t) = 2\pi\int_{-\infty}^{\infty} d\omega F_t(\omega)\,G_T(\pm\omega)\,. \tag{118}$$

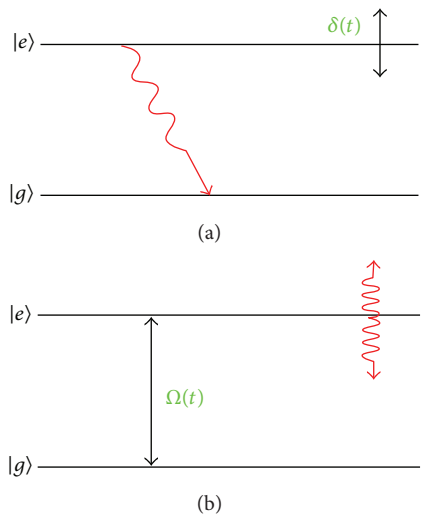

FIGURE 4: Schematic drawing of system and bath. (a) Amplitude noise (AN) (red) combatted by AC-Stark shift modulation (green). (b) Phase noise (PN) (red) combatted by resonant-field modulation (green).

Here the upper (lower) sign corresponds to the subscript $e(g)$, and

$$G_T(\omega) = (2\pi)^{-1} \int_{-\infty}^{\infty} \Phi_T(t)\, e^{i\omega t} dt \tag{119}$$

can be shown [161] to be nonnegative, with $G_T(-\omega) = e^{-\beta\omega} G_T(\omega)$, and vanishes for $\omega < 0$ at $T = 0$: $G_0(\omega) = 0$ $(\omega < 0)$. For the oscillator bath, one finds that

$$G_T(\omega) = [n(\omega) + 1]\, G_0(\omega) + n(-\omega)\, G_0(-\omega), \tag{120}$$

where $G_0(\omega) = \sum_\lambda |\kappa_\lambda|^2 \delta(\omega - \omega_\lambda)$ and $n(\omega) = (e^{\beta\omega} - 1)^{-1}$ is the average number of quanta in the oscillator (bath mode) with frequency ω.

We apply (118) to the case of *coherent modulation of quasiperiodic* form, (see (31)). Without a limitation of the generality, we can assume that $\sum_k |\epsilon_k|^2 = 1$. We then find, using (118), that the rates $R_{e(g)}(t)$ tend to the long-time limits

$$R_{e(g)} = 2\pi \int_{-\infty}^{\infty} d\omega F(\omega)\, G_T(\pm\omega), \tag{121}$$

where

$$F(\omega) = \lim_{t\to\infty} F_t(\omega) = \sum_k |\epsilon_k|^2 \delta(\omega - \omega_a - \omega_k), \tag{122}$$

or

$$R_{e(g)} = 2\pi \sum_k |\epsilon_k|^2 G_T(\pm(\omega_a + \omega_k)). \tag{123}$$

Equation (121) shows that $R_e(R_g)$ *is given by the overlap of the modulation spectrum* $F(\omega)$ *with the bath-CF spectrum* $G_T(\omega)[G_T(-\omega)]$. The limits (123) are approached when $\Omega t \gg 1$ and $t \gg t_c \equiv \max_k\{1/\xi(\pm(\omega_a + \omega_k)\}$. Here t_c is the bath memory (correlation) time, defined as the inverse of $\xi(\omega)$, the spectral interval over which $G_T(\omega)$ changes around the relevant frequencies.

Had we used the standard dipolar RWA hamiltonian in the case of an oscillator bath, dropping the antiresonant terms in $H_I(t)$, we would have arrived at the transition rates

$$R^{\mathrm{RWA}}_{e(g)} = 2\pi \int_0^{\infty} d\omega F(\omega)\, G_T(\pm\omega), \tag{124}$$

wherein the integration is performed from 0 to ∞, rather than from $-\infty$ to ∞, as in (121). This means that the RWA transition rates hold for a slow modulation, when $F(\omega) \simeq 0$ at $\omega < 0$, being peaked near ω_a. However, whenever the suppression of $R_{e(g)}$ requires modulation at a rate comparable to ω_a, the RWA is inadequate. For instance, (120) and (124) imply that, at $T = 0$, the rate R^{RWA}_g vanishes identically, irrespective of $F(\omega)$, in contrast to the true upward-transition rate R_g in (121), which may be comparable to R_e for ultrafast modulation. The difference between the RWA and non-RWA decay rates stems from the fact that the RWA implies that a downward (upward) transition is accompanied by emission (absorption) of a bath quantum, whereas the non-RWA (negative-frequency) contribution to $R_{e(g)}$ in (121) allows for just the opposite: downward (upward) transitions that are accompanied by absorption (emission). The latter processes are possible since the modulation may cause *level* $|e\rangle$ *to be shifted below* $|g\rangle$.

The validity of the (decohering) qubit model in the presence of modulation at a rate $\gtrsim \omega_a$ is now elucidated: it requires that $R_{e(g)j}t \ll 1$, $R_{e(g)j}$ being the effective transition rate from level $e(g)$ to *any other* level j, and, in particular, $R_{e(g)}t \ll 1$. If $R_{e(g)}$ are strongly suppressed by the modulation, the TLS model holds for long times.

7.3.2. Dynamically Modified Proper Dephasing. We turn now to proper dephasing when it dominates over decay. *The random frequency fluctuations* $\delta_d(t)$ are typically characterized by a (single) correlation time t_d, with ensemble mean $\overline{\delta}_d = 0$. When the field $V(t)$ is used only for gate operations, we assume that it does not affect proper dephasing. The ensemble average over $\delta_d(t)$ results in $R(t) \to R(t) + R_d(t)$ with the dephasing rate

$$R_d(t) = \int_0^t dt' \Phi_d(t'), \qquad \Phi_d(t) = \overline{\delta_d(t)\,\delta_d(0)}. \tag{125}$$

The dephasing CF $\Phi_d(t)$ is the counterpart of the bath CF $\Phi_T(t)$.

At $t \gg t_d$, the decoherence rate and shift approach their asymptotic values

$$R_d = \lim_{t\to\infty} R_d(t), \qquad \Delta_d = \lim_{t\to\infty} \Delta_d(t). \tag{126}$$

For the validity of (127), it is necessary that

$$R_d, |\Delta_d| \ll \frac{1}{t_d}. \tag{127}$$

We assume the secular approximation, which holds if

$$V_0(t) \gg R_d, |\Delta_d|. \tag{128}$$

By analogy with (118), one can obtain that

$$R_d(t) = \pi \int_{-\infty}^{\infty} d\omega F_t(\omega) G_d(\omega), \tag{129}$$

where $F_t(\omega)$ is given by (117) with

$$\epsilon(t) = \exp\left[-i \int_0^t V\left(t'\right) dt'\right], \tag{130}$$

$$G_d(\omega) = \frac{1}{\pi} \int_0^{\infty} \Phi_d(t) \cos \omega t \, dt. \tag{131}$$

As follows from (131), $G_d(\omega)$ is a symmetric function,

$$G_d(-\omega) = G_d(\omega). \tag{132}$$

The *proper dephasing* rate associated with

$$\Phi_d(t) = Ae^{-t/t_d} \tag{133}$$

is

$$R_d = At_d. \tag{134}$$

In the presence of a *constant* V_0 [cw $V(t)$], it is modified into

$$R_d = \frac{At_d}{V_0^2 t_d^2 + 1}. \tag{135}$$

For a sufficiently strong field, the dephasing rate R_d can be *suppressed* by the factor $1/(V_0 t_d)^2 \ll 1$. This suppression reflects the ability of strong, near-resonant Rabi splitting to shift the system out of the randomly fluctuating bandwidth, or average its effects. Quantum gate operations may be performed by *slight modulations* of the control field, which can flip the qubit without affecting proper dephasing. By comparison, the "bang-bang" (BB) method involving τ-periodic π-pulses [2, 82, 84] is an analog of the above "parity kicks." Using the analog of (121), such pulses can be shown to suppress R_d approximately according to (135) with $V_0 = \pi/\tau$. This BB method requires pulsed fields with Rabi frequencies $\gg 1/\tau$, that is, *much stronger fields than the cw field* in (135). Using $t_d \sim 10^{-7}$ s, cw Rabi frequencies exceeding 1 MHz achieve a significant dephasing suppression.

7.4. Modulation Arsenal. Any modulation with quasi-discrete, finite spectrum is deemed quasiperiodic, implying that it can be expanded as

$$\epsilon(t) = \sum_k \epsilon_k e^{-i\nu_k t}, \tag{136}$$

where ν_k ($k = 0, \pm 1, \ldots$) are arbitrary discrete frequencies such that

$$\left|\nu_k - \nu_{k'}\right| \geq \Omega \quad \forall k \neq k', \tag{137}$$

where Ω is the minimal spectral interval.

One can define the long-time limit of the quasi-periodic modulation, when

$$\Omega t \gg 1, \qquad t \gg t_c, \tag{138}$$

where t_c is the bath-memory (correlation) time, defined as the inverse of the largest spectral interval over which $G(\omega)$ and $G(-\omega)$ change appreciably near the relevant frequencies $\omega_a + \nu_k$. In this limit, the average decay rate is given by (Figure 5(a)) as

$$R_\uparrow = 2\pi \sum_k \left|\lambda_k\right|^2 G\left(\omega_a + \nu_k\right), \tag{139}$$

$$\lambda_k = \frac{\epsilon_k}{\epsilon_c}, \qquad \epsilon_c = \sum_k \left|\epsilon_k\right|^2. \tag{140}$$

7.4.1. Phase Modulation (PM) of the Coupling. Monochromatic Perturbation. Let

$$\epsilon(t) = \epsilon_0 e^{-i\Delta t}. \tag{141}$$

Then

$$R_\uparrow = 2\pi G\left(\omega_a + \Delta\right), \tag{142}$$

where $\Delta = \text{const.}$ is a frequency shift, induced by the AC Stark effect (in the case of atoms) or by the Zeeman effect (in the case of spins). In principle, such a shift may drastically enhance or suppress R relative to the Golden Rule decay rate, that is, the decay rate without any perturbation as

$$R_{\mathrm{GR}} = 2\pi G\left(\omega_a\right). \tag{143}$$

Equation (40) provides the *maximal change* of R achievable by an external perturbation, since it does not involve any averaging (smoothing) of $G(\omega)$ incurred by the width of $F_t(\omega)$: the modified R can even *vanish*, if the shifted frequency $\omega_a + \Delta$ is beyond the cutoff frequency of the coupling, where $G(\omega) = 0$ (Figure 5(d)). This would accomplish the goal of dynamical decoupling [81–87, 118, 162]. Conversely, the increase of R due to a shift can be much greater than that achievable by repeated measurements, that is, the anti-Zeno effect [97, 98, 101, 102]. In practice, however, AC Stark shifts are usually small for (cw) monochromatic perturbations, whence pulsed perturbations should often be used, resulting in multiple ν_k shifts, as per (139).

Dynamical Decoupling. Dynamical decoupling (DD) is one of the best known approaches to combat decoherence, especially dephasing [79–92, 95, 96]. A full description of this approach is beyond the scope of this work, but we present its most essential aspects and how it can be incorporated into the general framework described above.

7.4.2. Standard DD. DD is based on the notion that the phase-modulation control fields are short and strong enough such that the free evolution can be neglected during these pulses. Hence, the propagator can be decomposed into the free propagator, followed by the control-field propagator, free propagator, and so forth. The control fields used result in the periodic accumulation of π-phases; that is, each pulse has a total area of π, whose effects are similar to time-reversal or the spin-echo technique [94]. Thus, the free evolution propagator after the control π-pulse negates the effects of the

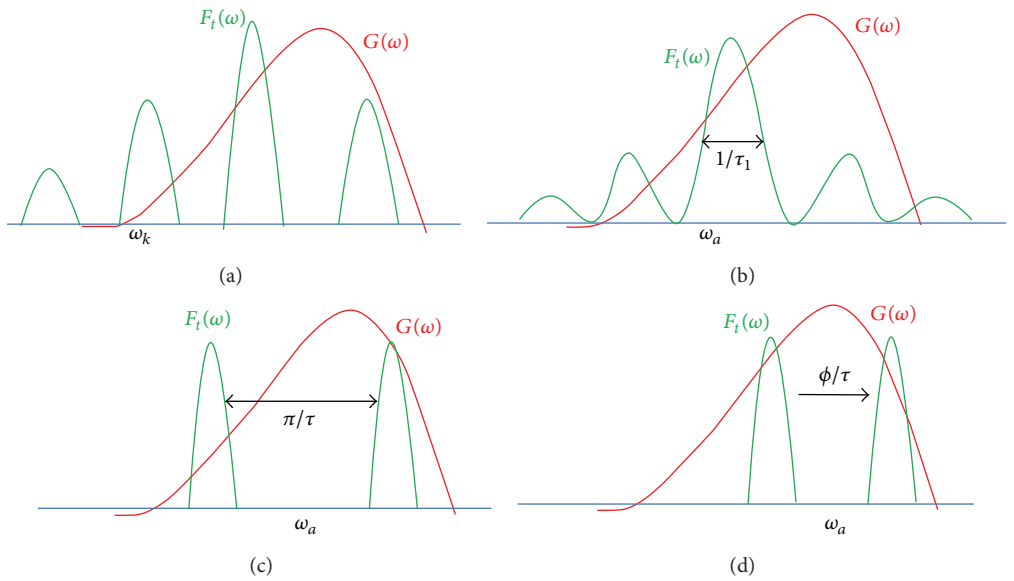

FIGURE 5: Spectral representation of the bath coupling, $G(\omega)$, and the modulation, $F_t(\omega)$. (a) General quasi-periodic modulation, with peaks at ω_k. (b) On-off modulation, with $1/\tau_1$ repetition rate for $\tau_1 \ll \tau_0$. (c) Impulsive phase modulation, (π-pulses), $\phi = \pi$. (d) Monochromatic modulation, or impulsive phase modulation, with small phase shifts, $\phi \ll 1$, and $1/\tau$ repetition rate.

free evolution propagator prior to the control fields, up to first order of the noise in the Magnus expansion.

While the formalism of dynamical decoupling is quite different from the formalism presented here, it can be easily incorporated into the general framework of universal dynamical decoherence control by introducing impulsive phase modulation. Let the phase of the modulation function periodically jump by an amount ϕ at times $\tau, 2\tau, \ldots$. Such modulation can be achieved by a train of identical, equidistant, narrow pulses of nonresonant radiation, which produce pulsed AC Stark shifts of ω_a. When $\phi = \pi$, this modulation corresponds to dynamical-decoupling (DD) pulses.

For sufficiently long times (see (138)), one can use (139), with

$$\nu_k = \frac{2k\pi}{\tau} - \frac{\phi}{\tau}, \qquad |\lambda_k|^2 = \frac{4\sin^2(\phi/2)}{(2k\pi - \phi)^2}. \tag{144}$$

For *small phase shifts*, $\phi \ll 1$, the $k = 0$ peak dominates,

$$|\lambda_0|^2 \approx 1 - \frac{\phi^2}{12}, \tag{145}$$

whereas

$$|\lambda_k|^2 \approx \frac{\phi^2}{4\pi^2 k^2} \quad (k \neq 0). \tag{146}$$

In this case, one can retain only the $k = 0$ term in (139), unless $G(\omega)$ is changing very fast with frequency. Then the modulation acts as a constant shift (Figure 5(d)) as

$$\Delta = -\frac{\phi}{\tau}. \tag{147}$$

As $|\phi|$ increases, the difference between the $k = 0$ and $k = 1$ peak heights diminishes, *vanishing* for $\phi = \pm\pi$. Then

$$|\lambda_0|^2 = |\lambda_1|^2 = \frac{4}{\pi^2}, \tag{148}$$

that is, $F_t(\omega)$ for $\phi = \pm\pi$ contains *two identical peaks symmetrically shifted in opposite directions* (Figure 5(c)) (the other peaks $|\lambda_k|^2$ decrease with k as $(2k-1)^{-2}$, totaling 0.19).

The foregoing features allow one to adjust the modulation parameters for a given scenario to obtain an *optimal* decrease or increase of R. Thus, the phase-modulation (PM) scheme with a small ϕ is preferable near a continuum edge (Figure 5(d)), since it yields a spectral shift in the required direction (positive or negative). The adverse effect of $k \neq 0$ peaks in $F_t(\omega)$ then scales as ϕ^2 and hence can be significantly reduced by decreasing $|\phi|$. On the other hand, if ω_a is near a *symmetric* peak of $G(\omega)$, R is reduced more effectively for $\phi \simeq \pi$, as in [80, 81], since the main peaks of $F_t(\omega)$ at ω_0 and ω_1 then shift stronger with τ^{-1} than the peak at $\omega_0 = -\phi/\tau$ for $\phi \ll 1$.

7.4.3. Optimal DD. One of the recent extensions of standard DD is the optimal DD, introduced by Uhrig [95]. While the standard DD applies an equidistant sequence of π-pulses, optimal DD finds the temporal spacing of the pulses such that dephasing is minimized. In [95], the optimal temporal spacing was found to satisfy a simple analytic equation and the resulting modulation power spectrum for $n\pi$-pulses during time t can be approximated by

$$F_t(\omega) \approx 2t(n+1)^2 \frac{J_{n+1}^2(\omega t/2)}{(\omega t/2)^2}, \tag{149}$$

where J is the Bessel function. This optimal DD sequence was derived by making the first n derivatives of $F_t(\omega)$

vanish. This requires the modulation spectrum to have higher frequency components, by minimizing the lower frequency peaks observed in the standard DD. However, it is important to note that this optimization is done irrespective of the coupling spectrum $G(\omega)$. Hence, this modulation is optimal only if there is weaker coupling to higher frequencies of the bath, which can be easily seen in (121) by noting that the coupling spectrum $G(\omega)$ must have lower values at higher frequencies for the optimal DD to be effective. By contrast, we analyze below an optimal modulation based on our universal formula [104] that takes the coupling spectrum into account.

Other Extensions. We considered here only two forms of dynamical decoupling that can be easily incorporated into the general framework. However, DD has many extensions that go beyond what has been discussed above. An important extension is the universal DD sequence [119] that combats all forms of coupling to a bath, namely, both amplitude and phase noises. The general formalism presented above has not yet addressed this issue, but attempts are currently being made to generalize the treatment.

Another important extension is known as concatenated DD [90] that treats increasingly higher order corrections of the noise, where each concatenation level of the control pulses reduces the previous level's induced errors. This powerful protocol cannot be easily incorporated into our formalism since it goes beyond the second-order approximation used in our derivation of the universal formula.

In general, two major differences make our universal formula approach advantageous compared to the DD approach. The first difference is that we relax the DD assumption that the control fields must be either very short or very strong. In our formalism, the control fields are considered *concurrently* with the coupling to the bath, hence allowing a much wider variety of pulse sequences, ranging from continuous modulation all the way to DD sequences. The second difference relates to the consideration of the bath spectrum. Dynamical decoupling suggests using the same pulse sequence (be it periodic, optimized, or concatenated), no matter what the shape of the bath spectrum. By contrast, our formalism explicitly considers the bath spectrum and allows optimal tailoring of the modulation to a given bath spectrum (see below).

7.5. Optimal Decoherence Control of a Qubit. The aforementioned arsenal of the modulation schemes is not general and neither it nor DD [82, 90, 95, 119, 163, 164] have shown optimality with respect to the decoherence suppression, for *any* given coupling spectrum. Here we apply variational principles to our universal-formula dynamical control of decoherence in order to find the *optimal modulation* for any given decoherence process. We first derive an equation for the *optimal, energy-constrained control by modulation* that minimizes decoherence, for any given bath-coupling spectrum and then numerically solve this equation and compare the optimal modulation to energy-constrained dynamical-decoupling pulses.

The objective is to minimize the average decoherence rate, $R(t)$, given a bath-coupling spectrum, $G(\omega)$, by finding the optimal phase modulation, $\epsilon(t) = e^{i\phi(t)}$ under an energy constraint, respectively, given by

$$R(t) = 2\pi \int_{-\infty}^{\infty} d\omega G(\omega) F_t(\omega),$$

$$G(\omega) = (2\pi)^{-1} \operatorname{Re} \int_{-\infty}^{\infty} dt \Phi(t) e^{i\omega t},$$

$$F_t(\omega) = \frac{\left|\epsilon_t(\omega)\right|^2}{t}, \qquad \epsilon_t(\omega) = \frac{1}{\sqrt{2\pi}} \int_0^t dt_1 e^{i\phi(t_1)} e^{i\omega t_1},$$

$$\int_0^T dt \left|\dot{\phi}(t)\right|^2 = E. \tag{150}$$

7.5.1. Calculus of Variations

7.5.2. Derivation of the Euler-Lagrange Equation. The boundary conditions for the accumulated phase are $\phi(0) = \dot{\phi}(0) = 0$, which results in a smooth solution and accounts for turning the control field on at $t = 0$. Eliminating λ, we find that the optimal control field shape is the solution to the following equation:

$$\ddot{\phi}(t) = \frac{-\sqrt{E} Z[t, \phi(t)]}{\sqrt{\int_0^T dt_1 \left| \int_0^{t_1} dt_2 Z[t_2, \phi(t_2)] \right|^2}}, \tag{151}$$

where λ is the Lagrange multiplier, and

$$Z[t, \phi(t)] = \frac{1}{T} \int_0^T dt_1 \widetilde{\Phi}(|t - t_1|) \times \sin[\phi(t) - \phi(t_1) + \Delta(t - t_1)]. \tag{152}$$

We may compare the optimal dephasing rate to the one obtained by the popular periodic DD control (bang bang) procedure. But to make the comparison meaningful, we impose the same energy constraint. Finite-duration periodic DD against pure dephasing is the "bang bang" application of $n\pi$-pulses and is given in our setting by

$$\Omega(t) = \begin{cases} \frac{\pi}{\nu} & j\tau \le t < j\tau + \nu, \ j = 0, \ldots, n-1, \\ 0 & \text{otherwise}, \end{cases} \tag{153}$$

where $\nu < \tau$ is the width of each pulse and τ is the interval between pulses. The energy constraint E and the total modulation duration $T = n\tau + \nu$ are related via $n = \nu E/\pi^2$. In the frequency domain, the spectral modulation intensity can be described by a series of peaks, where the two main peaks are at $\pm\pi/\tau$. Thus, the peaks are shifted in proportion to the energy invested in the modulation.

(a) Single-Peak Resonant Dephasing Spectrum. This simple dephasing spectrum describes a common scenario where $\Phi(t) = e^{-t/t_c}\gamma/t_c$, where γ is the long-time dephasing rate

$[R(t \to \infty) = 2\pi\gamma]$ and t_c is the noise correlation time. Figure 6(a) shows $R(T)$, normalized to the bare (unmodulated) dephasing rate, as a function of the energy constraint. As expected, the more energy is available for modulation, the lower is the dephasing rate. For low energies, the optimal modulation significantly outperforms DD, while at higher energies this difference disappears. These results can be understood from Figure 7(a), by noticing that the two central DD peaks have significant overlap with $G(\omega)$ at the low energy value shown. As E is increased at fixed T, the DD peaks move farther apart and have less overlap with $G(\omega)$, leading to improved performance. Applying the linearized EL equation with DD as initial guess yields only mild improvements (not shown). The explanation for the superior performance of the optimal modulation is also evident from Figure 7(a): since higher frequencies have lower coupling strength in this case, the optimal control "reshapes" so as to maximize its weight in the high-frequency range, to the extent permitted by the energy constraint. The modulation can be well approximated by $\Omega(t) = a[1 + e^{-t/T}(t/T - 1)]$, where a is determined by the energy constraint, which fits the results in Figure 6(a).

(b) Single-Peak Off-Resonant Dephasing Spectrum. This dephasing spectrum describes a variation on the aforementioned scenario, where the spectral peak is shifted ($\Delta \neq 0$ in $\Phi(t) = \widetilde{\Phi}(t)e^{i\Delta t}$), for example, coupling to a nonresonant bath. With no other constraints, the optimal modulation is trivially similar to the one of the resonant spectrum, with a shifted energy-constraint $E^{\text{non-res}} = E^{\text{res}} + \Delta$. To demonstrate how this formalism can accommodate additional constraints, we impose a positivity constraint, $\dot{\phi}(t) \geq 0$ (positive field amplitude) and obtain nontrivial behavior of $R(T)$ as a function of the energy constraint—see Figure 6(b). Here we used the linearized EL equation with the DD modulation (153) as an initial guess. For both the DD and optimal modulations, we observe an initial *increase* in the dephasing rate as a function of energy, followed by a decrease. For DD, this can be interpreted as a manifestation of the initial anti-Zeno effect and the subsequent quantum Zeno effect [100, 165]. Because of the positivity constraint, modulations with low energy (both DD and optimal) couple to more resonant modes of the bath (Figure 7(b)) and thus do worse than the unmodulated case. The DD modulation is optimal for small energy constraints, and hence the decoherence rates of DD and our optimal solution coincide. This is because the DD peaks do not overlap with the off-resonant spectral peak. However, as the positive-frequency main DD peak (Figure 7(b)) nears the off-resonant spectral peak, with increased energy, the optimal modulation diverges from the DD modulation and "reshapes" itself so as to couple to higher modes of the bath. In the time domain (Figure 6(b) inset), this is seen as a smoothing of the abrupt DD modulation. At even higher energy constraints, there is once more no improvement by the optimal modulation over DD, yet there is an improvement over the unmodulated case. Over the entire range of E, the optimal modulation results in a much flatter $R(T)$ than DD, which is an indicator of its robustness. While DD is strongly influenced by the off-resonant peak, the optimal modulation exploits the energy available to find the minimal overlap with the dephasing spectrum.

(c) $1/f$ Dephasing Spectrum. The ubiquitous $1/f$ dephasing spectrum that describes a variety of experiments—for example, charge noise in superconducting qubits [166]—is given in our notation by $G(\omega) \propto 1/\omega$, with cutoffs $\omega_{\min}$ and $\omega_{\max}$. Figure 6(c) shows that, as expected, the more the energy available for modulation, the lower the dephasing rate. Notice that due to the cut-off $\omega_{\min}$, a low-energy modulation does worse than the unmodulated case. Furthermore, since, as in case (a), higher frequencies now have lower coupling strength, the optimal control "reshapes" so as to have as high a weight in the high frequency range as the energy constraint allows (Figure 7(c)). This is expressed in the time domain (Figure 6(c) inset) as the initial increase in the modulation strength ($t < 50$). The later decrease in modulation strength can be attributed to the lower cutoff, where the optimal modulation benefits from lower frequencies, that is, lower modulation amplitudes. Upon comparing the $1/f$ case to the Lorentzian spectrum, Figure 6(a), we observe a similar optimal initial chirped modulation in the time domain.

Despite the differences in the long-time behavior (due to the lower cutoff in the $1/f$ case), these two examples allow us to generalize to any dephasing spectrum with a monotonically decreasing system-bath coupling strength as a function of frequency. The optimal modulation for such spectra will be an energy-constrained chirped modulation, with modifications due to other spectral characteristics, for example, cutoffs.

(d) Multipeaked Dephasing Spectrum. This describes the most general scenario, where there can be several resonances and noise correlation times. Figure 6(d) shows $R(T)$ as a function of the energy constraint. Once again, because DD does not account for the dephasing spectrum, its performance is much worse than our (universal-formula) optimal modulation, whose "reshaping" results in monotonically improving performance: the peaks of our optimal modulation are predominantly anticorrelated with the peaks of $G(\omega)$.

8. Multipartite Decoherence Control and Quantum Computing

Multipartite decoherence control, for many qubits coupled to thermal baths, is a much more challenging task than single-qubit control since (i) entanglement between the qubits is typically more vulnerable and more rapidly destroyed by the environment than single qubit coherence [73, 74, 108–113] (ii) the possibility of cross decoherence, whereby qubits are coupled to each other through the baths, considerably complicates the control. We have analyzed this situation and extended [107, 123] the decoherence control approach to multipartite scenarios, where the qubits are either coupled to zero- or finite-temperature baths.

Although our strategy applies in general to any number of excitations, simple closed-form solutions are obtainable

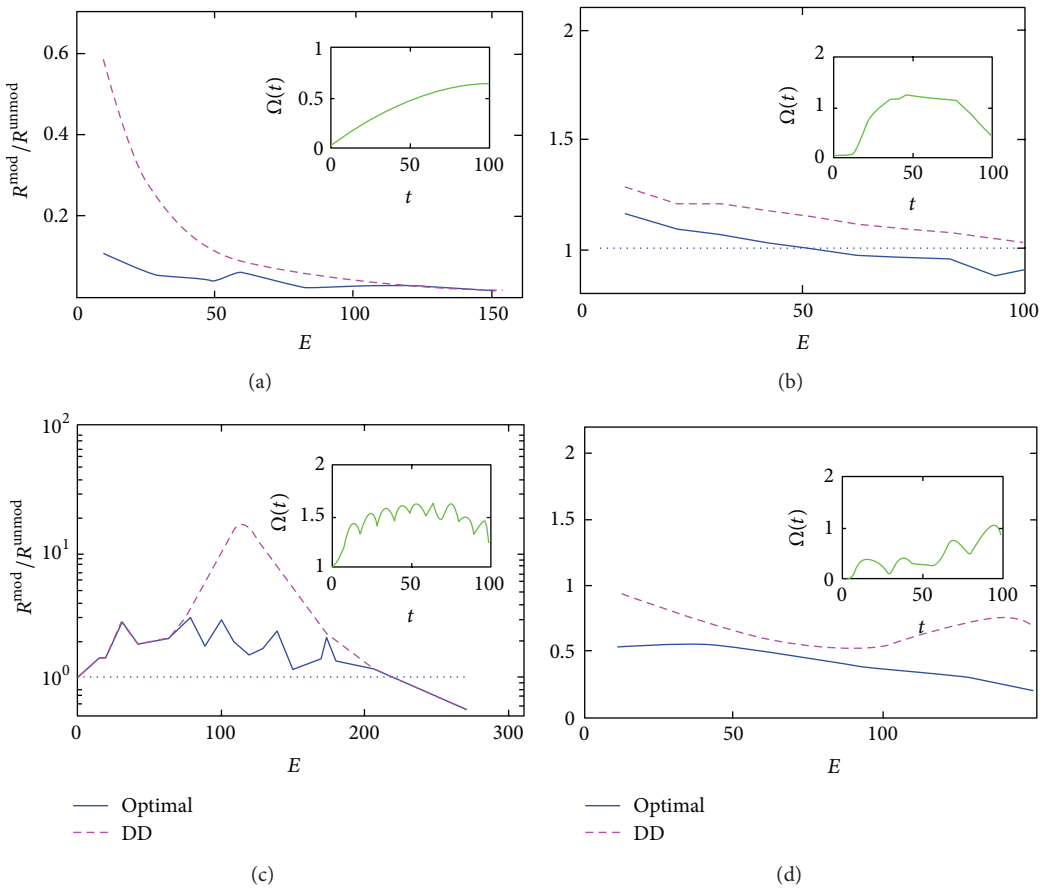

FIGURE 6: Average modified final decoherence rate $R(T)$, normalized with respect to the unmodulated rate, as a function of energy constraint. DD—dash, magenta. Optimal modulation—solid, blue. Insets: optimal modulation $\Omega(t)$ for different energy constraints. (a) Single-peak resonant dephasing spectrum (inset: $E = 20$). (b) Single-peak off-resonant spectrum (inset: $E = 50$). (c) $1/f$ spectrum (inset: $E = 30$). (d) Multipeaked spectrum (inset: $E = 30$).

for a *single* initial excitation of the system. Accordingly, the complete wave function is

$$|\Psi(t)\rangle = \sum_k \tilde{\alpha}_0^k(t)\,|k\rangle \bigotimes_{j=1}^{N} |g\rangle_j + \sum_{j=1}^{N}\sum_{n=1}^{M_j} \tilde{\alpha}_{j,n}(t)\,|n\rangle_j\,|\text{vac}\rangle \bigotimes_{j'\neq j} |g\rangle_{j'}. \tag{154}$$

We will denote the first and second RHS terms in (154) as the bath and system wave function, $|\Psi^B(t)\rangle$ and $|\Psi^S(t)\rangle$, respectively. In order to solve the Schrödinger equation, we shall follow the same procedure used for a single qubit in Section 3 (see (9)–(13)).

In order to analyze the time evolution of the wave function, written as a column vector $\alpha(t) = \{\alpha_{j,n}(t)\}$, it is expedient to express it in the interaction picture

$$\alpha_{j,n}(t) = e^{i\omega_{j,n}t + i\int_0^t d\tau\delta_{j,n}(\tau)}\tilde{\alpha}_n(t). \tag{155}$$

The Schrödinger equation for the coupled $\{\alpha_{j,n}(t)\}$ and $\{\alpha_0^k(t)\}$ amplitudes in (154) may be reduced, upon eliminating the $\{\alpha_0^k(t)\}$ amplitudes and transforming to the interaction picture, to the following exact integrodifferential equation:

$$\dot{\alpha}_{j,n}(t) = \int_0^t dt' \sum_{j',n'} \Phi_{jj',nn'}(t-t')\,\epsilon_{j,n}(t)\,\epsilon^*_{j',n'}(t') \times e^{i\omega_{j,n}t - i\omega_{j',n'}t'}\alpha_{j',n'}(t'). \tag{156}$$

Here $\Phi(t)$ is the reservoir-response matrix, given by

$$\Phi_{jj',nn'}(t) = \hbar^{-2}\sum_k \mu_{k,j,n}\mu^*_{k,j',n'}e^{-i\omega_k t}, \qquad \epsilon_{j,n}(t) = \tilde{\epsilon}_{j,n}(t)\,e^{i\int_0^t d\tau\delta_{j,n}(\tau)} \tag{157}$$

which accounts for both the modulation and the Stark shift.

Assuming that the amplitudes are slowly varying on the time scale of the bath response [99] and using the matrix representation, this equation has the general solution

$$\alpha(t) = T_+ e^{-tR(t)}\alpha(0), \tag{158}$$

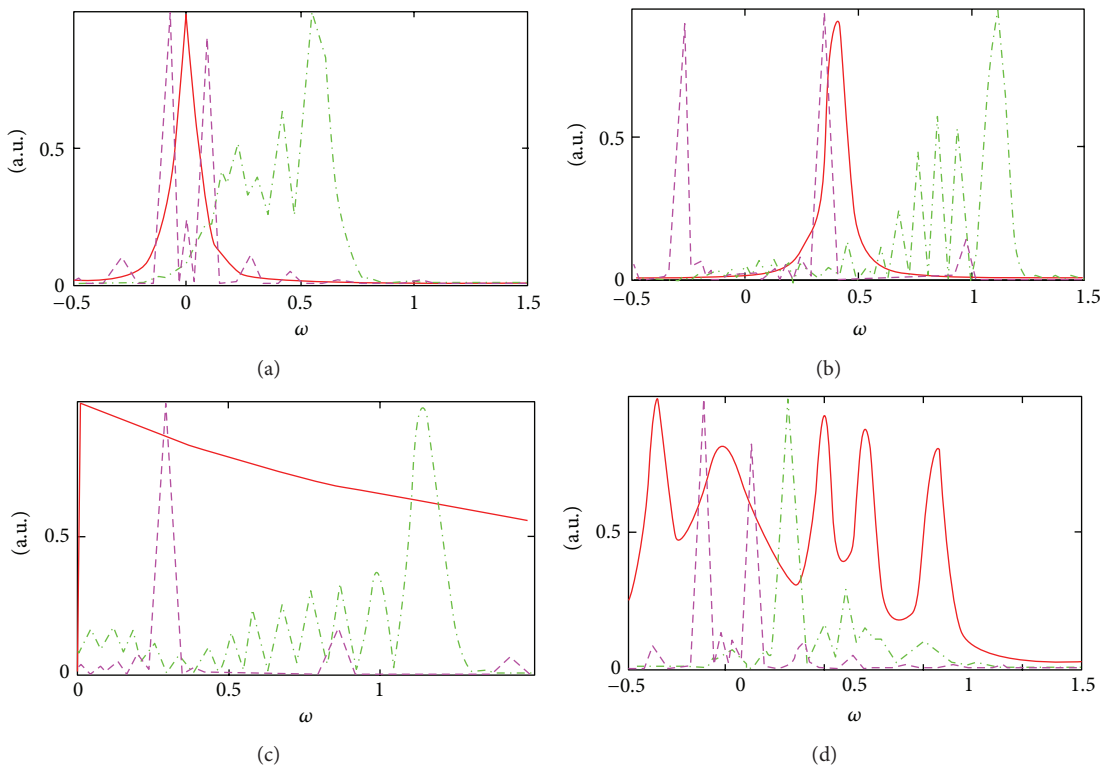

FIGURE 7: Dephasing spectrum $G(\omega)$ (solid, red), optimal (dot-dash, green), and DD (dash, magenta) modulation spectra $F_T(\omega)$, in arbitrary units (a.u.). Same parameters as in the insets of Figure 6.

where T_+ is the time-ordering operator and $R(t) = \{R_{jj',nn'}(t)\}$ is the dynamically modified decoherence matrix, determined by the following convolution (see (23)–(27)):

$$R_{jj',nn'}(t) = 2\pi \int_{-\infty}^{\infty} d\omega G_{jj',nn'}(\omega) F_{t,jj',nn'}(\omega), \quad (159)$$

$$G_{jj',nn'}(\omega) = \pi^{-1} \int_0^{\infty} dt \Phi_{jj',nn'}(t) e^{i\omega t}, \quad (160)$$

$$F_{t,jj',n''}(\omega) = \frac{\epsilon_{t,j,n}(\omega - \omega_{j,n}) \epsilon^*_{t,j',n'}(\omega - \omega_{j'n'})}{t}, \quad (161)$$

$$\epsilon_{t,j,n}(\omega) = \int_0^t d\tau \epsilon_{j,n}(\tau) e^{i\omega\tau}. \quad (162)$$

Here $G_{jj',nn'}(\omega)$ is the coupling spectrum matrix given by the environment and $F_{t,jj',nn'}(\omega)$ is the dynamical modulation matrix, which we design at will to suppress the decoherence. This general solution holds *for dynamically modified relaxation of singly excited multipartite entangled states into a zero-temperature bath.*

It is important to note that both the coupling spectrum matrix, $G_{jj',nn'}(\omega)$, and the dynamical modulation matrix, $F_{t,jj',nn'}(\omega)$, are *complex* and not real, as in the single-qubit scenario. This occurs because, opposed to the single-qubit scenario, the modulation matrix off-diagonal term may be complex due to phase-relations between different modulations of the relevant particles. Hence, one cannot separate the real and imaginary parts of the coupling spectrum matrix and obtain a real decoherence matrix. Nevertheless, the diagonal elements of the decoherence matrix are easily separable to real decay rates, similar to (26), and imaginary Lamb shifts.

In the following, we shall use as illustration an impulsive phase modulation, that is, a sequence of pulsed Stark shifts caused by fields whose amplitudes satisfy [99]

$$\epsilon_{j,n}(t) = e^{i[t/\tau_{j,n}]\theta_{j,n}}, \quad (163)$$

$$\epsilon_{t,j,n}(\omega) = \frac{\left(e^{i\omega\tau_{j,n}} - 1\right)\left(e^{i(\theta_{j,n}+\omega\tau_{j,n})[t/\tau_{j,n}]} - 1\right)}{i\omega\left(e^{i(\theta_{j,n}+\omega\tau_{j,n})} - 1\right)}. \quad (164)$$

Here $[\cdots]$ denotes the integer part, and $\tau_{j,n}$ and $\theta_{j,n}$ are the pulse duration and the phase change for level n of particle j, respectively. In the limit of weak pulses, of area $|\theta_{j,n}| \ll \pi$, (164) yields $\epsilon_{t,j,n}(\omega) \cong \epsilon_{t,j,n}\delta(\omega - \Delta_{j,n})$, where $\Delta_{j,n} = \theta_{j,n}/\tau_{j,n}$ is the effective spectral shift caused by the applied pulses.

It is expedient to rewrite the fidelity of the evolving system, $f(t) = |\langle\Psi^S(0)|\Psi^S(t)\rangle|^2$, as a product of two factors

$$f(t) = f_p(t) f_c(t),$$

$$f_p(t) = |A(t)|^2 = \sum_{j=1}^{N} \sum_{n=1}^{M_j} \left|\alpha_{j,n}(t)\right|^2, \quad (165)$$

$$f_c(t) = \frac{\left|\sum_{j=1}^{N} \sum_{n=1}^{M_j} \alpha^*_{j,n}(0) \alpha_{j,n}(t)\right|^2}{|A(t)|^2},$$

where $f_c(t)$ is the autocorrelation function, $|\langle\Psi^S(0)|\Psi^S(t)\rangle|^2$, normalized by the total excitation probability $|A(t)|^2$. Thus $1 - f_p(t)$ measures population loss from any $|n\rangle_j$, whereas $1 - f_c(t)$ is a measure of correlation preservation: $f_c = 1$ when the initial multipartite correlations are completely preserved. As shown below, population and correlation preservation can be *independently controlled* in the model of (154).

In the absence of dynamical control, $f_c(t)$ decays much faster than $f_p(t)$ and is much more sensitive to the asymmetry between local particle-bath couplings. Thus, for initial Bell singlet and triplet states, $|\Psi(0)\rangle = 1/\sqrt{2}(|g\rangle_A|n\rangle_B \pm |n\rangle_a|g\rangle_B)$, which do not experience cross decoherence but only different local decoherence rates, $\alpha_{A(B)}(t) = 1/\sqrt{2}e^{-tR_{A(B)}}(t)$. We find $f_p(t) = (e^{-2tR_A(t)} + e^{-2tR_B(t)})/2$; $f_c(t) = (1 + C(t))/2 = 1/2 + e^{-t\Delta R(t)}/(1 + e^{-2t\Delta R(t)})$, where $\Delta R(t) = R_A(t) - R_B(t)$ and $C(t)$ is the concurrence [167].

We shall first deal with N identical qubits and thus ignore the n subscript, that is, set $\omega_j \equiv \omega_0$. We also require that at any chosen time $t = T$, the AC Stark shifts in (158) satisfy $\int_0^T d\tau\delta_j(\tau) = 2\pi m$, where $m = 0, \pm 1, \ldots$. This requirement ensures that modulations only affect the decoherence matrix (159) but do not change the relative phases of the entangled qubits when their states are probed or manipulated by logic operations at $t = T$.

Without any modulations, decoherence in this scenario has no inherent symmetry. Our point is that one can *symmetrize the decoherence* by appropriate modulations. The key is that different, "local," phase-locked modulations applied to the individual particles, according to (161), can be chosen to cause *controlled interference* and/or spectral shifts between the particles' couplings to the bath. The $F_{t,jj'}(\omega)$ matrices (cf. (161)) can then satisfy $2N$ requirements at all times and be tailored to impose the advantageous symmetries described below. By contrast, a "global" (identical) modulation, characterized by $F_{t,jj'}(\omega) = |\epsilon_t(\omega)|^2$, is not guaranteed to satisfy $N \gg 1$ symmetrizing requirements at all times (Figure 9(a)).

The most desirable symmetry is that of *identical coupled particles* (ICP), which would emerge if all the modulated particles could acquire the *same* dynamically modified decoherence and cross decoherence yielding the following $N \times N$ fully symmetrized decoherence matrix

$$R_{jj'}^{\mathrm{ICP}}(t) = R(t) \quad \forall j, j'. \tag{166}$$

ICP would then give rise to a $(N - 1)$-dimensional decoherence-free subspace (DFS), the entire single-excitation sector except the totally symmetric entangled state. An initial state in this DFS [115] would have $f(t) = 1$ for all times, meaning that it would neither lose its population nor its initial correlations (or entanglement).

However, it is generally impossible to ensure this symmetry, since it amounts to satisfying $N(N-1)/2$ conditions using N modulating fields. Even if we accidently succeed with N particles, the success is not scalable to $N+1$ or more particles. Moreover, the ability to impose the ICP symmetry by local modulation fails completely if not all particles are coupled to all other particles through the bath, that is, if some $G_{jj'}(\omega)$ elements vanish.

A more limited symmetry that we may *ensure* for N qubits is that of *independent identical particles* (IIP). This symmetry is formed when spectral shifts and/or interferences imposed by N modulations cause the N different particles to acquire the *same* single-particle decoherence $r(t)$ and experience no cross decoherence. To this end, we may choose in (163) $\epsilon_{t,j}(\omega) \simeq \epsilon_{t,j}\delta(\omega - \Delta_j)$. The spectral shifts Δ_j can be different enough to couple each particle to a different spectral range of bath modes so that their cross coupling vanishes as

$$\begin{aligned} &R_{jj'}(t) \\ &\quad = \epsilon_{t,j}^{*}\epsilon_{t,j'} \int d\omega G(\omega)\, \delta\left(\omega - \Delta_j\right)\delta\left(\omega - \Delta_{j'}\right) \\ &\quad \longrightarrow 0. \end{aligned} \tag{167}$$

Here, the vanishing of $G_{jj'}(\omega)$ for some j, j' is not a limitation. The N single-particle decoherence rates can be equated by an appropriate choice of N parameters $\{\Delta_j\}$ as (Figure 8)

$$R_{jj'}^{\mathrm{IIP}}(t) = \left|\epsilon_{t,j}\right|^2 G_{jj}\left(\Delta_j\right) = \delta_{jj'}R(t), \tag{168}$$

where $\delta_{jj'}$ is Kronecker's delta (Figure 9(b)). The IIP symmetry results in complete correlation preservation, that is $f_c(t) = 1$, but still permits population loss, $f(t) = f_p(t) = e^{-2\,\mathrm{Re}\,r(t)}$. If the single-particle $r(t)$ may be dynamically suppressed, that is, if the spectrally shifted bath response $G_{jj}(\omega_j + \Delta_j)$ is small enough, this $f(t)$ will be kept close to 1 (Figure 10).

If IIP symmetry is imposed, the particles become effectively independent in terms of their coupling to the bath. Hence, collective coupling to the bath, which is a prerequisite for a DFS, *is not formed* in this case. In order to impose decoherence-free conditions, we extend the treatment to *multilevel* particles. We will show that the use of auxiliary levels and local modulations can *result in a decoherence-free singly excited N qubit* system, in a general and realistic coupling scenario.

To this end, we invoke three-level particles with excited states $|1\rangle$ and $|2\rangle$. In a single three-level particle, an external field can impose an intraparticle DFS if $|1\rangle$ and $|2\rangle$ decay at the same rate to the ground state $|0\rangle$; this DFS consists of $|0\rangle$ and the "dark" or trapping state [78], the antisymmetric superposition of the two excited states $1/\sqrt{2}(|1\rangle - |2\rangle)$. However, this intraparticle DFS would *be destroyed* in a system of N three-level particles that are coupled to the bath and/or experience cross decoherence. In order to remedy this problem, let us consider local modulations acting differently on the two excited levels within each particle. Such modulations can be tailored to impose what may be dubbed *"independent identical trapping"* (IIT) symmetry. This means that all particles acquire identical trapping states and become (effectively) independent, *without cross decoherence*. As discussed above, N spectral shifts Δ_j determined by $|\epsilon_{t,j}(\omega)|^2$ suffice to eliminate cross decoherence, (167). Under these conditions, N destructively interfering pairs of local fields will cause trapping in each particle (Figure 9(c)). This would result in an N-dimensional DFS, composed of N particles sharing single excitation with anti symmetrically superposed

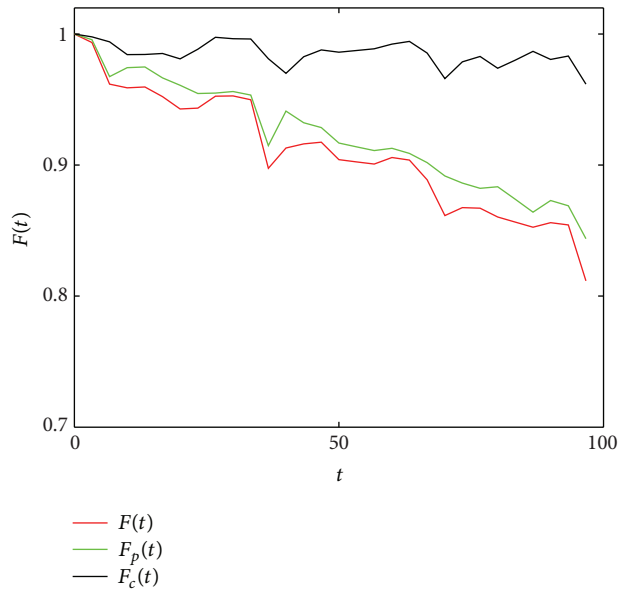

FIGURE 8: Fidelity of the IIP symmetry for two TLS coupled to zero-temperature baths. The initial state is entangled, $|\psi(0)\rangle = 1/\sqrt{2}(|g\rangle_A|e\rangle_B + |e\rangle_A|g\rangle_B)$.

excited states. Under the IIT symmetry, the decoherence matrix is block diagonal, each block corresponding to particle j with levels n, n' as

$$R^{\mathrm{IIT}}_{jj',nn'}(t) = \delta_{jj'} R_j(t). \tag{169}$$

Both disentanglement and population loss are nearly completely eliminated within the multipartite subspace, resulting in $F(t)$ very close to 1 (Figure 10).

As an example, the IIT recipe will be analyzed for two three-level particles, where each level of each particle experiences different coupling to the bath, and cross decoherence exists. Let us take the initial state of particles A, B to be $|\Psi_S(0)\rangle = (|-\rangle_A|0\rangle_B \pm |0\rangle_A|-\rangle_B)/\sqrt{2}$, where $(j = A, B)\ |-\rangle_j = (|1\rangle_j - |2\rangle_j)/\sqrt{2}$. The goal will be to keep this state intact, $|\Psi_S(t)\rangle \simeq |\Psi_S(0)\rangle$, by preventing cross decoherence and imposing intraparticle destructive interference. The bath response matrix will be taken to be $\Phi_{jj',nn'}(t) = \gamma d_n d_{n'}(e^{-t^2/4t^2_{j,n}} e^{-t^2/4t^2_{j',n'}}/k_0(r_{\min} + r_{jj'}))$ where γ is the single-particle unperturbed decay rate (satisfying Fermi's Golden Rule [78]), $d_n = \cos\eta_n$, with η_n being the angle of transition dipole, $t_{j,n}$ is the correlation time of level n of particle j, k_0 is the wavevector of the resonant transition $|0\rangle \leftrightarrow |1(2)\rangle$, and $r_{\min}$ is the distance below which the particles are identically coupled to the bath and $r_{jj'} = |r_j - r_{j'}|$, where r_j is the position of particle j. This model may describe the *distance-dependent cross-decoherence* of either radiatively or vibrationally relaxing atoms or ions at different sites in a trap, lattice or cavity [133, 168]. The parameters of the pulse sequence in (163) for creating the IIP or IIT symmetries were chosen such that the faster decaying particle experienced the stronger and/or faster pulses; that is, $\theta_{j,n}/\tau_{j,n}$ were adapted to the bath response parameters $\Phi_{jj,nn}$ of each particle. The pulse sequences were chosen to be different enough for each particle in order to eliminate the desired cross-decoherence terms, as per (167). Individual pulses were selected to obey the other IIP or IIT requirements described above. The very high fidelity achievable by IIT is seen in Figure 10.

8.1. Bipartite Entanglement and Decoherence Control. We shall henceforth analyze the case of bipartite systems, $N = 2$, and quantify entanglement by the often-used measure of concurrence C [167], given by

$$C(t) = \max\left\{0, \sqrt{\lambda_1} - \sqrt{\lambda_2} - \sqrt{\lambda_3} - \sqrt{\lambda_4}\right\}, \tag{170}$$

where λ_i are the positive eigenvalues, in decreasing order, of the matrix $\rho(\sigma_y \otimes \sigma_y)\rho^*(\sigma_y \otimes \sigma_y)$ where σ_y is the Y-Pauli matrix and the conjugation occurs in the computational basis $\{|gg\rangle, |ge\rangle, |eg\rangle, |ee\rangle\}$.

In order to explore the effects of dynamical modulations on the concurrence, we first define the following decoherence rate parameters.

(i) *Decoherence rate magnitude* is defined by $\nu_{e(g)}(t) = \sum_{j=1,2} |R^{e(g)}_{jj}(t)|$, where for the case of $\nu_{e(g)}(t) = 0$, we have no decoherence, with complete preservation of information and entanglement.

(ii) *Decoherence rate asymmetry* is defined as $\zeta(t) = |R^e_{11}(t) - R^e_{22}(t)|/\nu_e(t)$, where $\zeta(t) = 0$ is the fully symmetric case, and $\zeta(t) > 0$ measures the asymmetry. The decoherence rate asymmetry expresses the difference between the two systems with respect to the modulated coupling to the bath. Thus, protecting one system and neglecting the other can increase the asymmetry while preserving the decoherence rate magnitude.

(iii) *Cross decoherence* is defined as $\mu(t) = |R^e_{12}(t) + R^e_{21}(t)|/\nu_e(t)$, where $\mu(t) = 1$ denotes maximal cross-decoherence, and $\mu(t) = 0$ denotes completely separable, uncorrelated systems. The cross-decoherence expresses the "cross talk" between the two systems via the bath modes.

(iv) *Decoherence rate effective temperature* is defined as $\alpha(t) = 1/\ln(\nu_e(t)/\nu_g(t))$, where for unmodulated memoryless Markovian identical baths $\alpha = k_B T/\hbar\omega_a$.

What are the effects of dynamical control on the decoherence rate parameters? The decoherence rate magnitude, being the sum of all individual qubit decoherence rates, is best reduced by control schemes similar to those of single-qubit decoherence control, that is, reducing the overlap of the system-bath coupling and modulation spectra [80, 81, 84, 97]. The decoherence rate asymmetry, on the other hand, is best controlled by differently modulating the two TLS. One can increase the asymmetry by accelerating the decoherence of one qubit and reducing the other's [85, 97, 99, 121, 153], or decreasing it by equating the individual-qubit spectral overlap of the bath-coupling and modulation spectra.

Cross decoherence can be easily eliminated by choosing the appropriate modulations for each qubit. Thus, choosing

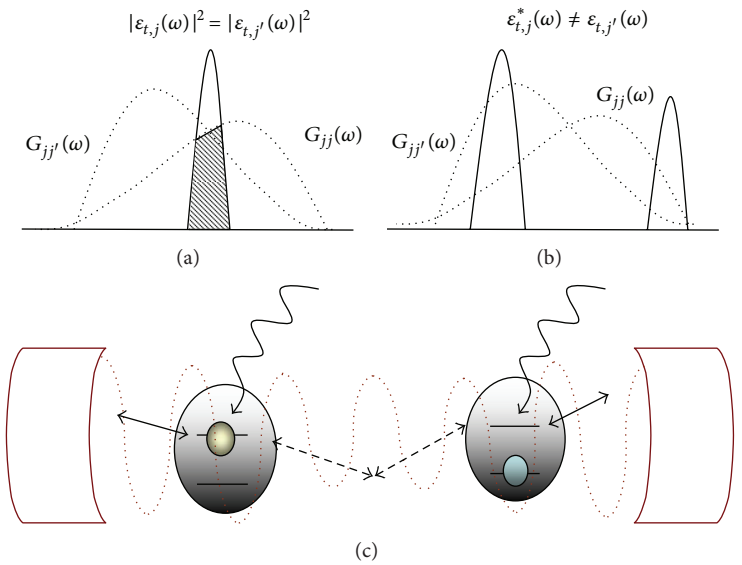

FIGURE 9: Two two-level particles in a cavity, coupled to the cavity modes (thin lines) and subject to local control fields (thick lines). ((a), (b)) Frequency domain overlap of coupling spectrum (dotted) and modulation matrix elements (solid), resulting in modified decoherence matrix elements (shaded), for (a) Global modulation (ICP symmetry) and (b) Cross-decoherence elimination (IIP symmetry). (c) General modulation scheme.

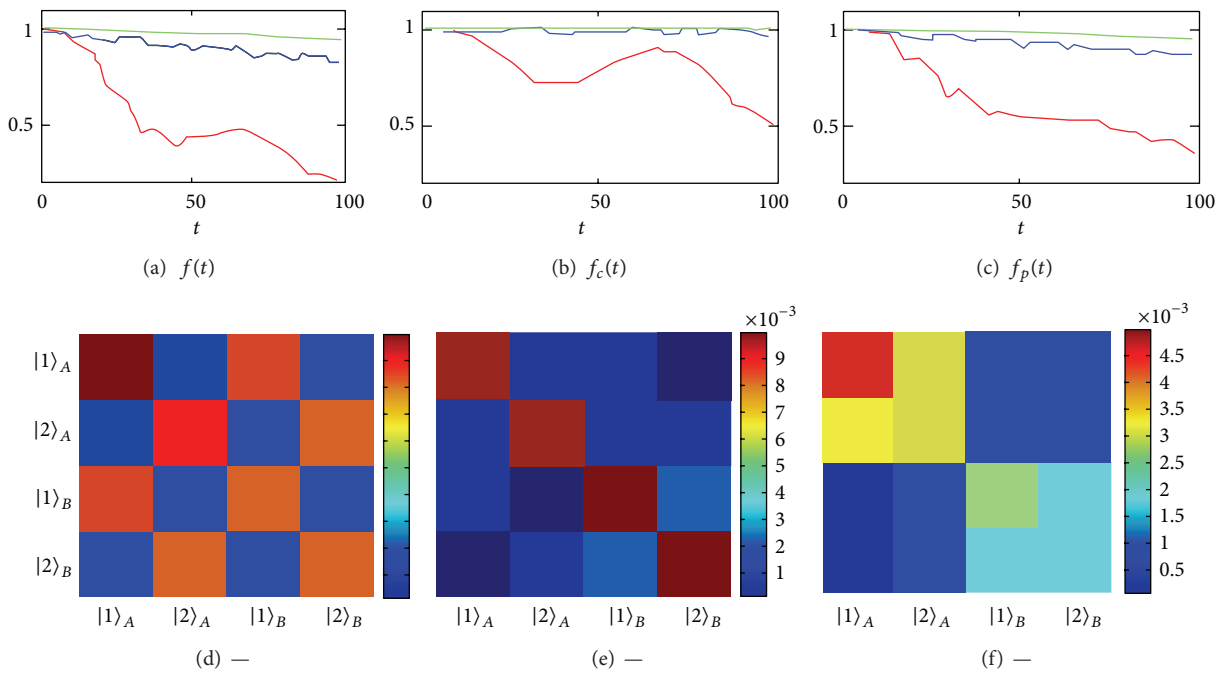

FIGURE 10: Fidelity as a function of time (in units of $(10\gamma)^{-1}$): (a) Overall fidelity, (b) Correlation preservation, and (c) Population preservation. ((d)–(f)) Decoherence matrix elements at time $t = 100$. (d) Global π-phase flips impose no symmetry (red) ($\tau_{j,n} = 1.1, \theta_{j,n}/\pi = 1.0$). (e) Independent identical particles (IIP) symmetry (blue) ($\tau_{j,n} = (0.75, 0.85, 0.95, 1.05), \theta_{j,n}/\pi = (0.834, 0.806, 0.836, 0.82)$); (f) Independent identical trapping (IIT) symmetry (green) ($\tau_{j,n} = (0.85, 0.85, 1.05, 1.05), \theta_{j,n}/\pi = (0.924, 0.9, 0.945, 0.91)$). The parameters are $\omega_1 = 0.5, \omega_2 = 0.6, \gamma = 0.1, k_0 r_{\min} = 1.0, t_{j,n} = (0.7, 1.0, 1.06, 1.1), r_j = (0.0, 0.1)$, and $\eta_n/\pi = (0.0, 0.1)$.

for each qubit such modulations that they are effectively coupled to different bath modes can completely eliminate cross decoherence [123].

The effective temperature cannot be independently controlled, as it is mainly governed by the bath temperature. However, ultrafast modulations can have very high spectral components, such that $\omega_{j,k} + \omega_a < 0$, and can influence the ratio of upward (R^g_{jj}) and downward (R^e_{jj}) transitions. Only the absence of the rotating-wave approximation in our analysis has allowed the elucidation of this effect, as "negative" frequencies are made accessible by modulations.

8.1.1. Disentanglement and Its Resuscitation. Next, we analyze the disentanglement of initial fully entangled bipartite states, that is, the Bell-states, $|\Phi_\pm\rangle = 1/\sqrt{2}(|e\rangle_1\,|e\rangle_2 \pm |g\rangle_1|g\rangle_2)$, $|\Psi_\pm\rangle = 1/\sqrt{2}(|e\rangle_1|g\rangle_2 \pm |g\rangle_1|e\rangle_2)$. The long-time limit concurrences of the Bell states for zero effective temperature are found to be

$$C\left(|\Phi_\pm\rangle\right)_{\mu=0} = e^{-t\nu}\left(1 - \sqrt{\left(1 - e^{-t\nu(1-\zeta)}\right)\left(1 - e^{-t\nu(1+\zeta)}\right)}\right), \qquad (171)$$

$$C\left(|\Psi_\pm\rangle\right)_{\zeta=0} = e^{-t\nu(1\pm\mu)}.$$

This demonstrates that an initial (pure) Bell state's entanglement decays exponentially for zero-temperature baths but does not vanish in finite time (the general case for $\mu, \zeta \neq 0$ is analytically solvable, but too cumbersome to be presented here). Conversely, coupling the two qubits to finite-temperature baths does result in entanglement sudden death [109, 112], that is, the concurrence vanishes in finite time, which we shall dub time of death (TOD), t^{TOD}.

Figure 11 presents the TOD of an initial Bell state as a function of effective temperature and either decoherence asymmetry (Figure 11(a)) or cross decoherence (Figure 11(b)). Equation (171) and Figure 11 imply that the TOD can be postponed by applying modulations that (i) reduce the decoherence magnitude, (ii) increase the asymmetry for $|\Phi_\pm\rangle$, (iii) reduce (increase) the cross decoherence for $|\Psi_+\rangle$ ($|\Psi_-\rangle$), or, (iv) decrease the effective temperature. While the reduction of effective temperature is a formidable challenge, asymmetry and cross decoherence are better controlled via modulations. Thus, for an initial $|\Phi_+\rangle$, increasing the decoherence asymmetry of an otherwise symmetric system guarantees the same prolonged time of death as that of a colder environment (Figure 11(a) inset).

This Bell state disentanglement analysis results in recipes for optimal control schemes of quantum information protocols, for example, quantum teleportation. We have shown that the singlet is always optimal, but it is not always experimentally accessible. For such a case, one should use the $|\Phi_\pm\rangle$ states and dynamically modulate each qubit so as to eliminate the cross decoherence if present [71] and maximize the decoherence asymmetry, thus achieving maximal entanglement preservation.

Moving from the long-time limit analysis, the analysis reveals that the *time-dependent* decoherence rates may exhibit oscillations that can be controlled via the *local modulations* applied on the individual qubits. These controlled oscillations and their effects on the partial resuscitation of entanglement are the main results of this section. We show that one can control the frequency as well as the magnitude of oscillations by choosing the appropriate modulations and thus resuscitate entanglement at specific desired times.

To demonstrate these effects, we shall investigate two distinct situations: (a) distant systems coupled to separate baths ($\Phi_{T,jj'}(t) = 0,\ j \neq j'$), whereby an initially entangled state is locally controlled and does not experience any cross decoherence (Figure 12(a)) and (b) adjacent systems coupled to the same bath, whereby local modulations may control the time dependent qubits' cross decoherence (Figure 12(c)).

Distant systems were extensively studied under various conditions [74, 108, 109, 112, 169, 170]. Here, we generalize these results under the universal dynamical control of decoherence approach and present new control schemes that facilitate entanglement sudden death and its controlled partial resuscitation (ESD-CPR).

Both the decoherence rate magnitude and asymmetry exhibit controlled oscillations on non-Markovian time scales (Figure 12(b) inset). This can be best observed by considering the most general quasistationary form of modulation, that is, quasi-periodic modulation, $\epsilon^+_j(t) = \sum_k \epsilon_{j,k} e^{-i\omega_{j,k}t}$, where $\omega_{j,k}$ are arbitrary discrete frequencies with minimal spectral distance $\Omega = \min(\omega_{j,k} - \omega_{j',k'})$ for all $j \neq j', k \neq k'$. In this case, the modulation spectrum, $F_{t,jj}(\omega)$, is a sum of terms peaked at $\omega = \omega_{j,k}$ that oscillate on non-Markovian time-scales [100, 105].

Thus, local modulations can control not only the magnitude of disentanglement but also its period of oscillation, which may give rise to entanglement sudden death controlled partial resuscitation (ESD-CPR). To demonstrate this, we use the Werner states as the initial partially entangled states, given by $\rho(0) = (1/3)(2\,|\Psi_+\rangle\langle\Psi_+| + (1 - a)|gg\rangle\langle gg| + a|ee\rangle\,\langle ee|)$, where $0 \leq a \leq 1$ [74, 113]. We numerically solve the modified Bloch equations for non-Markovian short time scales, and local (individual-qubit) impulsive-phase modulation, $\epsilon_j(t) = e^{\phi_j[t/\tau_j]}$, where $[\cdots]$ is the integer-part. We consider finite-temperature baths, with a Lorentzian bath-coupling spectra $G_{0,jj}(\omega) = \gamma_j(\Gamma_j^2/(\Gamma_j^2 + (\omega - \omega_0)^2))$, where γ_j is the coupling strength of TLS j to the bath, ω_0 is the center of the Lorentzian, $\Gamma_j = 1/t_{c_j}$, and $G_{0,jj'}(\omega) = 0$. Here $\gamma_j = \gamma$ and $\Gamma_j = \Gamma$ are taken to be equal for the two TLS, thus having no asymmetry for the unmodulated scenario ($\zeta(t) = 0$).

While the modulation can greatly decrease the decoherence rate magnitude, and thus maintain entanglement for longer durations, we have already shown that its effect is similar to that of the single-qubit decoherence case and is of less interest here. Hence, we present renormalized results such that the long-time limit of $\nu(t)$ is equal for all scenarios to that of the unmodulated case (Figure 12(b) inset). This is achieved by effectively changing the coupling strength γ for each scenario.

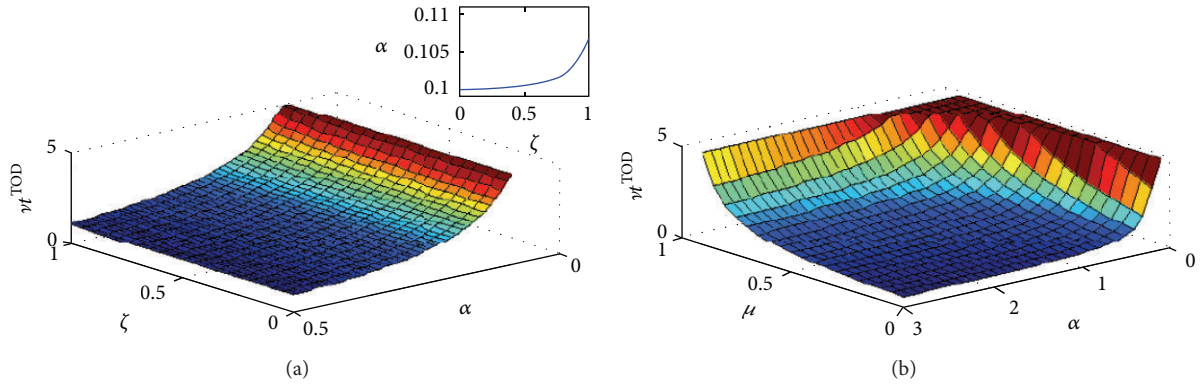

FIGURE 11: Time of death (TOD) as a function of decoherence rate parameters. (a) TOD of an initial $|\Phi_+\rangle$ as a function of effective temperature (α) and decoherence rate asymmetry (ζ), $\mu = 0$. Inset: effective temperature resulting in $\nu t^{\mathrm{TOD}} = 4.6$ as a function of asymmetry. (b) TOD of an initial $|\Psi\_\rangle$ as a function of effective temperature (α) and cross-decoherence (μ), $\zeta = 0$.

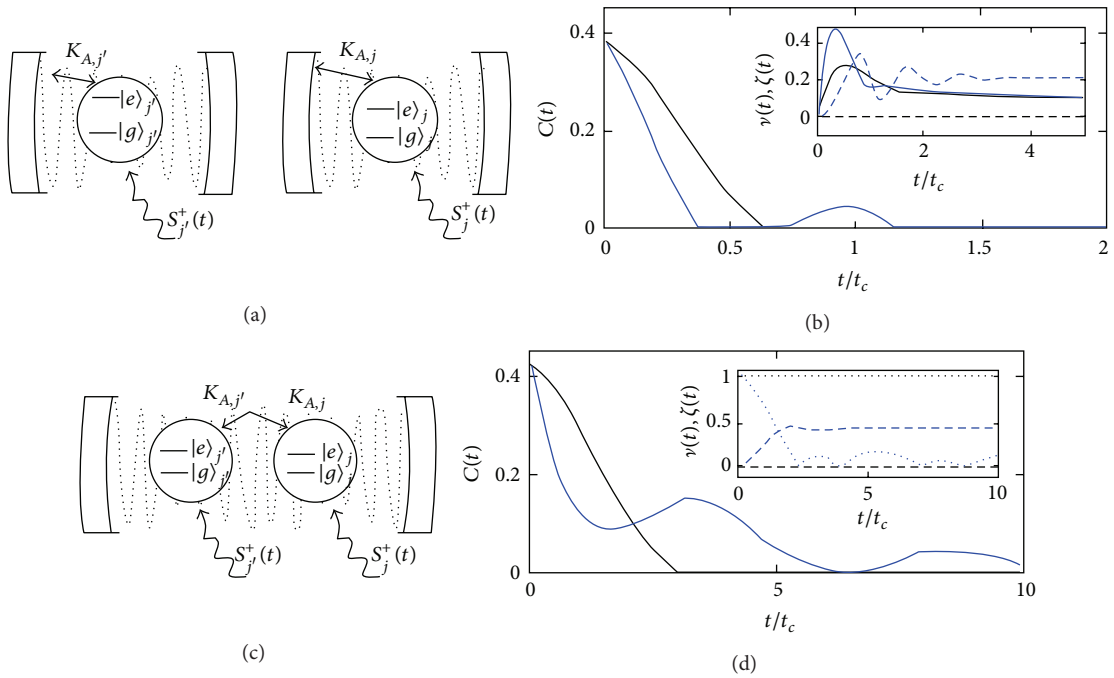

FIGURE 12: (a) Schematic drawing of two locally modulated atoms in separated cavities, coupled to the cavity modes. (b) Concurrence as a function of time. Unmodulated (black) and modulated (blue) scenarios, with no cross decoherence, $\mu = 0$. Inset: decoherence rate magnitude $\nu(t)$ (solid) and asymmetry $\zeta(t)$ (dashed) as a function of time. Parameters: $a = 0.75$, $\omega_a = 20/t_c$, $\omega_0 = 0.8\omega_a$, $\beta = 1/\omega_a$, $\gamma^{\mathrm{unmod}} = 0.032/t_c$, $\gamma^{\mathrm{mod}} = 2.65\gamma^{\mathrm{unmod}}$, $\tau_{1,2}/t_c = \{0.175, 0.1\}$, and $\phi_{1,2} = \pi/10$. (c) Schematic drawing of two locally modulated atoms in the same cavity, coupled to the cavity modes. (d) Concurrence as a function of time. Unmodulated (black) and modulated (blue) scenarios, with cross decoherence. Inset: cross-decoherence $\mu(t)$ (dotted) and asymmetry $\zeta(t)$ (dashed) as a function of time. Parameters: $a = 0.75$, $\omega_a = 20/t_c$, $\omega_0 = \omega_a$, $\beta = 10/\omega_a$, $\gamma^{\mathrm{unmod}} = 0.032/t_c$, $\gamma^{\mathrm{mod}} = 1.1\gamma^{\mathrm{unmod}}$, $\tau_{1,2}/t_c = \{0.175, 0.1\}$, $\phi_{1,2} = \pi/10$, and $\nu(t \gg t_c) = 0.28/t_c$.

Figure 12(a) presents the case with no cross decoherence, for example, two atoms in remote cavities. While the concurrence of the unmodulated scenario with zero asymmetry rapidly dies, the non-Markovian oscillation of the asymmetry due to the modulation results in ESD-CPR (Figure 12(b)). The rise of concurrence from the dead is substantial and can occur only at a time comparable to the correlation time of the bath t_c. During this time, the entanglement between the two TLS is "transferred" to the bath modes, which still retain some memory. The oscillations of the asymmetry facilitate the return of entanglement back to the two TLS. Notably, ESD-CPR is achieved here by *local modulations*; that is, the two TLS are not coupled through the control fields [108] nor through the bath modes [73, 110]. This novel result, of

controlling entanglement oscillations via local modulations, exemplifies the importance of a unified theory of non-Markovian time-scales multipartite decoherence control.

Next, we analyze the case of systems experiencing cross decoherence due to coupling to the same bath (Figure 12(c)). While this scenario has been less studied [73, 110], it demonstrates long (Markovian) time-scale controlled oscillations that result in ESD-CPR. To investigate this scenario, we set $G_{0,jj'}(\omega) = \sqrt{G_{0,jj}(\omega)G_{0,j'j'}(\omega)}$ and define cross decoherence as $\mu(t) = |R^e_{12}(t) + R^e_{21}(t)|/\nu_e(t)$, where $\mu(t) = 1$ denotes maximal cross decoherence, and $\mu(t) = 0$ denotes effectively separate systems. The cross decoherence expresses the locally modulated "crosstalk" between the two systems via the bath modes (Figure 12(c)).

As was previously discussed, the cross decoherence may vanish due to an imposed coupling of the two TLS to different bath modes. This becomes apparent for quasi-periodic modulation in the long-time limit, $\Omega t \gg 1$, where the cross-modulation spectrum, $F_{t,jj'}(\omega)$ becomes a series of $\delta(\omega_{j,k} - \omega_{j',k'})$. However, this long-time limit for the cross decoherence terms is reached only after the inverse of the minimal spectral distance of the two modulations, that is, $t \gg 1/\min(\omega_{j,k} - \omega_{j' \neq j,k'})$. This limit can be very long for similar, yet not equal, modulations, thus enabling a long oscillatory behavior of the cross decoherence (Figure 12(d) inset).

Figure 12(d) presents the effects of cross decoherence on concurrence. While it has been shown that some states (e.g., singlet) may benefit from cross decoherence [71], the Werner state's concurrence dies faster due to this "crosstalk." Applying different modulations on each TLS results in the reduction of cross decoherence and the increase of asymmetry, both beneficial for entanglement preservation. Furthermore, oscillations of the cross decoherence are long-lasting as the two modulations' peaks are close to one another, and can periodically kill and resuscitate the concurrence even in Markovian time scales ($t \gg t_c$).

This phenomenon can only be investigated by a general model that incorporates both arbitrary time-dependent control and the entire range of cross decoherence, from separate to adjacent systems. The universal dynamical disentanglement approach presented here is, to the best of our knowledge, the first that meets these requirements.

To conclude, the ESD-CPR scenario discussed has many aspects: (a) non-Markovian time-scale behavior [112, 169–171], (b) asymmetry between the two decoherence channels [108, 109, 169–172], (c) cross-decoherence of the two-qubits [73, 110, 171, 172], (d) finite temperature effects [109, 112], and (e) time-dependent control [108, 112, 170]. The universal dynamical control of disentanglement presented here generalizes all these aspects, as it describes *arbitrary* dynamical time-dependent control. Only by combining all these aspects into one formalism, one can fully exploit the control attained by locally modulating entangled systems, namely, oscillations of entanglement with controlled frequencies and amplitudes.

While postponing ESD by reducing the decoherence rate requires control schemes similar to those proposed for single-qubits, facilitating ESD-CPR by dynamically controlling the asymmetry and cross decoherence requires more elaborate local modulations. Based on these results, new control strategies for disentanglement reduction of quantum information processing can be suggested. By tailoring optimal control schemes for each scenario, one can locally control the entangled systems and thereby facilitate ESD-CPR at specific times. This may prove beneficial for many quantum computation and communication protocols.

8.2. Multipartite Decoherence Control. Here we address the problem of maintaining the fidelity of a multipartite entangled state, after it has been prepared [124, 173, 174]. In the context of *one-way quantum computing* [175], fidelity protection is more important than preventing disentanglement [126], since maintaining the *specific initial state* is essential for the success of the computation. Designing high-fidelity gates that are resistant to decoherence was addressed by us elsewhere [125] and its scaling with the number of qubits is beyond the scope of this paper.

We pose and answer the basic questions. How does decoherence scale with the number of qubits and is it state dependent? Can dynamical control combat decoherence and its scaling with the number of qubits as this number becomes large? What time scales are required for such control?

Fidelity in such systems can be protected by very general, not necessarily pulsed, dynamical control of decoherence [99, 100, 104, 118, 123–126, 174, 176]. In this approach, fields applied to the system can maintain its coherence, as long as their effects are faster than the correlation (memory) time of the environment, that is, they act on non-Markovian time scales. Thus far, single-qubit dynamic decoherence control has received more attention [99, 100, 104] than multipartite control [123, 174].

We show that by locally (specifically) modulating each qubit, one can drastically suppress the decoherence and its scaling through modifying the strength and number of effective decoherence channels. Our analysis yields the surprising result that a modulation which acts *after* the multipartite coherence time has decayed can still restore coherence to acceptable levels, if it is within the memory time of the bath, irrespective of the number of particles.

8.2.1. Scenarios. Our system is comprised of N qubits whose ground and excited states are $|g\rangle_j$ and $|e\rangle_j$, respectively, with $j = 1, \ldots, N$ and energy separation $\hbar\omega_a$ (Figure 1). Each qubit may be differently (weakly) coupled to a bath (henceforth we take $\hbar = 1$) as

$$H(t) = H_S + H_B + H_I + H_C(t),$$
$$H_S = \omega_a \sum_{j=1}^{N} |e\rangle_{jj}\langle e|, \qquad H_I = \sum_{j=1}^{N} \widehat{S}_j \widehat{B}_j, \tag{172}$$

where H_S, H_B, and H_I are the system, bath, and interaction Hamiltonians, respectively, $H_C(t)$ is the time-dependent control Hamiltonian, with $\widehat{B}_j$ being the jth qubit bath operator and $\widehat{S}_j$ the system-bath coupling operator of qubit j. We neglect *direct* interactions among bath modes and focus on scenarios where two or more qubits collectively couple to common bath modes (see Figure 13).

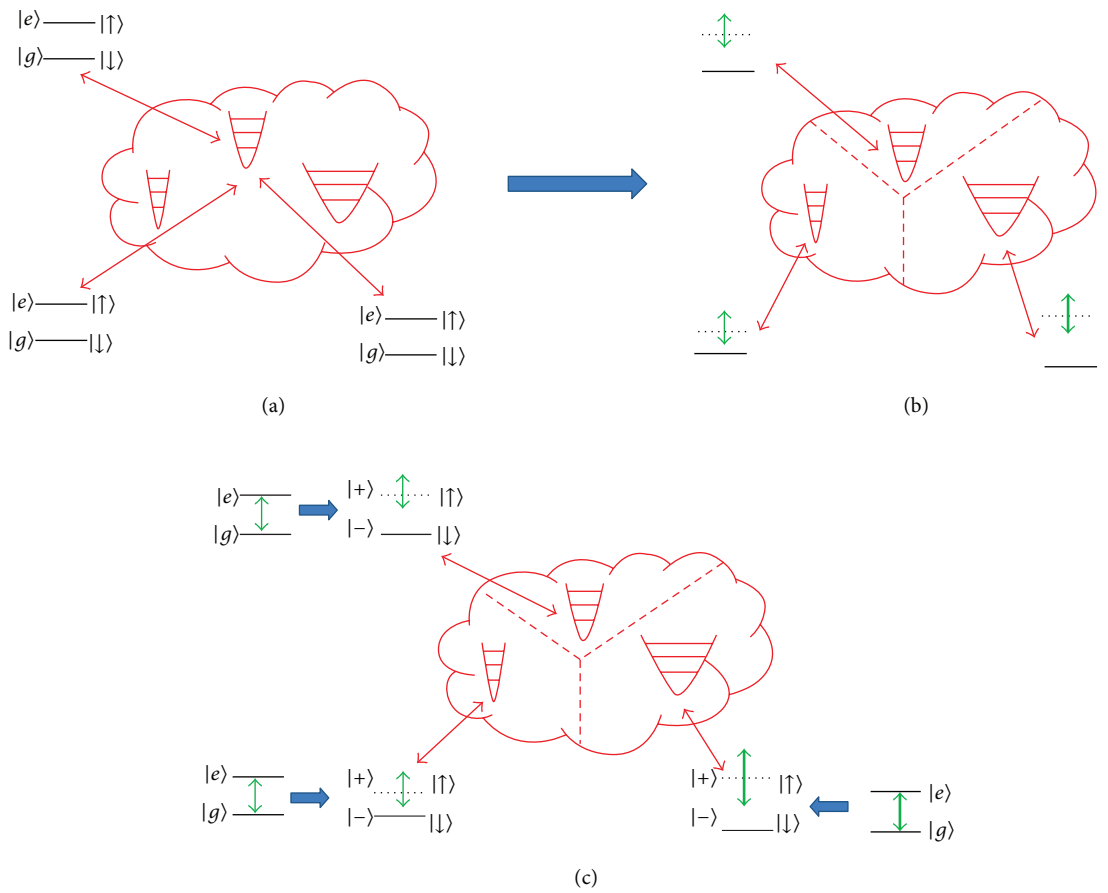

FIGURE 13: Multipartite systems (black) coupled to their environments (red) (color online). (a) Relaxation of identical qubits via coupling to the *same* bath modes causes cross decoherence. (b) *Different* AC-Stark shifts on individual qubits couple them to different bath modes, eliminating cross decoherence. (c) Different Rabi driving of dephasing qubits is analogous to (b).

Two kinds of decoherence can be similarly treated: (i) *relaxation* [123], caused by a system-bath coupling Hamiltonian that is off diagonal in the energy basis, with $\widehat{S}_j = |e\rangle_{jj}\langle g| + |g\rangle_{jj}\langle e|$ being the X-Pauli matrix of the jth qubit. Relaxation involves temperature-dependent level-population change, as well as erasure (scrambling) of the phase relations. Such a process is controllable if each qubit is subject to a strong but off-resonant driving field, $\hbar\eta_j(t)$, that causes an *AC Stark shift* (Figure 1(b)), that is, energy modulation of the system Hamiltonian [174], as

$$H_C(t) = \sum_{j=1}^{N} \eta_j(t)\,|e\rangle_{jj}\langle e|\,. \tag{173}$$

(ii) *Dephasing* [174] is caused by a system-bath coupling Hamiltonian that is diagonal in the energy basis, with $\widehat{S}_j = |e\rangle_{jj}\langle e| - |g\rangle_{jj}\langle g|$ being the Z-Pauli matrix of the jth qubit. Dephasing does not change level populations but only erases (scrambles) the phases. Such a process is controllable by near-resonant Rabi driving fields, $V_j(t)$, that cause transitions between qubit levels,

$$H_C(t) = \sum_{j=1}^{N} \left(V_j(t)\,e^{-i\omega_a t}|e\rangle_{jj}\langle g| + \text{h.c.}\right). \tag{174}$$

We first consider the unmodulated scenario, for which the ME becomes

$$\dot{\widehat{\rho}} = \sum_{j,j'=1}^{N} \left[r_{jj'}(t)\,\widehat{\sigma}_j^x\widehat{\rho}\widehat{\sigma}_{j'}^x - r_{jj'}(t)\,\widehat{\sigma}_{j'}^x\widehat{\sigma}_j^x\widehat{\rho} - r_{jj'}^*(t)\,\widehat{\rho}\widehat{\sigma}_{j'}^x\widehat{\sigma}_j^x + r_{jj'}^*(t)\,\widehat{\sigma}_{j'}^x\widehat{\rho}\widehat{\sigma}_j^x\right], \tag{175}$$

where $r_{jj'}(t)$ are the instantaneous decoherence rates. One can formally integrate (175) and get

$$\begin{aligned}\widehat{\rho}(t) = \widehat{\rho}(0) + \sum_{j,j'=1}^{N}\int_0^t dt' \Big[&r_{jj'}(t')\,\widehat{\sigma}_j^x\widehat{\rho}(t)\,\widehat{\sigma}_{j'}^x \\ &- r_{jj'}(t')\,\widehat{\sigma}_{j'}^x\widehat{\sigma}_j^x\widehat{\rho}(t) \\ &- r_{jj'}^*(t')\,\widehat{\rho}(t)\,\widehat{\sigma}_{j'}^x\widehat{\sigma}_j^x \\ &+ r_{jj'}^*(t')\,\widehat{\sigma}_{j'}^x\widehat{\rho}(t)\,\widehat{\sigma}_j^x\Big].\end{aligned} \tag{176}$$

We are interested in the fidelity, $f(t) = \mathrm{Tr}(\rho(0)^{1/2}\rho(t)\rho(0)^{1/2})$, of any initially pure state $|\psi\rangle$. To second-order in the system-bath coupling, we obtain from (176) the short-time form of $f(t)$ as

$$f_\psi(t) = 1 - t\Gamma_\psi(t;N), \tag{177}$$

$$\Gamma_\psi(t;N) = \sum_{j,j'=1}^{N} R_{jj'}(t)\left(\langle\psi|\,\widehat{\sigma}_j^x\widehat{\sigma}_{j'}^x\,|\psi\rangle - \langle\psi|\,\widehat{\sigma}_j^x\,|\psi\rangle\,\langle\psi|\,\widehat{\sigma}_{j'}^x\,|\psi\rangle\right), \tag{178}$$

$$R_{jj'}(t) = \frac{2}{t}\int_0^t dt' r_{jj'}\left(t'\right), \tag{179}$$

where $\Gamma_\psi(t;N)$ is the infidelity rate and $R_{jj'}(t)$ are elements of the (time-averaged) decoherence-rate matrix discussed below. While (177) and (178) are valid for all initial pure states, we henceforth focus our analysis on specific entangled multipartite states and discuss their decoherence scalability.

8.3. Decoherence Scalability

8.3.1. Multipartite Entangled States. We treat decoherence scaling with N for several distinct multipartite entangled states with clear N-dependence.

(i) GHZ states, $|\mathrm{GHZ}\rangle = (1/\sqrt{2})(\bigotimes_j|e\rangle_j + \bigotimes_j|g\rangle_j)$.

(ii) W-states, $|\mathrm{W}\rangle = (1/\sqrt{N})\sum_{j=1}^{N}(|e\rangle_j\bigotimes_{j\neq j'}|g\rangle_{j'})$.

(iii) Bright states, $|\mathrm{B}\rangle = |J = N/2, m = 0\rangle$, where $|J,m\rangle$ are the Dicke states [177], with J being the total angular momentum and m the excitation number.

(iv) Dark states, given by $|\mathrm{D}\rangle = \bigotimes_{j=2,4,\ldots,2N}|\Psi_-\rangle_{j-1,j}$ for even N, where $|\Psi_-\rangle_{j,j+1} = (1/\sqrt{2})(|g\rangle_j|e\rangle_{j+1} - |e\rangle_j|g\rangle_{j+1})$.

Equation (178) shows that the infidelity rate depends on the specific multipartite state and on the decoherence rates $R_{jj'}(t)$. The time dependence of these rates is revealed on non-Markovian time scales, yet they are constant on long (Markov) time scales. The diagonal elements of the decoherence-rate matrix, $R_{jj}(t)$, correspond to single-qubit decoherence, determined by the coupling of individual qubits (labeled by j) to their respective environments (baths). On the other hand, the off-diagonal elements, $R_{jj'}(t)$ with $j \neq j'$, represent *cross-decoherence* rates, that is, decoherence rates induced on the jth qubit by the j'th qubit. Such cross-decoherence rates are present only for qubits coupled to a common bath or if their dephasing noise is correlated. More explicitly, cross decoherence occurs because two qubits are coupled to the same bath (noise) mode (Figure 1(a)). In the second-order approximation, this means that qubit j interacts with a certain bath (or noise) mode and then the same mode interacts with qubit j' (cf. (178)). In the dephasing scenario, cross dephasing stems from the cross correlation of the stochastic noise functions of qubits j and j'. Thus, for example, ions subject to the same fluctuating magnetic field will experience cross dephasing.

In the absence of cross decoherence, when each qubit is locally coupled to an individual bath $R_{jj'}(t) = 0$, for all $j \neq j'$, the first state-dependent term of the infidelity rate in (178) scales linearly with N, for all states. The second term then appears only for unique states, for example, W-state, and can only lower the N scalability (Table 1), resulting in (at most) linear dependence on N for all states in systems without cross decoherence.

By contrast, the infidelity rate is much more *state-dependent* in systems with cross decoherence, since these systems have additional decoherence channels that may interfere, either constructively or destructively, depending on the initial entangled state via the phases of $\langle\psi|\,\widehat{\sigma}_j^x\widehat{\sigma}_{j'}^x\,|\psi\rangle$. Hence, the N scalability under cross decoherence can either mount to N^2 or vanish completely, a situation unattainable in the absence of cross decoherence.

More specifically, under global dephasing, the GHZ state becomes a bright state in the $|\pm\rangle$ basis and hence experiences constructive interference of all decoherence channels, so that its dephasing scales quadratically with N. The W-state and bright state, on the other hand, do not experience global dephasing since they are composed of a symmetric superposition of identically excited states and hence the dephasing becomes a global phase factor and does not influence decoherence. Remarkably, the dark state considered here is dark for global relaxation and dephasing, due to the invariance of the $|\Psi_-\rangle$ state under the basis rotation from $|e(g)\rangle$ to $|\pm\rangle$. For higher-order approximation this may not be valid.

8.3.2. Decoherence Scaling and the Zeno Regime. One may view decoherence scalability from a complementary aspect, that of the coherence time of the system. In this section, we consider an unmodulated scenario with identical coupling to all qubits, that is,

$$\Gamma_\psi(t;N) = c_\psi(N)\,R(t), \tag{180}$$

where $c_\psi(N)$ is the state-dependent scalability. We define the coherence time as the time at which the fidelity (177), or alternatively the error, $e(t) = 1 - f(t)$, reaches a certain threshold as

$$t_{\mathrm{coh}}\Gamma_\psi\left(t_{\mathrm{coh}};N\right) = 1 - f_{\mathrm{threshold}} \equiv e_{\mathrm{threshold}}. \tag{181}$$

This coherence time is an important measure, since its ratio to the time it takes to perform a single quantum operation (e.g., a two-qubit gate) [3] determines how many such operations can be performed successfully, that is, the complexity of the quantum computation.

The coherence time is usually identified with the inverse decoherence rate, since in the Markovian time-regime, the decoherence rate is constant, that is $R(t) = R$, yielding

$$t_{\mathrm{coh}}(N)\big|_{\mathrm{Markov}} = \frac{e_{\mathrm{threshold}}}{c_\psi(N)\,R}. \tag{182}$$

For example, linearly scaling systems $c_\psi(N) = N$, such as GHZ relaxation without cross decoherence, have Markovian

coherence time that scales inversely with N. However, for large systems, the fidelity threshold (181) is reached according to (177) after a time that may be much shorter than the correlation (memory) time of the bath, t_{corr}, so that the non-Markov time dependence of $R(t)$ starts playing a role. For still larger N, this threshold will be reached within the extremely short Zeno time-regime, t_{Zeno} [86, 97, 99, 102, 178, 179], in which the decoherence rate scales linearly with t, $R_{\text{Zeno}}(t) = t\dot{R}$ (see below). Hence, for sufficiently large systems, such that

$$c_\psi(N) \geq \frac{e_{\text{threshold}}}{t_{\text{Zeno}}^2 \dot{R}} \tag{183}$$

the coherence time is *always* that obtained in the Zeno time-regime as

$$t_{\text{coh}}(N)\big|_{\text{Zeno}} = \frac{e_{\text{threshold}}}{\sqrt{c_\psi(N)\,\dot{R}}}. \tag{184}$$

If $c_\psi(N) = N$, the Zeno coherence time scales as the *inverse square root* of N. This paradoxical result, namely, the inevitable improvement of the decoherence scaling law for sufficiently large systems, has been thus far overlooked. This result is a manifestation of the non-Markovian effects in decoherence dynamics.

8.3.3. Dynamically Modified Decoherence Rates. From (178), it is evident that the decoherence rates $R_{jj'}(t)$ are an important factor in the scaling of decoherence. Their time dependence stems from the non-Markovian master equation (ME) [126]. The same non-Markovian ME governs dynamical decoherence control. The resulting (time-averaged) decoherence rates then assume the form of spectral overlaps of the bath coupling spectrum matrix, $G_{jj'}(\omega)$, and the modulation power-spectrum matrix, $F_{t,jj'}(\omega)$ [174] as

$$R_{jj'}(t) = 2\pi\,\text{Re}\int_{-\infty}^{\infty} d\omega G_{jj'}(\omega)\,F_{t,jj'}(\omega), \tag{185}$$

$$F_{t,jj'}(\omega) = \frac{1}{t}\epsilon_{t,j}(\omega)\,\epsilon_{t,j'}^{*}(\omega), \tag{186}$$

where $G_{jj'}(\omega)$ is the Fourier transform of the system-bath correlation matrix $\Phi_{jj'}(\omega)$, and $F_{t,jj'}(\omega)$ is the time-dependent normalized modulation spectrum, where $\epsilon_{t,j}(\omega) = (1/\sqrt{2\pi})\int_0^t dt'\epsilon_j^+(t')e^{i\omega t'}$ is the finite-time Fourier transform of the modulation function. In the relaxation scenario, the modulation spectral function represents the effective change in qubit j's energy splitting or AC Stark shift (Figure 13(b)). In the dephasing scenario, it determines the time-dependent Rabi splitting of the $|\pm\rangle$ states (Figure 13(c)). In both scenarios, the spectral overlap $G_{jj'}(\omega)\epsilon_{t,j}^{*}(\omega)\epsilon_{t,j'}\omega)$ in (185) represents the effective coupling between the systems and the bath, whereby the dynamical control (modulation) determines which spectral bath modes the qubits are coupled to.

There is an important distinction between the controllability of single-qubit decoherence rates, $R_{jj}(t)$, and that of their cross-decoherence counterpart, $R_{jj'}(t)$. Namely, the single-qubit dynamically modified $R_{jj}(t)$ can only be reduced by decreasing the overlap between the modulation spectra $|\epsilon_{t,j}(\omega)|^2$ and the bath coupling spectra, $G_{jj}(\omega)$, both positive. No matter how fast the modulation is, $|\epsilon_{t,j}(\omega)|^2$ cannot decrease the single-qubit decoherence rate, if the bath coupling spectrum is spectrally flat (Markovian). By contrast, cross-decoherence rates $R_{jj'}(t)$ can be *completely* eliminated by choosing spectrally distinct local modulations whose spectral overlap $\epsilon_{t,j}^{*}(\omega)\epsilon_{t,j'}(\omega)$ vanishes, irrespective of the bath coupling spectrum, $G_{jj'}(\omega)$ even if it is Markovian (spectrally flat) (Figures 2(a) and 2(b)). The qubits effectively couple to orthogonal bath modes. Hence, by modulating each qubit differently, one can effectively decouple the qubits, as if they were interacting with separate baths.

8.3.4. Dynamically Modified Decoherence Scaling. How do these modulations affect decoherence scaling? Let us examine two limits of the general scenario more closely.

(A) Consider first the limit of *locally decohering* qubits. Due to the absence of a common bath, modulations cannot induce cross decoherence. Hence, they cannot change the scaling law, which is identical for most multipartite entangled states, namely, $\Gamma_\psi(t;N) \propto N$ (Table 1). Nevertheless, modulations can still improve the infidelity rate, by decreasing the overlap of each qubit's bath coupling and modulation spectra.

(B) The other limiting case is that of collective decoherence of qubits coupled to a common bath, but locally controlled. By exploiting the spectral distinction of N different local modulations, one can completely eliminate cross decoherence and effectively render the system similar to the aforementioned locally decohering qubits, in which for most states, decoherence scales linearly with N. Such local modulations may be advantageous for the relaxing bright state, or dephasing GHZ-state, by reducing its infidelity rate scaling by a factor of N.

On the other hand, one may enhance cross decoherence by local modulations: if the qubits are coupled to the same bath but with different strengths, then the modulations can be chosen to compensate for their unequal coupling strengths. Such enhanced cross decoherence can drastically improve the coherence time by rendering certain states completely dark: without modulation, partially dark states with unequal coupling have infidelity rate that scales as N, whereas under modulations that impose destructive interference of the decoherence channels, such states can acquire much longer coherence time by becoming fully dark.

8.3.5. Effective Modulation Time Scales. When do such local dynamic modulations become effective? Let us recall the relevant time scales. The longest one is the coherence time of a single-qubit without modulation, $t_{\text{coh}}(1) \cong 1/\Gamma_\psi$. Another is the correlation (memory) time of the bath, t_{corr}. It is the decay time of the correlation function, which is given by the product of the noise amplitude at time t with the noise amplitude at time $t+\tau$, averaged over realizations. In the frequency domain

Table 1: N-scalability of entangled states decoherence for relaxation and dephasing scenarios, with and without cross decoherence.

	Relaxation		Dephasing	
	No X-deco.	X-deco.	No X-deco.	X-deco.
GHZ	N	N	N	N^2
W-state	N	$3N-2$	$4(N-1)/N$	0
Bright state	N	$N+N^2/2$	N	0
Dark state	N	0	N	0

$1/t_{\text{corr}}$ is the width of the noise-coupling spectrum and in dephasing noise this is the noise bandwidth.

In the single qubit case, the weak-coupling assumption (see below) implies that the correlation time is shorter than the single-qubit coherence time [70] $t_{\text{corr}} \ll t_{\text{coh}}(1)$ or, equivalently, noise bandwidth much larger than dephasing rate [174]. In the unmodulated N-qubit scenario, this assumption is given by $t_{\text{corr}} \ll t_{\text{coh}}(N)$, whereas in the modulated case, it is the *modulated* coherence time that sets the limit for the weak coupling regime, $t_{\text{corr}} \ll t_{\text{coh}}^{\text{mod}}(N)$. Hence, even if for a large (unmodulated) system the weak coupling assumption does not hold, modulations that drastically increase the coherence time, for example, by eliminating cross decoherence, can make the system enter the valid regime for which the analysis holds.

Only modulations faster than the bath-(noise-) correlation time can affect the single-qubit decoherence rates $R_{jj}(t)$. Yet a crucial insight transpires: if each qubit decoheres individually (cross decoherence is eliminated), the (unmodulated) N-particle coherence time does not determine whether the control is effective. Neither does the infidelity rate (178). Rather, the modulation period, τ, must be shorter than t_{corr}, but can be much larger than $t_{\text{coh}}(1)/N$: it is unaffected by scaling!

We can now summarize the conditions for an effective increase of the coherence time of entangled multipartite systems by modulations with a period τ as

$$t_{\text{coh}}(N) \underbrace{\leq}_{\text{a}} \tau \underbrace{\leq}_{\text{b}} t_{\text{corr}} \underbrace{\leq}_{\text{c}} t_{\text{coh}}(1) \underbrace{\leq}_{\text{d}} t_{\text{coh}}^{\text{mod}}(N). \quad (187)$$

Here, (a) lays out the striking result that effective modulation can be slower than the coherence time of the system; (b) is the major requirement for effective modulation; (c) is the single-qubit weak-coupling assumption; (d) shows the main result, that is, the possibility of attaining (via effective modulations) multipartite coherence time $t_{\text{coh}}^{\text{mod}}(N)$ that is longer than the single-qubit coherence time.

8.3.6. Application to an Ion Trap. Our analysis is applicable to a broad variety of experimental setups. As an example, consider a string of ions in a linear trap [142, 180, 181], in which the qubits are encoded by two internal states of each ion ($|g(e)\rangle_j$) (Figure 14(c)). Fluctuating magnetic fields give rise to a *collective* fluctuation of qubit energies, thereby causing cross dephasing. Modulations that locally address each ion ($j = 1, \ldots, N$) may be realized by laser fields whose amplitude varies spatially and differently affects the jth "carrier" frequency $\omega_j(t)$ of the transition $|g\rangle_j \leftrightarrow |e\rangle_j$: a gradient of the laser field amplitude along the ion chain would suffice to achieve this.

Each local modulation may decrease the *individual* decoherence rate of each qubit by at least an order of magnitude, depending on the noise spectrum and available modulation frequencies. More importantly, local modulations may eliminate cross dephasing between ions, thereby increasing the coherence time of bright or GHZ states by a factor of N. For an ion trap with $t_{\text{coh}}(1) = 14.7\,\text{s}$, ($R \geq 10^{-2}\,\text{s}^{-1}$) [181], local modulations at intervals $\tau \cong 1\,\text{ms}$ can drastically increase the coherence times of GHZ or bright states, for example, $t_{\text{coh}}^{\text{mod}}(10) \cong t_{\text{coh}}(1) \cong 10\,\text{s}$ (Figure 14).

8.4. Validity of the Weak-Coupling Approximation

8.4.1. Thermal Baths. For coupling to a thermal bath, the first-order term is proportional to $\text{Tr}\langle H_I^B \rho_B\rangle$, where H_I^B is the bath part of the coupling Hamiltonian and ρ_B is the density matrix of the bath's thermal state. In the scenario considered here, H_I^B has only off-diagonal terms in the bath eigenbasis. For example, $H_I^B = \sum_k (\lambda_k a_k + \text{h.c.})$ for coupling to an oscillator bath, where λ_k is the coupling coefficient to mode k and a_k is the annihilation operator. This form renders the first-order term zero.

8.4.2. Validity of the ME. The master equation, (98), is valid as long as the density matrix does not change much within the correlation (memory) time of the bath, t_{corr}. In the entangled multipartite scenarios discussed here, this condition becomes $t_{\text{corr}} \sum_{j,j'=1}^{N} R_{jj'}(t_{\text{corr}}) \ll 1$.

8.4.3. Validity of the Fidelity. The fidelity derived above, (177) requires a stricter condition $t \sum_{j,j'=1}^{N} R_{jj'}(t) \ll 1$. Several important issues are raised by this approximation. The first is that it is N-dependent, meaning the time in which the approximation holds becomes shorter for larger systems. Furthermore, the N-dependency of the approximation depends on whether there is cross decoherence. With cross decoherence, the time within which the approximation holds depends on N^2, whereas without cross decoherence it depends on N.

In Figure 14, one can see that the single-qubit fidelity is within the validity domain of the approximation, whereas the fidelity of entangled states with $N = 10$ qubits without modulation becomes smaller and exit the validity regime rapidly. However, by applying different modulations on the qubits, one can not only reduce each qubit's decoherence rate, but also eliminate the cross decoherence and increase the fidelity by $N = 10$-fold, thus bringing it within the validity region of the weak-coupling approximation.

8.5. Fixed-Time Approach.

Assume that a quantity of interest ("score") can be written as a real-valued function $P(t) = P[\widehat{\varrho}(t)]$ of the system state $\widehat{\varrho}(t)$ at a given time t. This might be, for example, a measure of performance of some input-output device that is supposed to operate within a

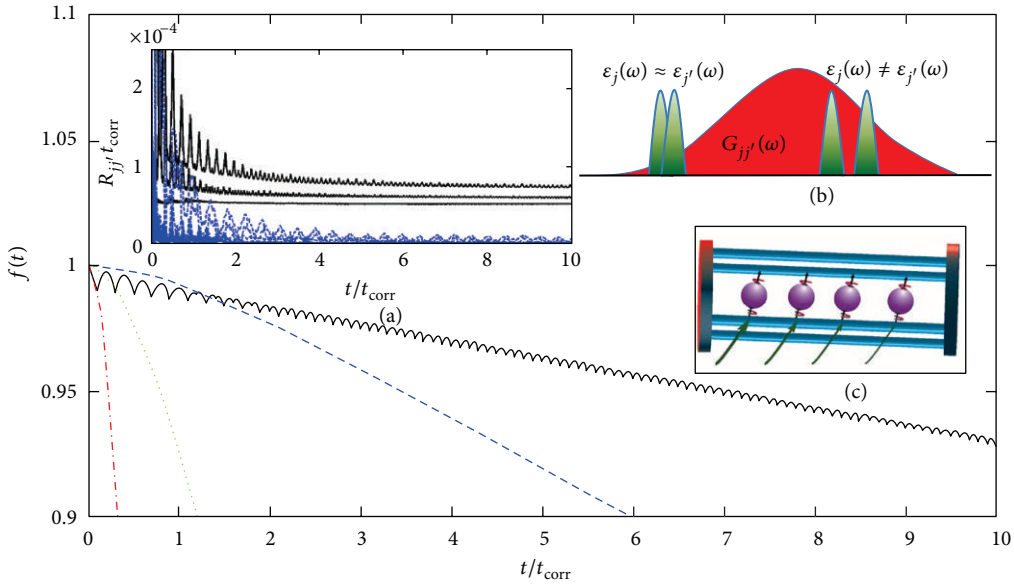

FIGURE 14: Fidelity as a function of time for entangled states experiencing collective relaxation under different modulations compared to that of a single qubit without modulation (blue, dashed) (color online): bright-state, $N = 10$ without modulation (red, dot-dashed); GHZ with $N = 10$ without modulation (green, dotted); bright-state with $N = 10$ under asymmetric modulation (black, solid). (a) Decoherence rates for $N = 3$ with asymmetric modulation. Single-qubit decoherence rates, $R_{jj}(t)$ (black, solid), undergo oscillations then attain constant nonzero values at $t \gg t_{\text{corr}}$; cross-decoherence rates $R_{jj'}(t)$ (blue, dashed) also oscillate but then decay to zero at $t \gg t_{\text{corr}}$. (b) For qubits j and j', the overlap of the bath coupling spectrum $G_{jj'}(\omega)$ (red area) and the modulation spectra $\epsilon_{t,j}(\omega)$ and $\epsilon_{t,j'}(\omega)$ (green areas) determine the decoherence rate. If the qubits undergo (asymmetric) different modulations $\epsilon_j(\omega) \neq \epsilon_{j'}(\omega)$, their lack of overlap eliminates cross decoherence. (c) Addressing individual ions in a trap by different control fields with different amplitudes induces asymmetric Rabi flippings and thereby eliminates cross decoherence.

predefined cycle/gate time t. Depending on the physical problem and model chosen, extensions and generalizations are conceivable, such as a comparison of the outcome for different t (on a time scale set by a constraint) [138], a time average $P = \int \mathrm{d}\tau f(\tau) P[\widehat{\varrho}(\tau)]$ with some probability density $f(\tau)$ [182], or a maximum $P(t) = \max_{\tau\in[0,t]} P[\widehat{\varrho}(\tau)]$ [183]. Here, we restrict ourselves to the "fixed-time" definition as given above. Our goal is to generate, by means of classical control fields applied to the system, a time dependence of the system Hamiltonian within the interval $0 \leq \tau \leq t$ that adjusts $P(t)$ to a desired value. In particular, this can be an optimum (i.e., maximum or minimum) of the possible values of P. Assume that the initial system state $\widehat{\varrho}(0)$ is given. The *change* to the "score" over time t, $P = P(t) - P(0)$, is then given by the first-order Taylor expansion in a chosen basis

$$P \approx \sum_{mn} \frac{\partial P}{\partial \varrho_{mn}} \Delta\varrho_{mn} = \mathrm{Tr}\left(\widehat{P}\Delta\widehat{\varrho}\right), \tag{188}$$

where $\Delta\widehat{\varrho} = \widehat{\varrho}(t) - \widehat{\varrho}(0)$ and the expansion coefficients

$$\left(\frac{\partial P}{\partial \varrho_{mn}}\right)_{t=0} \equiv \left(\widehat{P}\right)_{nm} \tag{189}$$

are the matrix elements (in the chosen basis) of a Hermitian operator $\widehat{P}$, which is the gradient of $P[\widehat{\varrho}(t)]$ with respect to $\widehat{\varrho}$ at $t = 0$; that is, we may formally write $\widehat{P} = (\nabla_{\widehat{\varrho}} P)^T_{t=0} = (\partial P/\partial\widehat{\varrho})^T_{t=0}$. In what follows, it is $\widehat{P}$ which contains all information on the score variable. Note that the transposition applied in (189) simply allows to express the sum over the Hadamard (i.e., entrywise) matrix product in (188) as a trace of the respective operator product $\widehat{P}\Delta\widehat{\varrho}$.

Let us illustrate this in two examples. If P is the expectation value of an observable (i.e., Hermitian operator) $\widehat{Q}$, so that $P = \mathrm{Tr}(\widehat{\varrho}\widehat{Q})$, then (189) just reduces to this observable $\widehat{P} = \widehat{Q}$. If P is the state purity, $P = \mathrm{Tr}(\widehat{\varrho}^2)$, then (189) becomes proportional to the state, $\widehat{P} = 2\widehat{\varrho}(0)$. Note that the score P is supposed to reflect the environment (bath) effects and not the internal system dynamics.

Equation (188) implies that $\Delta\widehat{\varrho}$ and with it P are small. Hence $\Delta\widehat{\varrho}$ must refer to the interaction picture and a weak interaction, while $P[\widehat{\varrho}(t)]$ should not be affected by the internal dynamics (so that no separate time dependence emerges in (188), which is not included in the chain-rule derivative). In the examples above, this is obvious for state purity, whereas an observable $\widehat{Q}$ might be thought of as coevolving with the internal dynamics.

Our starting point for what follows is simply the relation $P = \mathrm{Tr}(\widehat{P}\Delta\widehat{\varrho})$ with some Hermitian $\widehat{P}$, whose origin is not relevant.

8.6. Role of Averaged Interaction Energy. Equation (188) expresses the score P as an overlap between the gradient $\widehat{P}$ and the change of system state $\Delta\widehat{\varrho}$. In order to find expressions for

P in terms of physically insightful quantities, we decompose the total Hamiltonian into system, bath, and interaction parts,

$$\widehat{H}(t) = \widehat{H}_S(t) + \widehat{H}_B + \widehat{H}_I, \tag{190}$$

and consider the von Neumann equation of the total (system and environment) state in the interaction picture,

$$\frac{\partial}{\partial t}\widehat{\varrho}_{\text{tot}}(t) = -i\left[\widehat{H}_I(t), \widehat{\varrho}_{\text{tot}}(t)\right], \tag{191}$$

($\widehat{H}_I(t) = \widehat{U}_F^\dagger(t)\widehat{H}_I^{(S)}(t)\widehat{U}_F(t)$, (S) denoting the Schrödinger picture and $\widehat{U}_F(t) = T_+ e^{-i\int_0^t d\tau[\widehat{H}_S(\tau)+\widehat{H}_B]}$). Its solution can be written as Dyson (state) expansion

$$\begin{aligned}\widehat{\varrho}_{\text{tot}}(t) = {} & \widehat{\varrho}_{\text{tot}}(0) \\ & + (-i)\int_0^t dt_1 \left[\widehat{H}_I(t_1), \widehat{\varrho}_{\text{tot}}(0)\right] \\ & + (-i)^2 \int_0^t dt_1 \int_0^{t_1} dt_2 \left[\widehat{H}_I(t_1), \left[\widehat{H}_I(t_2), \widehat{\varrho}_{\text{tot}}(0)\right]\right] \\ & + \cdots,\end{aligned} \tag{192}$$

which can be obtained either by an iterated integration of (191) or from its formal solution

$$\widehat{\varrho}_{\text{tot}}(t) = \widehat{U}_I(t)\,\widehat{\varrho}_{\text{tot}}(0)\,\widehat{U}_I^\dagger(t), \quad \widehat{U}_I(t) = T_+ e^{-i\int_0^t dt' \widehat{H}_I(t')}, \tag{193}$$

by applying the Magnus (operator) expansion

$$\widehat{U}_I(t) = e^{-it\widehat{H}_{\text{eff}}(t)}, \tag{194}$$

$$\begin{aligned}\widehat{H}_{\text{eff}}(t) = {} & \frac{1}{t}\int_0^t dt_1 \widehat{H}_I(t_1) \\ & - \frac{i}{2t}\int_0^t dt_1 \int_0^{t_1} dt_2 \left[\widehat{H}_I(t_1), \widehat{H}_I(t_2)\right] + \cdots,\end{aligned} \tag{195}$$

expanding in (193) the exponential $\widehat{U}_I = \widehat{U}_I(\widehat{H}_{\text{eff}})$ and sorting the terms according to their order in $\widehat{H}_I$.

We assume that, initially, the system is brought in contact with its environment (rather than being in equilibrium with it), which corresponds to factorizing initial conditions $\widehat{\varrho}_{\text{tot}}(0) = \widehat{\varrho}(0) \otimes \widehat{\varrho}_B$. The environment is in a steady state $\widehat{\varrho}_B$, $[\widehat{\varrho}_B, \widehat{H}_B] = 0$, so it is more adequate to speak of a "bath." Tracing over the bath in (192) then gives the change of system state $\Delta\widehat{\varrho} = \widehat{\varrho}(t) - \widehat{\varrho}(0)$ over time t, which we must insert into (188). We further assume a vanishing bath expectation value of the interaction Hamiltonian,

$$\left\langle \widehat{H}_I \right\rangle_B \equiv \text{Tr}_B\left(\widehat{\varrho}_B \widehat{H}_I\right) = \widehat{0}. \tag{196}$$

As a consequence, the "drift" term corresponding to the first order in (192) vanishes, and we only consider the second order term as the lowest nonvanishing order approximation. Finally, we assume that the initial system state commutes with $\widehat{P}$,

$$\left[\widehat{\varrho}(0), \widehat{P}\right] = 0. \tag{197}$$

In the language of control theory, $\text{Tr}[\widehat{\varrho}(0)\widehat{P}]$ is a "kinematic critical point" [184] if (197) holds, since $\text{Tr}[e^{i\widehat{H}}\widehat{\varrho}(0)e^{-i\widehat{H}}\widehat{P}] = \text{Tr}[\widehat{\varrho}(0)\widehat{P}] + i\,\text{Tr}(\widehat{H}[\widehat{\varrho}(0), \widehat{P}]) + \mathcal{O}(\widehat{H}^2)$ for a small arbitrary system Hamiltonian $\widehat{H}$. Since we consider $\widehat{\varrho}$ in the interaction picture, (197) means that the score is insensitive (in first order) to a bath-induced unitary evolution (i.e., a generalized Lamb shift) [140]. The purpose of this assumption is only to simplify the expressions, but it is not essential. Physically, one may think of a fast auxiliary unitary transformation that is applied initially in order to diagonalize the initial state in the eigenbasis of $\widehat{P}$.

To the lowest (i.e., second) order, we then evaluate (188) for the score change as

$$P = t^2 \left\langle \left[\widehat{H}, \widehat{P}\right] \widehat{H} \right\rangle, \qquad \widehat{H} = \frac{1}{t}\int_0^t \mathrm{d}\tau\ \widehat{H}_{\text{I}}(\tau), \tag{198}$$

where $\langle\cdot\rangle = \text{Tr}[\widehat{\varrho}_{\text{tot}}(0)(\cdot)]$. This expresses the change of score in terms of the interaction Hamiltonian, averaged in the interaction picture over the time interval of interest. Our scheme is summarized in Figure 15.

8.7. Spectral Overlap. Alternatively, (198) can be written as an overlap of system and bath matrices, which allows a more direct physical interpretation. To do so, we assume d dimensional Hilbert space and expand the interaction Hamiltonian as a sum of products of system and bath operators,

$$\widehat{H}_{\text{I}} = \sum_{j=1}^{d^2-1} \widehat{S}_j \otimes \widehat{B}_j, \tag{199}$$

in such a way that $\langle \widehat{B}_j \rangle = 0$, which ensures that (196) is satisfied (otherwise we may shift $\widehat{B}_j' = \widehat{B}_j - \langle \widehat{B}_j \rangle \widehat{I}$, $\widehat{H}_{\text{S}}' = \widehat{H}_{\text{S}} + \sum_j \langle \widehat{B}_j \rangle \widehat{S}_j$). Considering (199) in the interaction picture and expanding $\widehat{S}_j(t) = \sum_k \epsilon_{jk}(t)\widehat{S}_k$ in terms of (Hermitian, traceless, orthonormalized to $\text{Tr}(\widehat{S}_j\widehat{S}_k) = d\delta_{jk}$) basis operators, $\widehat{S}_j$ defines a (real orthogonal) rotation matrix $\boldsymbol{\epsilon}(t)$ in the system's Hilbert space, with elements

$$\epsilon_{jk}(t) = \left\langle \widehat{S}_j(t)\,\widehat{S}_k \right\rangle_{\text{id}}, \tag{200}$$

where $\langle\cdot\rangle_{\text{id}} = \text{Tr}[d^{-1}\widehat{I}(\cdot)]$. These elements of the matrix $\boldsymbol{\epsilon}(t)$ may be regarded as the dynamical correlation functions of the basis operators. Analogously, we define a bath correlation matrix $\boldsymbol{\Phi}(t)$ with elements

$$\Phi_{jk}(t) = \left\langle \widehat{B}_j(t)\,\widehat{B}_k \right\rangle_{\text{B}}. \tag{201}$$

It contains the entire description of the bath behavior in our approximation. Finally, we define a Hermitian matrix $\boldsymbol{\Gamma}$ with elements

$$\Gamma_{kj} = \left\langle \left[\widehat{S}_j, \widehat{P}\right] \widehat{S}_k \right\rangle, \tag{202}$$

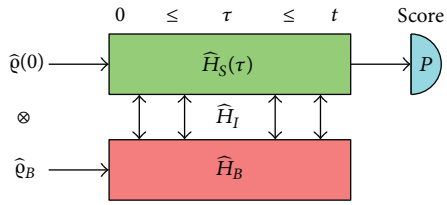

Figure 15: Our control scheme (color online): a system is brought in contact with a bath over a fixed time interval $0 \le \tau \le t$ during which the time dependence of the system Hamiltonian $\widehat{H}_S(\tau)$ is chosen such that a given system variable P is adjusted to a desired value at the final time t.

where $\langle\cdot\rangle = \mathrm{Tr}[\widehat{\varrho}(0)(\cdot)]$. The matrix $\mathbf{\Gamma}$ may be understood as a representation of the gradient $\widehat{P}$ with respect to the chosen basis operators $\widehat{S}_j$. Finally, we define the bath and (finite-time) system spectra according to

$$\mathbf{G}(\omega) = \int_{-\infty}^{\infty} dt e^{i\omega t} \mathbf{\Phi}(t),$$
$$\boldsymbol{\epsilon}_t(\omega) = \frac{1}{\sqrt{2\pi}} \int_0^t d\tau \mathrm{e}^{\mathrm{i}\omega\tau} \boldsymbol{\epsilon}(\tau). \tag{203}$$

This allows to express the score, (198), as the matrix overlap

$$P = \iint_0^t \mathrm{d}t_1 \mathrm{d}t_2 \, \mathrm{Tr}\left[\boldsymbol{\epsilon}^T(t_1) \mathbf{\Phi}(t_1 - t_2) \boldsymbol{\epsilon}(t_2) \mathbf{\Gamma}\right] \tag{204}$$

$$= \int_{-\infty}^{\infty} \mathrm{d}\omega \, \mathrm{Tr}\left[\boldsymbol{\epsilon}_t^\dagger(\omega) \mathbf{G}(\omega) \boldsymbol{\epsilon}_t(\omega) \mathbf{\Gamma}\right] \tag{205}$$

$$= t \int_{-\infty}^{\infty} \mathrm{d}\omega \, \mathrm{Tr}\left[\mathbf{F}_t(\omega) \mathbf{G}(\omega)\right]. \tag{206}$$

In (206), we have used the cyclic property of the trace to write the spectral overlap in a more compact form by combining the rotation matrix spectra $\boldsymbol{\epsilon}_t(\omega)$ and the gradient representation $\mathbf{\Gamma}$ to a system spectral matrix

$$\mathbf{F}_t(\omega) = \frac{1}{t} \boldsymbol{\epsilon}_t(\omega) \mathbf{\Gamma} \boldsymbol{\epsilon}_t^\dagger(\omega). \tag{207}$$

Analogously, (204) can be written in a more compact form by introducing the matrix

$$\mathbf{R}(t_1, t_2) = \boldsymbol{\epsilon}^T(t_1) \mathbf{\Phi}(t_1 - t_2) \boldsymbol{\epsilon}(t_2). \tag{208}$$

Equation (206) is a generalization of [105] and demonstrates that the change P over a given time t is determined by the spectral overlap between system and bath dynamics, analogously to DCM [185], or the measurement induced quantum Zeno and anti-Zeno control of open systems [97, 102]. The bath-spectral matrix $\mathbf{G}(\omega)$ must be positive semidefinite for all ω. If the same holds for the matrix $\mathbf{F}_t(\omega)$, then P is always positive. Below we will consider such a case where P reflects a gate error and the goal is then to minimize this error. The spectral overlap (206) can be made as small as desired by a rapid modulation of the system, such that the entire weight of the system spectrum is shifted beyond that of the bath, which is assumed to vanish for sufficiently high frequencies. Since this fast modulation may cause unbounded growth of the system energy, a meaningful posing of the problem requires a constraint.

In general, $\mathbf{F}_t(\omega)$ is Hermitian but need not necessarily be positive semi-definite, depending on the choice of score as encoded in $\mathbf{\Gamma}$. This reflects the fact that P can increase or decrease over t. Depending on the application, our goal can therefore also be to maximize P with positive and negative sign. In what follows, we will consider the question how to find a system dynamics that optimizes the score.

8.8. Euler-Lagrange Optimization

8.8.1. Role of Control, Score, and Constraint. Our considerations in the previous section suggest to define our control problem in terms of a triple $(\mathbf{f}, P, E)$ consisting of a control $\mathbf{f}$, a score P, and a constraint E.

The control is a set of real parameters f_l, which have been combined to a vector $\mathbf{f}$. These can either be timings, amplitudes, and/or phases of a given number of discrete pulses or can describe a time-continuous modulation of the system. Here, we focus on time-dependent control, where the $f_l(\tau)$ parametrize the system Hamiltonian as $\widehat{H}_S = \widehat{H}_S[\mathbf{f}(\tau)]$, or the unitary evolution operator $\widehat{U}(\tau) = T_+ e^{-i\int_0^\tau d\tau' \, \widehat{H}_S(\tau')} \equiv \widehat{U}[\mathbf{f}(\tau)]$. A direct parametrization of $\widehat{U}$ avoids the need of time-ordered integration of its exponent. The $\widehat{U}(\tau)$ thus obtained [176] can be then used to calculate the system Hamiltonian $\widehat{H}_S(\tau) = i[(\partial/\partial t)\widehat{U}(\tau)]\widehat{U}^\dagger(\tau)$.

Two explicit examples of the score P pertain to the fidelity of $\widehat{P}$ with a given pure state $F_\Psi = \langle\Psi|\widehat{\varrho}|\Psi\rangle$ (for which $\widehat{P} = |\Psi\rangle\langle\Psi|$), or to the von Neumann entropy which we can approximate (for nearly pure states) by the linear entropy, $S = -k\,\mathrm{Tr}(\widehat{\varrho}\ln\widehat{\varrho}) \approx S_L = k[1 - \mathrm{Tr}(\widehat{\varrho}^2)]$ (for which $\widehat{P} = -2k\widehat{\varrho}(0)$). The latter score can be used to maximize the fidelity with the maximally mixed state $\widehat{\varrho} \sim \widehat{I}$ (for which S_L becomes maximum), or to maximize the concurrence $C_{|\Psi_{AB}\rangle} = \sqrt{2(1 - \mathrm{Tr}\,\widehat{\varrho}_A^2)}$, $\widehat{\varrho}_A = \mathrm{Tr}_B|\Psi_{AB}\rangle\langle\Psi_{AB}|$, as a measure of entanglement of a pure state $|\Psi_{AB}\rangle$ of a bipartite system.

If a *constraint* is required to ensure the existence of a finite (physical) solution, its choice should depend on the most critical source of error. An example is the average speed with which the controls change, $E = \int_0^t d\tau \, \dot{\mathbf{f}}^2(\tau)$, which depend on the control bandwidth in the spectral domain. A parametrization-independent alternative is the mean square of the modulation energy, $E = \int_0^t d\tau \langle(\Delta\widehat{H})^2(\tau)\rangle_{\mathrm{id}}$, where $\langle\cdot\rangle_{\mathrm{id}}$ refers to a maximally mixed state and hence to a state-independent norm, and $\Delta\widehat{H}$ is the difference between the modulated and unmodulated (natural) system Hamiltonians.

8.8.2. A Projected Gradient Search. We want to find controls $\mathbf{f}$ that optimize a score $P(\mathbf{f})$ subject to a constraint $E(\mathbf{f})$. A numerical local optimization can be visualized in parameter space as shown in Figure 16.

We start at some initial point $\mathbf{f}_0$ for which $E(\mathbf{f}_0)$ is the desired value of the constraint. Simply following the gradient

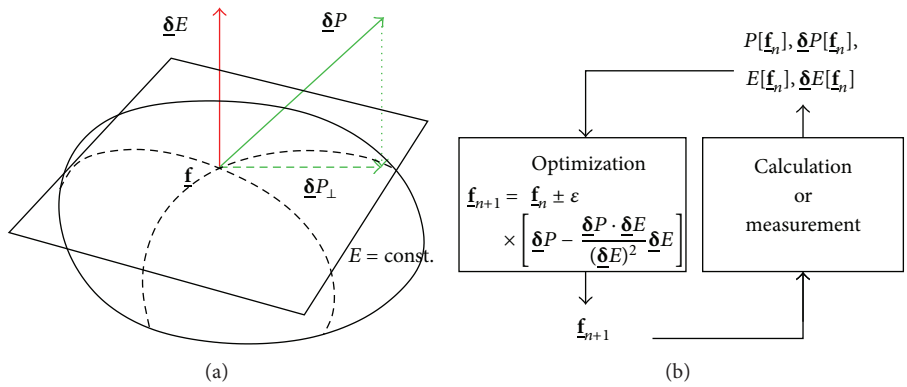

FIGURE 16: (a) Optimization of the score $P(\mathbf{f})$ subject to a constraint $E(\mathbf{f})$ in control space $\{\mathbf{f}\}$ by walking along the component $\boldsymbol{\delta}P_\perp$ of the gradient $\boldsymbol{\delta}P$ orthogonal to $\boldsymbol{\delta}E$. (b) Resulting iteration consisting in steps determined by a small parameter ϵ which yields a local solution depending on the starting point $\mathbf{f}_0$ (color online).

$\boldsymbol{\delta}P$ would maximize or minimize P but would also change E. To optimize P while keeping E constant, we therefore move along the projection of $\boldsymbol{\delta}P$ orthogonal to $\boldsymbol{\delta}E$, that is, along $\boldsymbol{\delta}P_\perp = \boldsymbol{\delta}P - ((\boldsymbol{\delta}P \cdot \boldsymbol{\delta}E)/(\boldsymbol{\delta}E)^2)\boldsymbol{\delta}E$. Since the gradients depend on $\mathbf{f}$, the iteration consists of small steps $\mathbf{f}_{n+1} = \mathbf{f}_n \pm \epsilon \boldsymbol{\delta}P_\perp(\mathbf{f}_n)$, $\epsilon \ll 1$. Assuming that neither $\boldsymbol{\delta}P$ nor $\boldsymbol{\delta}E$ vanishes, the iteration will come to a halt where $\boldsymbol{\delta}P_\perp$ vanishes, because the gradients are parallel,

$$\boldsymbol{\delta}P = \lambda \boldsymbol{\delta}E. \tag{209}$$

This condition constitutes the Euler-Lagrange (EL) equation of the extremal problem, with the proportionality constant λ being the Lagrange multiplier. Its concrete form depends on the choice of P and E. Since the solutions of the EL optimization represent local optima of the constrained P, we may repeat the search with randomly chosen $\mathbf{f}_0$ a number of times and select the best solution. The gradients at each point $\mathbf{f}_n$ may be obtained either from a calculation based on prior knowledge of the bath or experimentally from data measured in real time. A discretization of the time interval $0 \le \tau \le t$ then reduces the variational $\boldsymbol{\delta}$ to a finite-dimensional vector gradient $\boldsymbol{\nabla}$.

8.9. Optimal Gate Protection

8.9.1. Gate Error as Average Fidelity Decline. A particular application of our formalism is decoherence protection of a given quantum operation by bath-optimal minimal-energy control (BOMEC) [176, 185]. Consider the implementation of a predetermined quantum gate, that is, unitary operation within a given "gate time" t. It is sufficient to consider a pure input state $|\Psi\rangle$. In the interaction picture with respect to the desired gate operation and in the absence of bath effects, we should therefore observe at time t the initial state $|\Psi\rangle$. The quantity of interest is here the fidelity $\langle\Psi|\widehat{\varrho}(t)|\Psi\rangle$, and we use the projector $\widehat{P} = \widehat{\varrho}(0) = |\Psi\rangle\langle\Psi|$ as the gradient operator, so that (197) is satisfied and (198) gives the fidelity change as the score

$$P = \langle\Psi|\,\Delta\widehat{\varrho}\,|\Psi\rangle = -t^2\langle\langle\Psi|\,\widehat{H}^2|\Psi\rangle - \langle\Psi|\,\widehat{H}|\Psi\rangle^2\rangle_{\mathrm{B}}, \tag{210}$$

which is given by $\widehat{H}$ defined in (198).

Since a quantum gate is supposed to act on an unknown input state, we need to get rid of the dependence on $|\Psi\rangle$. One possibility is to perform a uniform average over all $|\Psi\rangle$. We may apply, (see [186, 187])

$$\overline{\langle\Psi|\,\widehat{A}\,|\Psi\rangle\,\langle\Psi|\,\widehat{B}\,|\Psi\rangle} = \frac{\mathrm{Tr}\,\widehat{A}\widehat{B} + \mathrm{Tr}\,\widehat{A}\,\mathrm{Tr}\,\widehat{B}}{d\,(d+1)} \tag{211}$$

which gives the average

$$\overline{P} = -t^2\frac{d}{d+1}\left\langle\widehat{H}^2\right\rangle_{\mathrm{id}}, \tag{212}$$

where $\langle\cdot\rangle_{\mathrm{id}} = \mathrm{Tr}[d^{-1}\widehat{I}\otimes\widehat{\varrho}_B(\cdot)]$. In (212), we have used $\mathrm{Tr}_S\widehat{H} = \widehat{0}$, which corresponds to $\mathrm{Tr}\,\widehat{S}_j = 0$ in Section 8.7. Because of this and because of (196), $\langle\widehat{H}\rangle_B = \langle\widehat{H}_I\rangle_B = \widehat{0}$, we have $\langle\widehat{H}\rangle_{\mathrm{id}} = 0$, and (212) also describes the variance $\mathrm{Var}(\widehat{H}) = \langle\widehat{H}^2\rangle_{\mathrm{id}} - \langle\widehat{H}\rangle^2_{\mathrm{id}}$. On the other hand, $\widehat{P} = -2k\widehat{\varrho}(0)$ that gives the change ΔS of entropy $S = -k\,\mathrm{Tr}(\widehat{\varrho}\ln\widehat{\varrho})$ is (up to a proportionality factor of $-2k$) the same as the $\widehat{P}$ used here to give the change of fidelity, and we have $\Delta S = -2kP$. If we define a *gate error* $\mathscr{E}$ as the average fidelity decline, $\mathscr{E} = -\overline{P}$, with $\overline{P}$ given in (212), we can summarize the following proportionalities: gate error $\equiv$ average fidelity decline $\sim$ average entropy increase (purity decline) $\overline{\Delta S}$ $\sim$ square (variance) of the average interaction energy $\widehat{H}$ as

$$\mathscr{E} \equiv -\overline{P} = \frac{\overline{\Delta S}}{2k} = t^2\frac{d}{d+1}\left\langle\widehat{H}^2\right\rangle_{\mathrm{id}} = t^2\frac{d}{d+1}\,\mathrm{Var}\left(\widehat{H}\right). \tag{213}$$

In the matrix representation of Section 8.7, the average over the initial states in the matrix $\boldsymbol{\Gamma}$ defined in (202) gives $\overline{\boldsymbol{\Gamma}} = -(d/(d+1))\mathbf{I}$ (using $\mathrm{Tr}(\widehat{S}_j\widehat{S}_k) = d\delta_{jk}$ and $\mathrm{Tr}\,\widehat{S}_j = 0$), so that

$$\mathscr{E} = \frac{d}{d+1}\int_{-\infty}^{\infty}\mathrm{d}\omega\;\;\mathrm{Tr}\left[\boldsymbol{\epsilon}_t(\omega)\,\boldsymbol{\epsilon}_t^\dagger(\omega)\,\mathbf{G}(\omega)\right] \tag{214}$$

in agreement with [176] (except a different normalization $\mathrm{Tr}(\widehat{S}_j\widehat{S}_k) = 2\delta_{jk}$ leading there to a prefactor $(2/(d+1))$). From the requirement that $\mathscr{E} \ge 0$ must hold for any positive semi-definite matrix $\boldsymbol{\epsilon}_t(\omega)\boldsymbol{\epsilon}_t^\dagger(\omega)$, we conclude that $\mathbf{G}(\omega)$ must be a

positive semi-definite matrix for any ω. The task of BOMEC is then to find a system evolution $\widehat{U}(\tau)$ (cf. the control examples in the previous section) that minimizes $\mathscr{E}$, subject to the boundary condition that the final $\widehat{U}(t)$ is the desired gate.

8.10. Comparison of BOMEC with DD. It is appropriate to compare the effect of dynamical decoupling (DD) [82, 188] with that of BOMEC. DD does not change with the bath spectrum $\mathbf{G}(\omega)$. With an increasing number of pulses, DD shifts the weight of the system spectrum $\mathbf{F}(\omega)$ towards higher frequencies, until the overlap equation (206) has become sufficiently small. This is illustrated for two different numbers of pulses of periodic DD (PDD, pulses periodic in time), in the upper row of Figure 17 in the case of a 1D single qubit modulation (i.e., all pulses are given by an arbitrary but fixed Pauli matrix).

Aperiodic DD such as UDD [188] suppresses low-frequency components (to the left of the main peak) in the system spectrum, which retain the system-bath coupling even if the main peak of the system spectrum has been shifted beyond the bath cut-off frequency (Figure 17). The plots indicate that this suppression of low frequency components is achieved at the price of a smaller shift of the main peak; that is, shifting the main peak beyond a given cutoff requires more pulses in UDD than in PDD. Note that optimized DD sequences with improved asymptotics exist [189], which we will not consider here.

System modulation spectra obtained with BOMEC are shown in Figure 18.

The plot refers to a qubit subject to pure dephasing (i.e., Z-coupling) by a bath whose spectrum $G(\omega)$ has a Lorentzian peak and low-frequency tail. The BOMEC optimizes $\widehat{U}(\tau)$ simultaneously for 3D Pauli matrix couplings to the bath (Z, Y, and X). The resulting system spectrum $F(\omega)$ is shown for different energy constraints E which are increased in small and equal steps. For low E, $F(\omega)$ has a single peak on the left of the bath peak. Increasing E causes a second peak of $F(\omega)$ to emerge on the right of the bath peak, which continues to grow, while the peak on the left diminishes, until for high E, only the right peak remains. Figure 18 hence demonstrates that the spectrum $F(\omega)$ generated by BOMEC changes continuously as E increases but avoids overlap with the maxima of $G(\omega)$ irrespective of E. BOMEC can therefore be superior to all forms of DD including UDD, especially if the bath has high cutoff but bandgaps at low frequencies.

8.11. Purity Control of a Qubit. To give an example of the opposite case, where the goal is to maximize the system-bath coupling, we apply our approach of constrained optimization to the linear entropy $S_L = 2[1 - \mathrm{Tr}(\widehat{\varrho}^2)]$ of a qubit (note that here S_L has been normalized to 1 by setting the coefficient $k = d/(d-1) = 2$, cf. Section 8.8). We assume an initial mixture

$$\widehat{\varrho}(0) = p\,|1\rangle\langle 1| + (1-p)\,|0\rangle\langle 0| \tag{215}$$

of a ground (excited) state $|0\rangle$ ($|1\rangle$), where $0 \le p \le 0.5$ is related to S_L by $p = (1 - \sqrt{1 - S_L})/2$. With $\widehat{S}_j = \widehat{\sigma}_j$ denoting for $d = 2$ the Pauli matrices, (215) can be written in terms of $\widehat{H}_0 = (\omega_0/2)\widehat{\sigma}_3$ as $\widehat{\varrho}(0) = (e^{-\beta\widehat{H}_0}/\mathrm{Tr}(e^{-\beta\widehat{H}_0})) = (|1\rangle\langle 1|/(1 + e^{\beta\omega_0})) + (|0\rangle\langle 0|/(1 + e^{-\beta\omega_0}))$, where $\beta = \ln(p^{-1} - 1)/\omega_0$ is the inverse temperature. Purity and temperature are hence related via the energy scale ω_0. Our goal is a constrained optimization of ΔS_L, that is, $\widehat{P} = -4\,\widehat{\varrho}(0)$ in (189). Unlike the gate error equation (213), ΔS_L can be negative or positive, which can be understood as cooling or heating, respectively.

The time evolutions resulting from a minimization of ΔS_L for the initial state equation (215) are illustrated in Figure 19. The optimization refers to a bath spectrum as shown in Figure 20. The f_j shown in Figure 19(a) are defined by $\widehat{U}(\tau) = e^{-(i/2)f_3(\tau)\widehat{\sigma}_3}e^{-(i/2)f_2(\tau)\widehat{\sigma}_2}e^{-(i/2)f_1(\tau)\widehat{\sigma}_3}$, whereas the ω_j shown in Figure 19(b) are given by $\widehat{H}_S(\tau) = \sum_j \omega_j(\tau)\widehat{\sigma}_j$. The chosen constraint $E = (1/2)\int_0^t d\tau\,\mathrm{Tr}(H_S - \widehat{H}_0)^2(\tau)$ can be written in terms of the f_j as $E = (1/4)\int_0^t dt_1[\dot{f}_1^2 + \dot{f}_2^2 + (\dot{f}_3 - \omega_0)^2 + 2\dot{f}_1(\dot{f}_3 - \omega_0)\cos f_2]$. (Note that we have set $\hbar = 1$, so that the dimension of energy becomes inverse time and hence corresponds to that of angular frequency. By measuring time in units of some characteristic correlation time of the bath chosen in the plots, time, energy, and angular frequency have been made dimensionless.) The overlap between the evolving system state $\widehat{\varrho}(\tau)$ (in the Schrödinger picture) and the ground state $|0\rangle$ shown in Figure 19(c) indicates the fast unitary system modulation through short time population inversions without significantly altering the state purity as verified in Figure 19(d). This can be visualized as fast π-rotations of the state inside the Bloch sphere, which, together with smaller rotations, here result in the final reduction of $S_L(t)$ seen in Figure 19(d). Figure 19(d) also confirms that for the chosen time and coupling strength, differences between various methods of approximation are small.

In contrast to gate protection, no initial-state averaging is performed here, that is, (215) is known. Consequently, as Figure 20 shows, the relevant components $F_j \equiv (\mathbf{F}_t)_{jj}(\omega)$ of the system modulation spectrum contributing to the spectral overlap Equation (206) depend on the initial state $\widehat{\varrho}(0)$ via the matrix $\mathbf{\Gamma}$ Equation (202). (We assume an uncorrelated bath, that is, $G_{jk}(\omega) = 0$ for $j \neq k$ and $G_j \equiv G_{jj}(\omega)$.) This influence is clearly visible in case of a constant (unmodulated, i.e., free) Hamiltonian (middle column), for which we set $\omega_0 = 2\pi/t$ with the final t being in the order of the bath correlation time. Cooling (heating) is achieved by realizing negative (positive) ΔS_L via maximum negative (positive) spectral overlap, as shown in the left (right) column of Figure 20. This is the opposite to system-bath decoupling, where the goal is to minimize the overlap.

The plots illustrate the role of the energy constraint E: increasing E allows to establish overlap with higher frequency components of the bath spectrum. This also suggests that for a bath spectrum with a finite frequency cutoff, increasing E beyond a certain saturation value will not lead to further improvement of the optimization. In the time domain, increasing E leads to more rapid changes in the physical Hamiltonian, however, requiring higher resolution of the numerical treatment. On the contrary, for attempted cooling

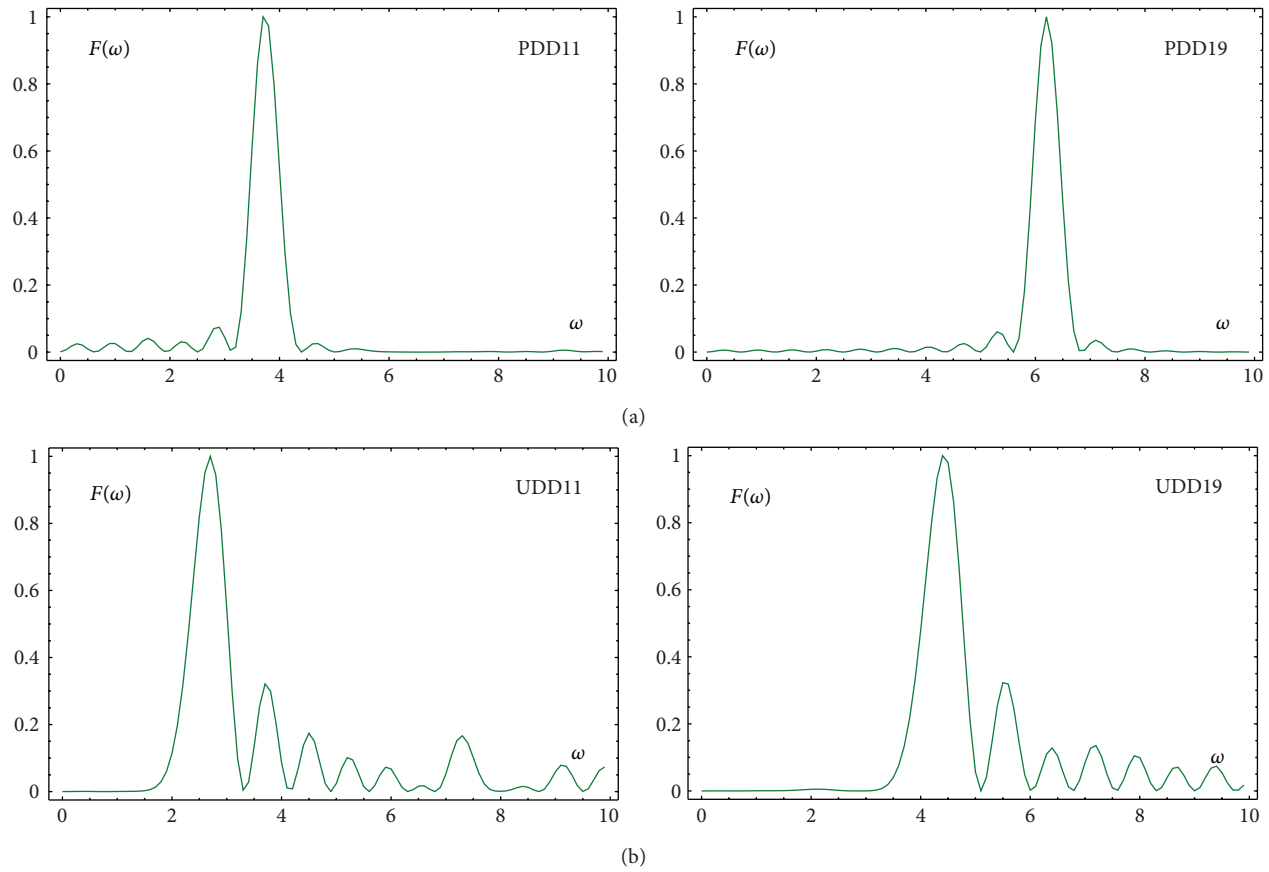

FIGURE 17: System modulation spectra $F(\omega)$ (scaled to 1 with respect to their maximum value, scaling of ω as in Figure 18) generated by two methods of DD. Upper row: periodic dynamical decoupling with $n\pi$-pulses (PDDn), lower row: Uhrig dynamical decoupling with the same number of π-pulses (UDDn), compared for $n = 11$ (left column) and $n = 19$ (right column) pulses (color online).

(heating) by minimization (maximization) of ΔS_L, a given E may be too small to lead to negative (positive) ΔS_L. The obtained ΔS_L may then be understood as "reduced heating" (reduced cooling) as compared to a ΔS_L obtained with an unmodulated $\widehat{H}_0$. This is shown in Figure 21. The figure also illustrates once more that the $\widehat{\varrho}(0)$ dependence of the spectra shown in Figure 20 is accompanied by a $\widehat{\varrho}(0)$ dependency of the achievable change ΔS_L for a given bath. For a maximally mixed state in particular ($p = 0.5$), the matrix $\mathbf{\Gamma}$ equation (202) vanishes and with it ΔS_L.

A possibility to achieve negative (positive) ΔS_L by its minimization (maximization) even for weak modulation (i.e., for small E) is to adapt the temperature of the bath such that for an undriven system Hamiltonian $\widehat{H}_0$, no change is observed, $\Delta S_L = 0$, which is a necessary condition for a system-bath equilibrium. This would require nonunitary system modulation, for example, the effect of repeated measurements [191–193].

8.12. Bound Estimation. Our goal is to give constraint-independent upper and lower bounds for the maximum change $P = \mathrm{Tr}(\widehat{P}\Delta\widehat{\varrho})$ that can be achieved with a given bath and $\widehat{P}$ under the condition (197). We assume that $\boldsymbol{\epsilon}$, $\mathbf{\Gamma}$, and $\mathbf{G}(\omega)$ are quadratic $(d^2 - 1)$-dimensional matrices. If $\max[\mathrm{Tr}\,\mathbf{G}(\omega)] < \infty$, we can estimate P by using that $\mathrm{Tr}(\mathbf{AB}) \leq \mathrm{Tr}(\mathbf{A})\,\mathrm{Tr}(\mathbf{B})$ for positive semi-definite matrices $\mathbf{A}$, $\mathbf{B}$ and applying Hölder's inequality in the form of $\int_{-\infty}^{\infty} d\omega |f(\omega)g(\omega)| \leq \sup\{|g(\omega)|\} \int_{-\infty}^{\infty} d\omega |f(\omega)|$. Decomposing $\mathbf{\Gamma} = \mathbf{\Gamma}_1 - \mathbf{\Gamma}_2$ into positive semi-definite matrices $\mathbf{\Gamma}_i$ and making use of $(1/t)\int_{-\infty}^{\infty} d\omega \boldsymbol{\epsilon}_t{}^{\dagger}(\omega)\boldsymbol{\epsilon}_t(\omega) = \widehat{I}$, we thus get

$$-P_2 \leq P \leq P_1, \quad P_i = t \sup\left[\mathrm{Tr}\,\mathbf{G}(\omega)\right] \mathrm{Tr}\,\mathbf{\Gamma}_i. \tag{216}$$

This reveals that for given t and $\mathbf{G}(\omega)$, the bounds P_i depend on $\widehat{\varrho}(0)$ and $\widehat{P}$ via $\mathbf{\Gamma}$.

9. Discussion

A comprehensive approach for dynamical protection of quantum information processing (QIP) systems from the deleterious effects of decoherence was presented. Below, we discuss several theoretical and practical implications of this general approach. We first examine the temporal and spectral domains in order to increase our understanding of the underlying physical mechanisms of dynamical decoherence control. A practical approach, whereby one uses the universal decoherence control formalism to first reconstruct the noise

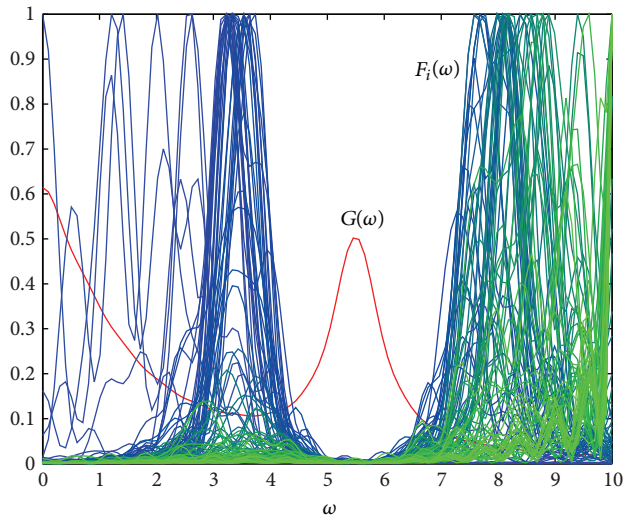

FIGURE 18: BOMEC minimization of the gate error for a single qubit π-gate caused by pure dephasing with a given bath spectrum ($G(\omega)$, bold red line, scaled to 0.61 with respect to its maximum value, scaling of ω with respect to the chosen bath resonance, i.e., in units of the inverse bath correlation time). The Z-components of the obtained system modulation spectra $F_i(\omega)$ are shown for energy constraints $E_i = 0.1 + 4(i-1)$, $i = 1, 2, \ldots, 101$, (thin lines, blue to green) individually scaled to 1 (color online).

spectra and then optimize the modulation to combat decoherence in experimental scenarios is then discussed. We next consider a theoretical approach, whereby one gains insight into the mechanism and dynamics of entanglement, which is both an essential resource for QIP and the main reason for decoherence.

9.1. Temporal and Spectral Aspects. The universal dynamical decoherence control formula was first developed for single qubit decay due to interaction with a zero-temperature bath in Section 3 [97, 102] and was later extended to decay and dephasing due to interaction with finite-temperature baths in Section 7 [100, 124] and finally to multipartite systems in Section 8. One can examine the universal dynamical decoherence and disentanglement formalism presented above from two complementary perspectives, namely, the time and spectral domains.

9.1.1. Temporal Domain. In the temporal domain, one can express the gist of the formalism by the following equation [104, 107]:

$$R_{ij}(t) = \int_0^t dt' \Phi_{ij}\left(t - t'\right) \epsilon_i(t) \epsilon_j^*\left(t'\right), \tag{217}$$

where $R_{ii}(t)$ is the decoherence rate (either due to decay or dephasing) of the ith qubit, $R_{ij}(t)$ is the average cross-decoherence of qubits i and j, $\Phi_{ii}(t)$ is the bath response (or memory) function due to coupling of qubit i, $\Phi_{ij}(t)$ is the cross-response function due to coupling of qubits i and j, and $\epsilon_i(t)$ is the temporal modulation function of qubit i.

The bath response function is usually associated with a characteristic correlation or memory time, t_c, which separates the non-Markovian ($t \ll t_c$) and the Markovian ($t \gg t_c$) temporal regimes, for example, $\Phi(t) \propto e^{-t/t_c}$. Within the bath memory time, the bath modes oscillate coherently and in unison and maintain "memory" of their interaction with the system, whereas after the correlation time has passed, the modes lose their coherent oscillations and "forget" their prior interactions [178].

The temporal modulation function usually has two factors, namely, a system factor of the form $e^{i\omega_a t}$, where $\hbar\omega_a$ is the energy separation of the two-level system, and a modulation or control factor that can represent either amplitude ($\widetilde{\epsilon}(t)$) or phase ($\phi(t)$) modulation, $\epsilon(t) = \widetilde{\epsilon}(t) e^{i\omega_a t + i\phi(t)}$.

In order to affect the system-bath coupling and control, or modulate the decoherence due to this coupling, one must dynamically modulate the system faster than the correlation time. Slower modulation will have no effect on the loss of coherence and will thus not be able to control it. Modulating the system faster than the correlation time can effectively "reset" the clock. Applying a modulation sequence repeatedly can thus drastically change the decoherence and impose a continued coherent evolution of the system-bath coupling [86, 178].

Moreover, during the short non-Markovian time regime, the decoherence rates are time dependent and may even acquire a negative sign [178]. This can result in novel behavior such as rapid cooling of a system coupled to a finite temperature bath, below the bath temperature. By repeatedly disturbing the free evolution by frequent measurements or phase modulations, one can maintain this behavior of the time-dependent decoherence rate over long times and thus accumulate the short-time cooling.

Another novel feature that is apparent from (217) is the effect of local modulations on cross decoherence, where local modulations refer to different modulation of each qubit, $\epsilon_i(t) \neq \epsilon_j(t)$. Due to the phase difference of the local modulations, one can exploit interference effects between two decoherence channels. As shown in Section 8 [123], by applying different modulation to each qubit, faster than the cross correlation time, one can create destructive interference and thus eliminate the cross decoherence. On the other hand, by applying tailored modulations to different qubits, one can create constructive interference that can generate a decoherence-free subspace (DFS).

9.1.2. Spectral Domain. In the spectral domain, one can express the same decoherence rate as in (217) by the following equation:

$$R_{ij}(t) = 2\pi \int_{-\infty}^{\infty} d\omega G_{ij}(\omega) F_{t,ij}(\omega), \tag{218}$$

$$F_{t,ij}(\omega) = \frac{1}{t} \epsilon_{t,i}(\omega) \epsilon_{t,j}^*(\omega), \tag{219}$$

where $G_{ii}(\omega)$ is the coupling spectrum of the ith qubit to the decohering bath (either a decay-inducing bath, a dephasing-inducing bath, or the spectrum of the classical proper-dephasing), $G_{ij}(\omega)$ is the cross-coupling spectrum of qubits i

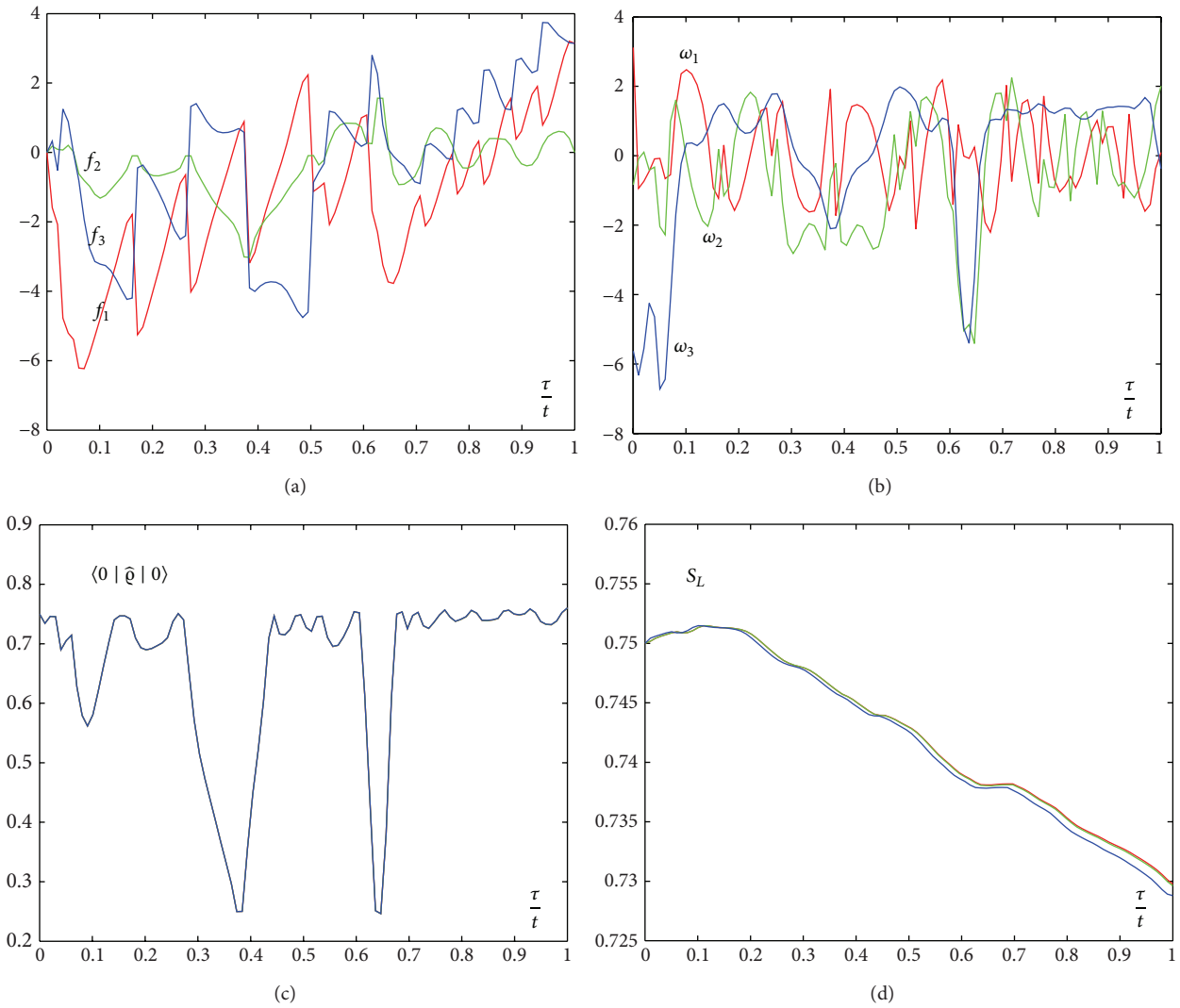

FIGURE 19: Evolution within $0 \leq \tau \leq t$ for an optimized cooling with initial $p = 0.25$ of (a) effective and (b) instantaneous controls (1 red, 2 green, and 3 blue graphs show x, y, and z component), (c) ground state overlap of the system state, and (d) linear entropy (upper red, middle green, and lower blue graphs show numerical integration of the time-convolutionless equation [190], of the Nakajima-Zwanzig equation, and second-order approximation of the solution as given in (192), respectively, which are all indistinguishable in (c)) (system-bath coupling strength $\kappa = 10^{-2}$, $\omega_0 = 2\pi/t$, $t = 10$ in units of effective bath correlation time, $E = 100$) (color online).

and j, and $\epsilon_{t,i}(\omega)$ is the ith qubit time-dependent modulation spectrum.

The temperature-dependent coupling spectrum is the Fourier transform of the bath response function in (217), and it usually has a certain width proportional to the inverse of the correlation time. The time-dependent modulation spectrum is the finite-time Fourier transform of the modulation function, $\epsilon_i(t)$.

Equation (218) identifies the source of decoherence as the coupling of the time-dependent modulated system to the bath modes. Thus, for an unmodulated system in the long-time regime, the single-qubit modulation power spectrum given by $F_{t,ii}(\omega) = |\epsilon_{t,i}(\omega)|^2$ becomes a δ-function centered at the system energy-separation, ω_a. This Golden Rule result can be viewed as the coupling between the system and the corresponding mode of the bath, with coupling strength $G(\omega_a)$.

However, one can analyze more complex scenarios using (218). The modulation spectrum is a time-dependent function and for an unmodulated system it becomes a sinc function with a time-dependent width. For short times, the modulation spectrum is wide, expressing the time-energy uncertainty, whereby the system energy separation is not well defined and the system is effectively coupled to many bath modes. Depending on the coupling spectrum, $G(\omega)$, the decoherence rate oscillates and can acquire negative values, until, after the correlation time, it settles to the Golden Rule value, expressing the well-defined energy separation.

Another important insight gained from the frequency-domain analysis is the optimal shape of the modulation

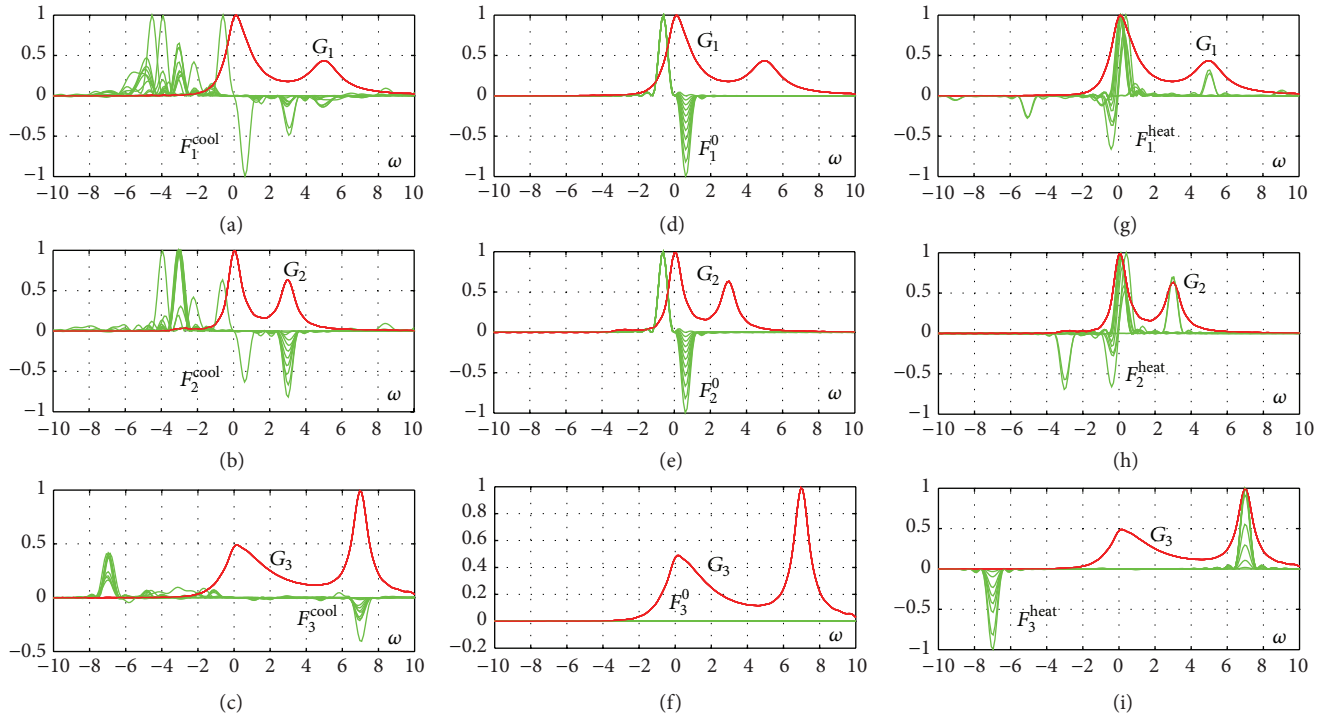

FIGURE 20: Cooling and heating of a TLS by minimization (left: (a), (b), (c)) and maximization (right: (g), (h), (i)) of the change of linear entropy for a given bath spectrum (G_j, red) with $j = 1, 2, 3$ denoting x, y, and z components. The optimized system spectra (F_j, green) are shown for an energy constraint $E = 10^2$ (left) and $E = 10^3$ (right) as contrasted to the unmodulated Hamiltonian $\widehat{H}_0$ (i.e., for $E = 0.001, 0.05, 0.1, \ldots, 0.45, 0.499$). All graphs are individually scaled to 1 with respect to their maximum value, and scaling of ω is the same as in Figure 18 (color online).

that reduces the decoherence rate. Given a specific coupling spectrum, one should choose a modulation so as to decrease the overlap between the modulation and coupling spectra [104]. This optimal modulation means that the system is effectively coupled to bath modes with lower coupling strength. Furthermore, since the coupling spectrum has a width proportional to the inverse correlation time, in order to reduce decoherence one should drive the system with a higher frequency than this width, that is, faster than the correlation time. One can also choose to increase the decoherence (i.e., impose the anti-Zeno effect) by applying a modulation that would couple the system to more strongly-coupled bath modes.

Finally, cross decoherence can be understood from the spectral-domain analysis as the coupling of two systems via common bath modes; that is, (218) is the overlap of three functions, namely, cross coupling spectrum and the individual modulation spectra of the two systems. For example, if two systems couple to different modes, then in the absence of modulations, they will not experience any cross decoherence. Hence, in order to impose cross decoherence, one should modulate the systems in such a way that they effectively couple to the same modes with the same strength. On the other hand, if one wishes to eliminate cross decoherence, one should apply local modulations, such that the modulation spectra have different peaks, which would result in the two systems coupling to different modes and thus experiencing no cross decoherence.

9.2. A User Manual for Decoherence Control. The goal of any practical modulation scheme is to reduce, or, if possible, eliminate, all the elements of the decoherence matrix in (218) (see [123] for an alternative solution). However, in order to obtain the optimal modulation [104], one must first know the system-bath coupling spectra of the qubits in question. This information is usually not available *a priori* and thus most experimentalists have resorted to the suboptimal dynamical-decoupling (or bang-bang) modulation, which does not require this knowledge.

Instead, we suggest a practical and general two-step approach to optimally combat decoherence.

(1) Use known, prescribed modulations to reveal the unknown decoherence parameters, that is, the system-bath coupling spectra.

(2) Tailor optimal modulations for the obtained parameters.

9.2.1. Use of Modulations to Reconstruct Coupling Spectra. Equation (218) can be expressed via three matrices: (i) The coupling spectra matrix, $G_{ij}(\omega)$, is usually unknown and is the objective of this analysis. (ii) The modulation power spectra matrix, $F_{t,ij}(\omega) = (1/t)\epsilon_{t,i}(\omega)\epsilon^*_{t,j}(\omega)$, can be calculated for each specific *known* modulation. (iii) The average decoherence matrix, $R_{ij}(t)$, can be experimentally obtained via measurements of the decohering system.

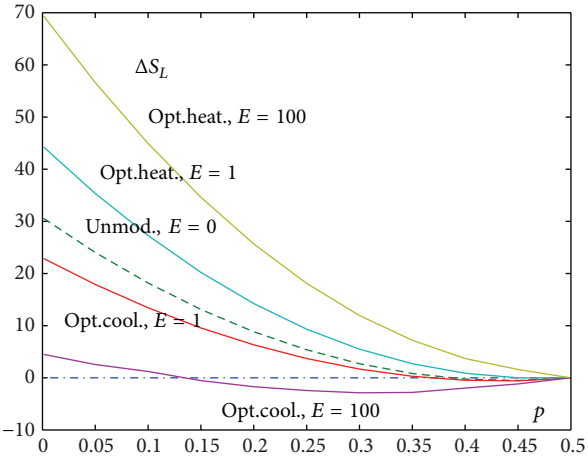

FIGURE 21: Change of linear entropy in units of the system-bath coupling strength obtained by minimization (attempted cooling) and maximization (attempted heating) of ΔS_L under different constraints $E = 0, 1, 100$ as a function of the initial p for a bath as shown in Figure 20 (color online).

Thus, the protocol outlined here is to use a parameterized modulation arsenal (see [124] for a comprehensive analysis of modulation pulses) and measure the decoherence rate for each such modulation. This results in a vector of decoherence rates that depends on the modulation parameters. By using simple numerical methods, one can then find the coupling spectrum that best fits the calculated $(F_{t,ij}(\omega))$ and the measured $(R_{ij}(t))$ quantities.

For example, one can apply to a single qubit an impulsive phase modulation, $\epsilon(t) = e^{i[t/\tau]\phi}$, with varying phase ϕ and pulse intervals τ. This can be applied as a time-dependent AC-Stark shift to combat decay or a time-dependent resonant field to combat dephasing [100, 107]. This modulation scheme has the following power spectrum:

$$F_{n\tau}(\omega) = \frac{2\sin^2(\omega\tau/2)\sin^2[n(\phi+\omega\tau)/2]}{\pi n\tau\omega^2\sin^2[(\phi+\omega\tau)/2]}, \qquad (220)$$

where $n = [t/\tau]$.

For each modulation parameters pair, $\{\phi, \tau\}$, one experimentally measure the average decoherence rate of the qubit, $R(t)$ (either decay of an initially excited state or dephasing of an initial superposition of ground and excited states). Then one runs a simple numerical algorithm that finds the coupling spectrum, $G(\omega)$, that best fits the observed results.

An alternative approach to obtain the coupling spectrum is to use the fact that within the bath response (memory) time, the decoherence rate changes with time, even if no modulation is applied. Thus, for non-Markovian time scales and no modulation, the "modulation" power spectrum is given by a sinc function. Measuring the excited-state population (for decay control) or coherence (for dephasing control) for short times compared to the bath response time should reveal a nonexponential, nonmonotonic decoherence and thus divulge the underlying coupling spectrum.

Furthermore, if one has a multipartite system, and thus a decoherence matrix, one must perform multiple modulation schemes that address the different qubits, on top of performing the aforementioned single-qubit scheme for all the qubits. This is essential to ascertain the cross-coupling spectra of all the possible qubit pairs. As discussed in [107, 123, 126], these cross-coupling spectra are extremely important in reducing disentanglement and allow, in certain circumstances, a complete elimination of decoherence.

To summarize, the methods of applying different modulations or measuring decoherence at different times effectively sample the frequency space, ω, and thus address different bath modes and allow measuring their coupling strength to the system. Thereafter, one can numerically obtain the coupling spectra that best fits the measured data.

9.2.2. Optimal Modulation for Decoherence Control. After one obtains the system-bath coupling spectra by applying specific, parameterized modulation schemes, one can finally tailor the specific modulation that would optimally reduce or eliminate decoherence. However, two aspects should be considered carefully, namely, the specific QIP application used and the specific modulation constraints.

As shown in [107, 125, 126, 183], each QIP application has its own figure-of-merit that assesses the effectiveness of the dynamical decoherence control scheme. In general, we have shown that this effectiveness is related to the decoherence matrix of the form given by (218). Yet, if some of its elements cannot be drastically reduced, one can still have a dramatic effect and increase the appropriate figure of merit.

We have shown in Section 8 [107] that if the systems in question have three levels, one can completely eliminate decoherence and disentanglement by imposing a special symmetry using the appropriate modulation. Thus, even if drastic reduction of all the decoherence matrix elements is not possible, then by using local modulations, one may equate the intraparticle elements, eliminate the interparticle elements, and code the quantum information in the ground and antisymmetric "dark" state of the two excited levels and consequently completely preserve coherence and entanglement.

Furthermore, we have shown [125, 137] that, in multiqubit quantum computation, it is vital to consider all possible modulations and fields, and not only those that directly perform a quantum logic gate. Thus, while usually one only requires the optimization of the fields applied to perform the gate, we have stressed that the gate fidelity can be greatly increased if one also applies and optimizes all other possible fields.

However, these schemes can only be applied after obtaining an approximate form of the system-bath coupling spectra, without which one cannot tailor the local modulations that equate or eliminate specific elements of the decoherence matrix.

In any optimization problem, one must consider the constraints of the modulations. In [104], we have considered an energy constraint of the resonant field applied in order to optimally reduce dephasing and have derived the appropriate Euler-Lagrange equation. However, an experimental system may have additional constraints, such as the dynamical range of the modulator, other resonances within the system, heating, and so forth. Each such scenario must be taken

into account when considering the available repertoire of modulation parameters. Usually, one will have to resort to numerical optimization given the system-bath coupling spectra matrix and the possible modulations.

To summarize, after obtaining the general shape of the system-bath coupling spectra matrix of the multipartite system by applying parameterized, known modulations, one can optimize the appropriate QIP-dependent figure of merit while obeying the constraints of the available modulations.

9.3. Entanglement: Decoherence Interplay. Entanglement is the main resource of quantum information processing, without which quantum computation will not be faster than its classical counterpart [3] and quantum communication protocols will not work [194–196]. Moreover, as shown in [194–196], the impact of nonmaximally entangled quantum channels is identical to a nonmaximally entangled Bell measurement. Thus, entanglement is crucial for all nonlocal stages of quantum protocols, namely, the quantum channel preparation as well as bipartite Bell measurement.

However, entanglement is also the main source of decoherence, when the decohering agent is a quantum bath (as opposed to classical proper dephasing [100, 107, 125]). We have shown here that a similar formula for dynamical decoherence control, (218) is obtained for decay and dephasing due to coupling to a bath of harmonic oscillators. In these scenarios, as well as the scenario detailed in [178], the source of decoherence is the entanglement of the system to the bath's degrees of freedom. Because the latter are inaccessible to both modulation and probing, they are traced out and this results in loss of coherence of the system.

Nevertheless, not all is lost when interacting with a bath. During short times, much shorter than the bath memory times, the system and bath still interact coherently and the effects of the bath can be remedied by applying the appropriate modulations. This can understood from (218) by noting that the width of $G(\omega)$ is proportional to the inverse of the memory time. Thus, one can apply rapidly repeating modulations, corresponding to a multipeaked modulation power spectrum, where the peaks are positioned at the high frequency range. The spectral overlap between the system-bath coupling spectrum and the modulation power spectrum can be greatly reduced if the modulations are temporally separated by a shorter interval than the bath correlation time.

These frequent modulations can be viewed as driving the system to higher frequencies in which the bath modes are dramatically more weakly coupled than those modes coupled without modulation. This reduced coupling results in less entanglement with the bath modes and thus less decoherence.

A novel interplay between entanglement as a QIP resource and entanglement as the source of decoherence was detailed in Section 8 [126]. Two entangled qubits were analyzed, each coupled to a bath via common modes. The non-Markovian time scale was considered, as well as dynamical modulations. It was shown how the entanglement of the qubits could vanish after a finite time (entanglement sudden death—ESD), but later restored by non-Markovian modulation-induced oscillations of the system-bath coherence.

Thus, an exchange between two-qubit entanglement and system-bath entanglement may take place and be dynamically controlled by modulations. If the systems couple to two baths that have common modes, one can observe the transfer of coherence and buildup of entanglement between the two systems via these modes. If, on the other hand, the baths were completely separate, the coherence transfer between each system and its bath can modulate the amount of system-system entanglement, first lost and then regained.

Another striking example of entanglement-mediated dynamics was presented in [178]. There we considered a two-level system that first reaches the state of equilibrium with a bath of harmonic oscillators, a state in which large system-bath entanglement is present, but no further dynamics. Then, a quantum probe is coupled to the system and performs a quantum nondemolition (QND) measurement of the system's excited-level population. This QND measurement results in system-probe entanglement and the consequent loss of system-bath coherence, or vanishing of the off-diagonal elements of the system-bath density matrix. After this impulsive, nonselective, QND measurement, the state is no longer in equilibrium and begins to evolve.

We have shown that immediately after the measurement the system and bath always "heat up", that is, get excited. Remarkably, for certain system-bath coupling spectra, one can also observe a system that has lower excited-state population than the equilibrium state, that is, a purer system. This occurs despite the fact that the system has effectively recoupled with the bath and has become entangled with it.

This interplay between system-bath entanglement, and system-probe entanglement and its effect on system cooling is still under active investigation by our group.

Entanglement in open systems is a fascinating concept that is not yet fully understood. It is essential for QIP, yet it is also the origin of decoherence. The interplay between system-system entanglement, system-probe entanglement and system-bath entanglement on non-Markovian timescales is an intriguing field that deserves more attention.

10. Conclusions

In this paper, we have expounded our universal approach to the dynamical control of qubits subject to AN and PN, by either off- or on-resonant modulating fields, respectively. It is based on a general non-Markovian master equation valid for weak system-bath coupling and arbitrary modulations, since it does not invoke the rotating wave approximation. The resulting universal convolution formulae provide intuitive clues as to the optimal tailoring of modulation and noise spectra. Our analysis of multiple, field-driven, qubits which are coupled to partly correlated or independent baths or undergo locally varying random dephasing has resulted in the universal formula (129) for coupling to zero-temperature bath, and (61) for Bell-state preservation under local proper dephasing.

Our general analysis allows one to come up with an optimal choice between global and local control, based on the observation that the maximal suppression of decoherence is

not necessarily the best one. Instead, we demand an optimal *phase-relation* between different, but *synchronous,* local modulations of each particle. The merits of local versus global modulations have been shown to be essentially twofold:

(i) Local modulation can effectively decorrelate the different proper dephasings of the multiple TLS, resulting in equal dephasing rates for all states. For two TLS, we have shown that the singlet and triplet Bell states acquire the same dynamically modified dephasing rate. This should be beneficial compared to the standard global "Bang-Bang" (π-phase flips) if both states are used (intermittently) for information transmission or storage.

(ii) For different couplings to a zero-temperature bath, one can better preserve any initial state by using local modulation which can reduce the decay as well as the mixing with other states, than by using global modulation. It was shown that local modulation which eliminates the cross decoherence terms increases the fidelity more than the global modulation alternative. For two TLS, it was shown that local modulation better preserves an initial Bell state, whether a singlet or a triplet, compared to global π-phase "parity kicks."

In this paper, we have expounded our comprehensive approach to the dynamical control of decay and decoherence. Our analysis of dynamically modified coupling between a qubit and a bath has resulted in the universal formula (25) for the dynamically modified decay rate into a zero-temperature bath, as well as its counterparts (121) for excited- and ground-state dynamical decay into finite-temperature baths. This ground-state dynamically induced decay results from RWA violation by ultrafast modulation. For multilevel systems with partly interfering decaying levels (Section 5), the merits of *global* (common to all levels) versus *local* (specific to each level) modulations have been compared.

The previous ground-breaking works on dynamical decoupling [80–87, 118] are more restrictive than the universal approach detailed in Sections 2–5 of this paper.

(i) In most works [82–87], the coupling between the system and the bath had only proper dephasing elements, that is, $H_I = \hbar\sigma_z \sum_\lambda (\kappa_\lambda a_\lambda + \kappa_\lambda^* a_\lambda^\dagger)$. This coupling means that there is no population decay to the bath and the decoherence is only via the phase. In other pioneering works [80, 81, 118], off-diagonal coupling to a Lorentzian bath was considered within the rotating-wave approximation (RWA). The Hamiltonians in all of these works should be contrasted with the more general Hamiltonians, 1, which account for both dephasing and decay into arbitrary baths, without the RWA.

(ii) The "parity kicks" [80, 118] or "bang-bang" (BB) pulses have usually been considered [81–87] to be so strong and fast that during the pulses there is no coupling to the bath, while between the pulses there is natural evolution of the system coupled to the bath. By contrast, the approach outlined in the present paper allows for modulations that are effected *during* the coupling to the bath.

(iii) The BB pulses [82] that have been previously proposed flip the phase of the system state by π, so that to achieve suppression of the decoherence. In particular, in [86] it was shown that the use of BB pulses results in suppression of the low-frequency modes of the spectral density, thus effectively suppressing the decoherence due to $1/f$-type spectral densities. The BB pulses formalism then yields for $R_d(t_{2N})t_{2N}$ the same expression (see [83], Equation (4)) as our universal approach, if one chooses in our (129) the specific form [83] $G_d(\omega) = \coth(\beta\omega/2)G(\omega)$ and adopts

$$F_{t_{2N}}(\omega) = 2\tan^2\left(\frac{\omega\tau}{2}\right)\frac{1-\cos\omega t_{2N}}{\pi\omega^2 t_{2N}}, \tag{221}$$

which coincides with our result in (52) upon setting $\phi = \pi$ and $n = 2N$, $t_{2N} = 2N\tau$.

(iv) As shown in Section 7.3.2, a new field may be more effective (much less energy consuming) in suppressing proper dephasing as BB pulses.

(v) The pioneering results [80, 108, 118] on dynamical suppression of decay into a Lorentzian or Gaussian bath coincide with ours, advocating $\phi = \pi$ phase flips as the most appropriate (48). However, our more general results and (123) identify small periodic phase shifts $\phi \ll 1$ as being far more suitable near the Debye cut-off frequency of a phonon bath.

(vi) Our innovative treatment of *multilevel decay via coupling to partly correlated* baths in Section 5 gives a flavor for the pros and cons of decay suppression via local versus *global* phase modulations.

(vii) The ground-breaking theory and experiment [106] concerning decay to the continuum in a periodically tilted washboard potential coincide with our results on amplitude modulation (Section 3.6), but our treatment also covers other parameter ranges, suitable for modulated Josephson junctions [100].

In Section 6, we have outlined a method complementary to the one in Sections 2–5. We have demonstrated that a "counterintuitively" ordered sequence of abrupt changes of the detuning between an atomic transition and a continuum edge (the photonic band cutoff) is able to protect the atomic state from spontaneous emission more effectively than the intuitively obvious alternative, which is to fix the resonance frequency well within the forbidden bandgap, as far as possible from the continuum edge. This method is effective even under conditions of *strong coupling to the continuum*, since it is based on phase-dependent changes of the atomic state that is "dressed" by the continuum, rather than on modulation of the "bare" state that is weakly perturbed by the bath [81, 99, 118], as opposed to all previously proposed dynamical modulation strategies [81, 97, 99, 118], including that of Sections 2–5. The ability to maintain high fidelity of quantum states and quantum-logic operations in

the presence of decoherence by nonadiabatic interference, contrary to the prevailing adiabatic approach to quantum-state control [1, 11, 12, 129, 142], may pave the way to new methods of controlling decay and decoherence in spectrally structured continua [2, 85, 87, 119].

Peculiarity of the Approach. In summary, we have considered a way of finding a time dependence of the system Hamiltonian over a fixed time interval such that a given system observable attains a desired value at the end of this interval. The peculiarity of our approach is that it relies on knowledge of the bath coupling spectrum and adapts the spectrum of the system modulation to it. This allows to adjust the modulation to bandgaps or peaks in the bath coupling spectrum. In contrast to dynamic decoupling of system and bath, which can be achieved by shifting the entire system-modulation spectrum beyond some assumed bath cutoff frequency, an enhancement of the coupling requires more detailed knowledge on the peak positions of the bath spectrum. In this way, our approach may comprise suppression and enhancement of the system-bath coupling in a unified way for executing more general tasks than decoherence suppression. The same approach can also be applied to map out the bath spectrum by measuring the coherence decay rate for a narrow-band modulation centered at different frequencies [197].

As far as the controls are concerned, we here consider time-continuous modulation of the system Hamiltonian, which allows for vastly more freedom compared to control that is restricted to stroboscopic pulses as in DD [82, 188, 189]. We do not rely on rapidly changing control fields that are required to approximate stroboscopic π-pulses. These features allow efficient optimization under energy constraint. On the other hand, the generation of a sequence of well-defined pulses may be preferable experimentally. We may choose the pulse timings and/or areas as continuous control-parameters and optimize them with respect to a given bath spectrum. Hence, our approach encompasses both pulsed and continuous modulation as special cases.

Open Issues. An open issue of the approach is the inclusion of higher orders in the system-bath coupling, which becomes important for strong or resonant system-bath coupling, so that a perturbative expansion cannot be applied. This may be the case especially when this coupling is to be enhanced in order to achieve a nonunitary operation (e.g., cooling), since in this case an optimization of the coupling may take us out of the domain of validity of the entire approach.

Another concern regards the initial conditions. Here we have assumed a factorized initial state of the system and bath. This prevents us from taking into account system-bath interactions that may have occurred prior to that time. In particular, if the system is in equilibrium with the bath, their states are entangled or correlated [191, 198].

An immediate problem of both higher order coupling and system-bath correlations is that their consideration requires knowledge of the corresponding parameters. It may be difficult to obtain such data with sufficient experimental precision. Moreover, its consideration renders the theory cumbersome and the intuition gained from the spectral overlap approach presented here is lost. A way out is offered by replacing the "open" iteration loop in Figure 16 with a "closed" loop [199], where the calculation of the score, constraint, and their gradients are based on actual measurements performed on the controlled system in real time rather than on prior model assumptions, that is, knowledge of bath properties. Such closed loop control would allow efficient optimization, but at the cost of losing any insight into the physical mechanisms behind the result obtained.

From a fundamental point of view, it is interesting to derive analytic bounds of a desired score (under a chosen constraint) and see if this bound can be achieved by means of some (global) optimization, that is, if the bound is tight. The need for a constraint in such optimization is not obvious if the task requires coupling enhancement, especially when the bath spectrum has a single maximum.

Our investigation of the scalability of decoherence control has revealed several general, basic insights. The first is that for small systems the coherence time is inversely proportional to the state-dependent scalability, $c_\psi(N)$, while for sufficiently large systems, this scaling is *always* inversely proportional to the *square root* of $c_\psi(N)$, due to the transition to a Zeno-like behavior of the decoherence rates.

We have then shown that whenever qubits *collectively* couple to common bath modes (e.g., in ion traps [180, 181] or cavities [200–202]) local modulations of individual qubits can eliminate cross decoherence, thus changing the scalability in a scenario-dependent manner (Table 1). (i) Local distinct modulations can eliminate cross decoherence, causing decoherence scaling to be linear in N for most entangled states. (ii) Imposing cross decoherence equality by local modulations can render states truly dark, regardless of N. (iii) Very large systems may revert from their unmodulated Zeno-like behavior to their Markov-like behavior, by either strong enough or scenario-tailored local modulations. Our major result is that the modulation must be faster than the correlation time of the bath, but can be much slower than the (unmodulated) multipartite coherence time, and still be effective.

These results show that dynamical control of decoherence is a promising avenue for combatting multipartite decoherence, since their rate is not required to become faster as the system grows. Coherence-time scalability with N is particularly crucial for one-way quantum computing [175], since the initial state is highly entangled and the computation, performed by measurements, is done in a serial manner. On the fundamental side, these results may pave the way to understanding and controlling "quantumness" in large multipartite systems. These findings identify local dynamic control as a promising path to the protection of quantum information from the environment in large multipartite systems.

References

[1] C. A. Sackett, D. Kielpinski, B. E. King et al., "Experimental entanglement of four particles," *Nature*, vol. 404, no. 6775, pp. 256–259, 2000.

[2] L. A. Wu and D. A. Lidar, "Creating decoherence-free subspaces using strong and fast pulses," *Physical Review Letters*, vol. 88, Article ID 207902, 4 pages, 2002.

[3] M. A. Nielsen and I. L. Chuang, *Quantum Computation and Quantum Information*, Cambridge University Press, Cambridge, UK, 2000.

[4] P. R. Hemmer, A. V. Turukhin, M. S. Shahriar, and J. A. Musser, "Raman-excited spin coherences in nitrogen-vacancy color centers in diamond," *Optics Letters*, vol. 26, no. 6, pp. 361–363, 2001.

[5] T. Takagahara, "Electron-phonon interactions in semiconductor nanocrystals," *Journal of Luminescence*, vol. 70, no. 1–6, pp. 129–143, 1996.

[6] J. D. Joannopoulos, R. D. Meade, and J. N. Winn, *Photonic Crystals: Molding the Flow of Light*, Princeton University Press, 1995.

[7] G. Kurizki and A. G. Kofman, *The Encyclopedia of Optical Engineering*, Dekker, 2003.

[8] H. Gießen, J. D. Berger, G. Mohs, P. Meystre, and S. F. Yelin, "Cavity-modified spontaneous emission: from Rabi oscillations to exponential decay," *Physical Review A*, vol. 53, no. 4, pp. 2816–2821, 1996.

[9] T. Quang, M. Woldeyohannes, and S. John, "Coherent control of spontaneous emission near a photonic band edge: a single-atom optical memory device," *Physical Review Letters*, vol. 79, pp. 5238–5241, 1997.

[10] G. K. Brennen, C. M. Caves, P. S. Jessen, and I. H. Deutsch, "Quantum logic gates in optical lattices," *Physical Review Letters*, vol. 82, no. 5, pp. 1060–1063, 1999.

[11] T. Calarco, A. Datta, P. Fedichey, E. Pazy, and P. Zoller, "Spin-based all-optical quantum computation with quantum dots: understanding and suppressing decoherence," *Physical Review A*, vol. 68, no. 1, Article ID 012310, 2003.

[12] J. J. García-Ripoll, P. Zoller, and J. I. Cirac, "Speed optimized two-qubit gates with laser coherent control techniques for ion trap quantum computing," *Physical Review Letters*, vol. 91, Article ID 157901, 4 pages, 2003.

[13] L. Landau and E. Lifshitz, *Quantum Mechanics*, Pergamon, Oxford, UK, 1977.

[14] S. John and J. Wang, "Quantum electrodynamics near a photonic band gap: photon bound states and dressed atoms," *Physical Review Letters*, vol. 64, pp. 2418–2421, 1990.

[15] M. Woldeyohannes and S. John, "Coherent control of spontaneous emission near a photonic band edge," *Journal of Optics B*, vol. 5, no. 2, pp. R43–R82, 2003.

[16] S. Y. Zhu, Y. Yang, H. Chen et al., "Spontaneous radiation and lamb shift in three-dimensional photonic crystals," *Physical Review Letters*, vol. 84, pp. 2136–2139, 2000.

[17] B. S. Ham, M. S. Shahriar, M. K. Kim, and P. R. Hemmer, "Frequency-selective time-domain optical data storage by electromagnetically induced transparency in a rare-earth-doped solid," *Optics Letters*, vol. 22, no. 24, pp. 1849–1851, 1997.

[18] D. Petrosyan and G. Kurizki, "Photon-photon correlations and entanglement in doped photonic crystals," *Physical Review A*, vol. 64, no. 2, Article ID 023810, 2001.

[19] A. G. Kofman and G. Kurizki, "Acceleration of quantum decay processes by frequent observations," *Nature*, vol. 405, pp. 546–550, 2000.

[20] A. G. Kofman and G. Kurizki, "Universal dynamical control of quantum mechanical decay: modulation of the coupling to the continuum," *Physical Review Letters*, vol. 87, Article ID 270405, 4 pages, 2001.

[21] A. G. Kofman and G. Kurizki, "Unified theory of dynamically suppressed qubit decoherence in thermal baths," *Physical Review Letters*, vol. 93, Article ID 130406, 2004.

[22] G. Gordon and G. Kurizki, "Preventing multipartite disentanglement by local modulations," *Physical Review Letters*, vol. 97, Article ID 110503, 8 pages, 2006.

[23] G. Gordon, N. Erez, and G. Kurizki, "Universal dynamical decoherence control of noisy single- and multi-qubit systems," *Journal of Physics B*, vol. 40, S75, 2007.

[24] A. M. Lane, "Decay at early times: larger or smaller than the golden rule?" *Physics Letters*, vol. 99, pp. 359–360, 1983.

[25] A. G. Kofman and G. Kurizki, "Quantum Zeno effect on atomic excitation decay in resonators," *Physical Review A*, vol. 54, pp. R3750–R3753, 1996.

[26] P. Facchi and S. Pascazio, "Quantum Zeno phenomena: pulsed versus continuous measurement," *Progress in Physics*, vol. 49, pp. 941–947, 2001.

[27] Y. Castin and J. Dalibard, "Relative phase of two Bose-Einstein condensates," *Physical Review A*, vol. 55, pp. 4330–4337, 1997.

[28] M. Lewenstein and L. You, "Quantum phase diffusion of a Bose-Einstein condensate," *Physical Review Letters*, vol. 77, pp. 3489–3493, 1996.

[29] E. M. Wright, D. F. Walls, and J. C. Garrison, "Collapses and revivals of Bose-Einstein condensates formed in small atomic samples," *Physical Review Letters*, vol. 77, pp. 2158–2161, 1996.

[30] M. Javanainen and M. Wilkens, "Phase and phase diffusion of a split Bose-Einstein condensate," *Physical Review Letters*, vol. 78, pp. 4675–4678, 1997.

[31] A. Vardi and J. R. Anglin, "Bose-Einstein condensates beyond mean field theory: quantum backreaction as decoherence," *Physical Review Letters*, vol. 86, pp. 568–571, 2001.

[32] J. R. Anglin and A. Vardi, "Magic numbers and erratic level crossings of double-well Bose-Einstein condensates," *Physical Review A*, vol. 64, Article ID 013605, 2001.

[33] M. Greiner, M. O. Mandel, T. Hänsch, and I. Bloch, "Collapse and revival of the matter wave field of a Bose-Einstein condensate," *Nature*, vol. 419, pp. 51–54, 2002.

[34] T. Schumm, S. Hofferberth et al., "Matter-wave interferometry in a double well on an atom chip," *Nature Physics*, vol. 1, pp. 57–62, 2005.

[35] Y. Shin, "Interference of Bose-Einstein condensates split with an atom chip," *Physical Review A*, vol. 72, Article ID 021604, 4 pages, 2005.

[36] G.-B. Jo, "Long phase coherence time and number squeezing of two Bose-Einstein condensates on an atom chip," *Physical Review Letters*, vol. 98, Article ID 030407, 2007.

[37] I. E. Mazets, G. Kurizki, N. Katz, and N. Davidson, "Optically induced polarons in Bose-Einstein condensates: monitoring composite quasiparticle decay," *Physical Review Letters*, vol. 94, Article ID 190403, 2005.

[38] E. W. Streed, "Continuous and pulsed quantum Zeno effect," *Physical Review Letters*, vol. 97, Article ID 260402, 2006.

[39] G.-B. Jo, "Phase-sensitive recombination of two Bose-Einstein condensates on an atom chip," *Physical Review Letters*, vol. 98, Article ID 180401, 2007.

[40] M. Anderlini, J. Sebby-Strabley, J. Kruse et al., "Controlled atom dynamics in a double-well optical lattice," *Journal of Physics B*, vol. 39, article S19, 2006.

[41] J. Sebby-Strabley, B. L. Brown, and M. Anderlini, "Preparing and probing atomic number states with an atom interferometer," *Physical Review Letters*, vol. 98, Article ID 200405, 2007.

[42] S. Folling, S. Trotzky, and P. Cheinet, "Direct observation of second-order atom tunnelling," *Nature*, vol. 448, Article ID 06112, 2007.

[43] W. H. Zurek, "Decoherence, einselection, and the quantum origins of the classical," *Reviews of Modern Physics*, vol. 75, pp. 715–775, 2003.

[44] P. J. Y. Louis, P. M. R. Brydon, and C. M. Savage, "Macroscopic quantum superposition states in Bose-Einstein condensates: decoherence and many modes," *Physical Review A*, vol. 64, Article ID 053613, 2001.

[45] Y. P. Huang and M. G. Moore, "Creation, detection, and decoherence of macroscopic quantum superposition states in double-well Bose-Einstein condenates," *Physical Review A*, vol. 73, Article ID 023606, 2006.

[46] I. Tikhonenkov, J. R. Anglin, and A. Vardi, "Quantum dynamics of Bose-Hubbard Hamiltonians beyond the Hartree-Fock-Bogoliubov approximation: the Bogoliubov back-reaction approximation," *Physical Review A*, vol. 75, no. 6, Article ID 013613, 2007.

[47] I. Tikhonenkov, J. R. Anglin, and A. Vardi, "Erratum to: Quantum dynamics of Bose-Hubbard Hamiltonians beyond the Hartree-Fock-Bogoliubov approximation: the Bogoliubov back-reaction approximation," *Physical Review A*, vol. 75, Article ID 069910, 2007.

[48] J. R. Anglin, "Cold, dilute, trapped bosons as an open quantum system," *Physical Review Letters*, vol. 79, pp. 6–9, 1997.

[49] L. Fonda and G. C. Ghirardi, "Some remarks on the origin of the deviations from the exponential decay law of an unstable particle," *Nuovo Cimento A*, vol. 7, pp. 180–184, 1972.

[50] B. Misra and E. C. G. Sudarshan, "The Zeno's paradox in quantum theory," *Journal of Mathematical Physics*, vol. 18, article 756, 8 pages, 1977.

[51] A. G. Kofman and G. Kurizki, "Acceleration of quantum decay processes by frequent observations," *Nature*, vol. 405, no. 6786, pp. 546–550, 2000.

[52] A. G. Kofman and G. Kurizki, "Universal dynamical control of quantum mechanical decay: modulation of the coupling to the continuum," *Physical Review Letters*, vol. 87, Article ID 270405, 4 pages, 2001.

[53] P. Facchi, H. Nakazato, and S. Pascazio, "From the quantum Zeno to the inverse quantum Zeno effect," *Physical Review Letters*, vol. 86, pp. 2699–2703, 2001.

[54] A. M. Lane, "Decay at early times: larger or smaller than the golden rule?" *Physics Letters A*, vol. 99, pp. 359–360, 1983.

[55] M. C. Fischer, B. Gutierrez-Medina, and M. G. Raizen, "Observation of the quantum Zeno and anti-Zeno effects in an unstable system," *Physical Review Letters*, vol. 87, Article ID 040402, 2001.

[56] J. J. Sakurai, *Modern Quantum Mechanics*, Addison-Wesley, 1994.

[57] C. J. Myatt, B. E. King, Q. A. Turchette et al., "Decoherence of quantum superpositions through coupling to engineered reservoirs," *Nature*, vol. 403, no. 6767, pp. 269–273, 2000.

[58] E. Yablonovitch, "Inhibited spontaneous emission in solid-state physics and electronics," *Physical Review Letters*, vol. 58, pp. 2059–2062, 1987.

[59] A. G. Kofman, G. Kurizki, and B. Sherman, "Spontaneous and induced atomic decay in photonic band structures," *Journal of Modern Optics*, vol. 41, pp. 353–384, 1994.

[60] J. Stenger, S. Inouye, A. P. Chikkatur et al., "Bragg spectroscopy of a Bose-Einstein condensate," *Physical Review Letters*, vol. 82, pp. 4569–4573, 1999.

[61] M. Kozuma, L. Deng, E. W. Hagley et al., "Coherent splitting of Bose-Einstein condensed atoms with optically induced Bragg diffraction," *Physical Review Letters*, vol. 82, pp. 871–875, 1999.

[62] R. Ozeri, N. Katz, J. Steinhauer, and N. Davidson, "Colloquium: bulk Bogoliubov excitations in a Bose-Einstein condensate," *Reviews of Modern Physics*, vol. 77, no. 1, pp. 187–205, 2005.

[63] M. Kramer, C. Menotti, L. Pitaevskii, and S. Stringari, "Bose-Einstein condensates in 1D optical lattices," *European Physical Journal D*, vol. 27, pp. 247–261, 2003.

[64] C. Menotti, M. Kramer, L. Pitaevskii, and S. Stringari, "Dynamic structure factor of a bose-einstein condensate in a one-dimensional optical lattice," *Physical Review A*, vol. 67, Article ID 053609, 2003.

[65] S. T. Beliaev, "Energy-spectrum of a non-ideal Bose gas," *Soviet Physics*, vol. 2, p. 299, 1958.

[66] S. Tsuchiya and A. Griffin, "Damping of Bogoliubov excitations in optical lattices," *Physical Review A*, vol. 70, no. 2, Article ID 023611, 4 pages, 2004.

[67] N. N. Bogoliubov, "On the theory of superfluidity," *Journal of Physics-USSR*, vol. 11, article 23, 1947.

[68] N. Katz, J. Steinhauer, R. Ozeri, and N. Davidson, "Baliaev damping of quasi-particles in a Bose-Einstein condensate," *Physical Review Letters*, vol. 89, Article ID 220401, 2002.

[69] E. E. Rowen, N. Bar-Gill, and R. Pugatch, "Energy-dependent damping of excitations over an elongated Bose-Einstein condensate," *Physical Review A*, vol. 77, Article ID 033602, 2008.

[70] H.-P. Breuer and F. Petruccione, *The Theory of Open Quantum Systems*, Oxford University Press, Oxford, UK, 2002.

[71] K. Banaszek, A. Dragan, W. Wasilewski, and C. Radzewicz, "Experimental demonstration of entanglement-enhanced classical communication over a quantum channel with correlated noise," *Physical Review Letters*, vol. 92, no. 25, Article ID 257901, 2004.

[72] J. Ball, A. Dragan, and K. Banaszek, "Exploiting entanglement in communication channels with correlated noise," *Physical Review A*, vol. 69, no. 4, Article ID 042324, 2004.

[73] S. Bandyopadhyay and D. A. Lidar, "Entangling capacities of noisy two-qubit Hamiltonians," *Physical Review A*, vol. 70, no. 1, Article ID 010301, 2004.

[74] T. Yu and J. H. Eberly, "Finite-time disentanglement via spontaneous emission," *Physical Review Letters*, vol. 93, no. 14, pp. 1–140404, 2004.

[75] T. Yu and J. H. Eberly, "Sudden death of entanglement: classical noise effects," *Optics Communications*, vol. 264, no. 2, pp. 393–397, 2006.

[76] C. Cohen-Tannoudji, J. Dupont-Roc, and G. Grynberg, *Atom-Photon Interactions*, Wiley, New York, NY, USA, 1992.

[77] J. Clarke, A. N. Cleland, M. H. Devoret, D. Esteve, and J. M. Martinis, "Quantum mechanics of a macroscopic variable: the phase difference of a Josephson junction," *Science*, vol. 239, no. 4843, pp. 992–997, 1988.

[78] M. O. Scully and M. S. Zubairy, *Quantum Optics*, Cambridge University Press, Cambridge, Mass, USA, 1997.

[79] G. S. Agarwal, "Control of decoherence and relaxation by frequency modulation of a heat bath," *Physical Review A*, vol. 61, Article ID 013809, 2000.

[80] G. S. Agarwal, M. O. Scully, and H. Walther, "Accelerating decay by multiple 2π pulses," *Physical Review A*, vol. 63, no. 4, Article ID 044101, 2001.

[81] G. S. Agarwal, M. O. Scully, and H. Walther, "Inhibition of decoherence due to decay in a continuum," *Physical Review Letters*, vol. 86, no. 19, pp. 4271–4274, 2001.

[82] L. Viola and S. Lloyd, "Dynamical suppression of decoherence in two-state quantum systems," *Physical Review A*, vol. 58, no. 4, pp. 2733–2744, 1998.

[83] K. Shiokawa and D. A. Lidar, "Dynamical decoupling using slow pulses: efficient suppression of 1/f noise," *Physical Review A*, vol. 69, no. 3, Article ID 030302, 2004.

[84] D. Vitali and P. Tombesi, "Heating and decoherence suppression using decoupling techniques," *Physical Review A*, vol. 65, no. 1, Article ID 012305, 2002.

[85] P. Facchi and S. Pascazio, "Quantum Zeno and inverse quantum Zeno effects," *Progress in Optics*, vol. 42, pp. 147–217, 2001.

[86] P. Facchi, D. A. Lidar, and S. Pascazio, "Unification of dynamical decoupling and the quantum Zeno effect," *Physical Review A*, vol. 69, no. 3, Article ID 032314, 2004.

[87] P. Zanardi and S. Lloyd, "Topological protection and quantum noiseless subsystems," *Physical Review Letters*, vol. 90, no. 6, Article ID 067902, 2003.

[88] L. Viola and E. Knill, "Robust dynamical decoupling of quantum systems with bounded controls," *Physical Review Letters*, vol. 90, no. 3, Article ID 037901, 2003.

[89] C. Uchiyama and M. Aihara, "Multipulse control of decoherence," *Physical Review A*, vol. 66, Article ID 032313, 2002.

[90] K. Khodjasteh and D. A. Lidar, "Fault-tolerant quantum dynamical decoupling," *Physical Review Letters*, vol. 95, no. 18, Article ID 180501, 2005.

[91] M. Stollsteimer and G. Mahler, "Suppression of arbitrary internal coupling in a quantum register," *Physical Review A*, vol. 64, Article ID 052301, 2001.

[92] L. Faoro and L. Viola, "Dynamical suppression of 1/f noise processes in qubit systems," *Physical Review Letters*, vol. 92, Article ID 117905, 2004.

[93] C. Search and P. R. Berman, "Suppression of magnetic state decoherence using ultrafast optical pulses," *Physical Review Letters*, vol. 85, no. 11, pp. 2272–2275, 2000.

[94] U. Haeberlen, *High Resolution NMR in Solids: Selective Averaging*, Academic, New York, NY, USA, 1976.

[95] G. S. Uhrig, "Keeping a quantum bit alive by optimized pipulse sequences," *Physical Review Letters*, vol. 98, Article ID 100504, 2007.

[96] M. J. Biercuk, H. Uys, A. P. VanDevender, N. Shiga, W. M. Itano, and J. J. Bollinger, "Optimized dynamical decoupling in a model quantum memory," *Nature*, vol. 458, no. 7241, pp. 996–1000, 2009.

[97] A. G. Kofman and G. Kurizki, "Acceleration of quantum decay processes by frequent observations," *Nature*, vol. 405, no. 6786, pp. 546–550, 2000.

[98] A. G. Kofman and G. Kurizki, "Frequent observations accelerate decay: the anti-Zeno effect," *Zeitschrift fur Naturforschung*, vol. 56, no. 1-2, pp. 83–90, 2001.

[99] A. G. Kofman and G. Kurizki, "Universal dynamical control of quantum mechanical decay: modulation of the coupling to the continuum," *Physical Review Letters*, vol. 87, Article ID 270405, 2001.

[100] A. G. Kofman and G. Kurizki, "Unified theory of dynamically suppressed qubit decoherence in thermal baths," *Physical Review Letters*, vol. 93, no. 13, Article ID 130406, 2004.

[101] A. G. Kofman, G. Kurizki, and T. Opatrný, "Zeno and anti-Zeno effects for photon polarization dephasing," *Physical Review A*, vol. 63, Article ID 042108, 2001.

[102] A. G. Kofman and G. Kurizki, "Quantum Zeno effect on atomic excitation decay in resonators," *Physical Review A*, vol. 54, no. 5, pp. R3750–R3753, 1996.

[103] S. Pellegrin and G. Kurizki, "Nonadiabatic relaxation control of qubits strongly coupled to continuum edge," *Physical Review A*, vol. 71, no. 3, Article ID 032328, 2005.

[104] G. Gordon, G. Kurizki, and D. A. Lidar, "Optimal dynamical decoherence control of a qubit," *Physical Review Letters*, vol. 101, no. 1, Article ID 010403, 2008.

[105] A. G. Kofman and G. Kurizki, "Theory of dynamical control of qubit decay and decoherence," *IEEE Transactions on Nanotechnology*, vol. 4, no. 1, pp. 116–123, 2005.

[106] M. C. Fischer, B. Gutiérrez-Medina, and M. G. Raizen, "Observation of the quantum Zeno and anti-Zeno effects in an unstable system," *Physical Review Letters*, vol. 87, no. 4, Article ID 040402, 2001.

[107] G. Gordon, G. Kurizki, and A. G. Kofman, "Universal dynamical control of local decoherence for multipartite and multilevel systems," *Optics Communications*, vol. 264, no. 2, pp. 398–406, 2006.

[108] K. Zyczkowski, P. Horodecki, M. Horodecki, and R. Horodecki, "Dynamics of quantum entanglement," *Physical Review A*, vol. 65, no. 1, Article ID 012101, 2002.

[109] M. Ban, S. Kitajima, and F. Shibata, "Decoherence of entanglement in the Bloch channel," *Journal of Physics A*, vol. 38, no. 19, pp. 4235–4245, 2005.

[110] C. Anastopoulos, S. Shresta, and B. L. Hu, "Quantum entanglement under non-markovian dynamics of two qubits interacting with a common electromagnetic field," http://arxiv.org/abs/quant-ph/0610007.

[111] M. P. Almeida, F. De Melo, M. Hor-Meyll et al., "Environment-induced sudden death of entanglement," *Science*, vol. 316, pp. 579–582, 2007.

[112] F. F. Fanchini and R. D. J. Napolitano, "Continuous dynamical protection of two-qubit entanglement from uncorrelated dephasing, bit flipping, and dissipation," *Physical Review A*, vol. 76, no. 6, Article ID 062306, 2007.

[113] J. H. Eberly and T. Yu, "The end of an entanglement," *Science*, vol. 316, pp. 555–557, 2007.

[114] L. Viola, E. Knill, and S. Lloyd, "Dynamical generation of noiseless quantum subsystems," *Physical Review Letters*, vol. 85, no. 16, pp. 3520–3523, 2000.

[115] P. Zanardi and M. Rasetti, "Noiseless quantum codes," *Physical Review Letters*, vol. 79, no. 17, pp. 3306–3309, 1997.

[116] D. A. Lidar, I. L. Chuang, and K. B. Whaley, "Decoherence-free subspaces for quantum computation," *Physical Review Letters*, vol. 81, no. 12, pp. 2594–2597, 1998.

[117] L.-A. Wu and D. A. Lidar, "Creating decoherence-free subspaces using strong and fast pulses," *Physical Review Letters*, vol. 88, Article ID 207902, 2002.

[118] G. S. Agarwal, "Control of decoherence and relaxation by frequency modulation of a heat bath," *Physical Review A*, vol. 61, no. 1, Article ID 013809, 2000.

[119] L. Viola, E. Knill, and S. Lloyd, "Dynamical decoupling of open quantum systems," *Physical Review Letters*, vol. 82, no. 12, pp. 2417–2421, 1999.

[120] *Decoherence, Entanglement and Information Protection in Complex Quantum Systems*, V. M. Akulin, A. Sarfati, G. Kurizki,

and S. Pellegrin, Eds., vol. 189 of *NATO Science Series II: Mathematics, Physics and Chemistry*, Springer, 2005.

[121] A. Barone, G. Kurizki, and A. G. Kofman, "Dynamical control of macroscopic quantum tunneling," *Physical Review Letters*, vol. 92, no. 20, Article ID 200403, 2004.

[122] G. Gordon, G. Kurizki, and A. G. Kofman, "Universal dynamical control of decay and decoherence in multilevel systems," *Journal of Optics B*, vol. 7, no. 10, pp. S283–S292, 2005.

[123] G. Gordon and G. Kurizki, "Preventing multipartite disentanglement by local modulations," *Physical Review Letters*, vol. 97, no. 11, Article ID 110503, 2006.

[124] G. Gordon, N. Erez, and G. Kurizki, "Universal dynamical decoherence control of noisy single- and multi-qubit systems," *Journal of Physics B*, vol. 40, pp. S75–S93, 2007.

[125] G. Gordon and G. Kurizki, "Universal dephasing control during quantum computation," *Physical Review A*, vol. 76, no. 4, Article ID 042310, 2007.

[126] G. Gordon, "Entanglement sudden death and its controlled partial resuscitation," *Europhysics Letters*, vol. 83, no. 3, Article ID 30009, 2008.

[127] D. A. Lidar, D. Bacon, and K. B. Whaley, "Concatenating decoherence-free subspaces with quantum error correcting codes," *Physical Review Letters*, vol. 82, no. 22, pp. 4556–4559, 1999.

[128] P. Facchi and S. Pascazio, "Quantum zeno subspaces," *Physical Review Letters*, vol. 89, Article ID 080401, 2002.

[129] R. G. Unanyan and M. Fleischhauer, "Decoherence-free generation of many-particle entanglement by adiabatic ground-state transitions," *Physical Review Letters*, vol. 90, no. 13, pp. 133601/1–133601/4, 2003.

[130] E. Brion, V. M. Akulin, D. Comparat et al., "Coherence protection by the quantum Zeno effect and nonholonomic control in a Rydberg rubidium isotope," *Physical Review A*, vol. 71, no. 5, Article ID 052311, 2005.

[131] D. Loss and D. P. Divincenzo, "Quantum computation with quantum dots," *Physical Review A*, vol. 57, no. 1, pp. 120–126, 1998.

[132] D. Schrader, I. Dotsenko, M. Khudaverdyan, Y. Miroshnychenko, A. Rauschenbeutel, and D. Meschede, "Neutral atom quantum register," *Physical Review Letters*, vol. 93, Article ID 150501, 2004.

[133] A. Kreuter, C. Becher, G. P. T. Lancaster et al., "Spontaneous emission lifetime of a single trapped *Ca+* ion in a high finesse cavity," *Physical Review Letters*, vol. 92, no. 20, Article ID 203002, 2004.

[134] F. Schmidt-Kaler, H. Häffner, M. Riebe et al., "Realization of the Cirac-Zoller controlled-NOT quantum gate," *Nature*, vol. 422, no. 6930, pp. 408–411, 2003.

[135] X. Li, Y. Wu, D. Steel et al., "An all-optical quantum gate in a semiconductor quantum dot," *Science*, vol. 301, no. 5634, pp. 809–811, 2003.

[136] M. Fiorentino, T. Kim, and F. N. C. Wong, "Single-photon two-qubit SWAP gate for entanglement manipulation," *Physical Review A*, vol. 72, no. 1, Article ID 012318, 2005.

[137] G. Gordon and G. Kurizki, "Dynamical protection of quantum computation from decoherence in laser-driven cold-ion and cold-atom systems," *New Journal of Physics*, vol. 10, Article ID 045005, 2008.

[138] B. M. Escher, G. Bensky, J. Clausen, and G. Kurizki, "Optimized control of quantum state transfer from noisy to quiet qubits," *Journal of Physics B*, vol. 44, no. 15, Article ID 154015, 2011.

[139] K. G. H. Vollbrecht, C. A. Muschik, and J. I. Cirac, "Entanglement distillation by dissipation and continuous quantum repeaters," *Physical Review Letters*, vol. 107, no. 12, Article ID 120502, 2011.

[140] D. D. Bhaktavatsala Rao, N. Bar-Gill, and G. Kurizki, "Generation of macroscopic superpositions of quantum states by linear coupling to a bath," *Physical Review Letters*, vol. 106, no. 1, Article ID 010404, 2011.

[141] D. Boschi, S. Branca, F. De Martineand, and L. Hardy, "Experimental realization of teleporting an unknown pure quantum state via dual classical and Einstein-Podolsky-Rosen channels," *Physical Review Letters*, vol. 80, pp. 1121–1125, 1998.

[142] J. I. Cirac and P. Zoller, "Quantum computations with cold trapped ions," *Physical Review Letters*, vol. 74, no. 20, pp. 4091–4094, 1995.

[143] D. Petrosyan and G. Kurizki, "Scalable solid-state quantum processor using subradiant two-atom states," *Physical Review Letters*, vol. 89, Article ID 207902, 2002.

[144] T. Opatrný, B. Deb, and G. Kurizki, "Proposal for translational entanglement of dipole-dipole interacting atoms in optical lattices," *Physical Review Letters*, vol. 90, Article ID 250404, 2003.

[145] A. G. Kofman, G. Kurizki, and B. Sherman, "Spontaneous and induced atomic decay in photonic band structures," *Journal of Modern Optics*, vol. 41, pp. 353–384, 1994.

[146] S. Nakajima, "On quantum theory of transport phenomena," *Progress of Theoretical Physics*, vol. 20, article 948, 1958.

[147] R. Zwanzig, "Ensemble method in the theory of irreversibility," *The Journal of Chemical Physics*, vol. 33, no. 5, pp. 1338–1341, 1960.

[148] G. Lindblad, *Non-Equilibrium Entropy and Irreversibility*, vol. 5 of *Mathematical Physics Studies*, Reidel, Dordrecht, The Netherlands, 1983.

[149] G. Gordon, G. Kurizki, S. Mancini, D. Vitali, and P. Tombesi, "Open-loop stochastic control of quantum coherence," *Journal of Physics B*, vol. 40, pp. S61–S73, 2007.

[150] L. A. Khalfin, "Phenomenological theory of k_0 mesons and the non-exponential character of the decay," *JETP Letters*, vol. 8, pp. 65–68, 1968.

[151] L. Fonda, G. Ghirardi, A. Rimini, and T. Weber, "Quantum foundations of the exponential decay law," *Nuovo Cimento A*, vol. 15, article 689, 1973.

[152] B. Misra and E. C. G. Sudarshan, "The Zeno's paradox in quantum theory," *Journal of Mathematical Physics*, vol. 18, no. 4, pp. 756–763, 1976.

[153] A. M. Lane, "Decay at early times: larger or smaller than the golden rule?" *Physics Letters A*, vol. 99, no. 8, pp. 359–360, 1983.

[154] B. Sherman, G. Kurizki, and A. Kadyshevitch, "Nonclassical field dynamics in photonic band structures: atomic-beam resonant interaction with a spatially periodic field mode," *Physical Review Letters*, vol. 69, no. 13, pp. 1927–1930, 1992.

[155] Y. Japha and G. Kurizki, "Spontaneous emission from tunneling two-level atoms," *Physical Review Letters*, vol. 77, no. 14, pp. 2909–2912, 1996.

[156] Q. Niu and M. G. Raizen, "How Landau-Zener tunneling takes time," *Physical Review Letters*, vol. 80, no. 16, pp. 3491–3494, 1998.

[157] M. Born and E. Wolf, "This frequency distribution mimics the monochromatic-wave spatial intensity distribution produced by a line diffraction grating," in *Principles of Optics*, Pergamon, Oxford, UK, 1980.

[158] R. Cook, "What are quantum jumps," *Physica Scripta*, vol. 21, pp. 49–51, 1988.

[159] W. M. Itano, D. J. Heinzen, J. J. Bollinger, and D. J. Wineland, "Quantum Zeno effect," *Physical Review A*, vol. 41, no. 5, pp. 2295–2300, 1990.

[160] H.-P. Breuer, B. Kappler, and F. Petruccione, "The time-convolutionless projection operator technique in the quantum theory of dissipation and decoherence," *Annals of Physics*, vol. 291, no. 1, pp. 36–70, 2001.

[161] E. M. Lifshitz and L. P. Pitaevskii, *Statistical Physics*, vol. 2, Pergamon, Oxford, UK, 1980.

[162] R. Alicki, M. Horodecki, P. Horodecki, R. Horodecki, L. Jacak, and P. Machnikowski, "Optimal strategy for a single-qubit gate and the trade-off between opposite types of decoherence," *Physical Review A*, vol. 70, Article ID 010501, 2004.

[163] P. Zanardi, "Symmetrizing evolutions," *Physics Letters A*, vol. 258, pp. 77–82, 1999.

[164] D. Vitali and P. Tombesi, "Using parity kicks for decoherence control," *Physical Review A*, vol. 59, no. 6, pp. 4178–4186, 1999.

[165] P. Facchi, S. Tasaki, S. Pascazio, H. Nakazato, A. Tokuse, and D. A. Lidar, "Control of decoherence: analysis and comparison of three different strategies," *Physical Review A*, vol. 71, no. 2, Article ID 022302, 2005.

[166] Y. Nakamura, Y. A. Pashkin, T. Yamamoto, and J. S. Tsai, "Charge echo in a cooper-pair box," *Physical Review Letters*, vol. 88, Article ID 047901, 2002.

[167] W. K. Wootters, "Entanglement of formation of an arbitrary state of two qubits," *Physical Review Letters*, vol. 80, pp. 2245–2248, 1998.

[168] S. Fölling, F. Gerbier, A. Widera, O. Mandel, T. Gericke, and I. Bloch, "Spatial quantum noise interferometry in expanding ultracold atom clouds," *Nature*, vol. 434, no. 7032, pp. 481–484, 2005.

[169] M. Yönaç, T. Yu, and J. H. Eberly, "Pairwise concurrence dynamics: a four-qubit model," *Journal of Physics B*, vol. 40, no. 9, article no. S02, pp. S45–S59, 2007.

[170] M. Yönaç and J. H. Eberly, "Qubit entanglement driven by remote optical fields," *Optics Letters*, vol. 33, no. 3, pp. 270–272, 2008.

[171] S. Maniscalco, F. Francica, R. L. Zaffino, N. Lo Gullo, and F. Plastina, "Protecting entanglement via the quantum zeno effect," *Physical Review Letters*, vol. 100, no. 9, Article ID 090503, 2008.

[172] S. Natali and Z. Ficek, "Temporal and diffraction effects in entanglement creation in an optical cavity," *Physical Review A*, vol. 75, no. 4, Article ID 042307, 2007.

[173] O. Kern and G. Alber, "Controlling quantum systems by embedded dynamical decoupling schemes," *Physical Review Letters*, vol. 95, no. 25, Article ID 250501, 2005.

[174] G. Gordon, "Dynamical decoherence control of multi-partite systems," *Journal of Physics B*, vol. 42, Article ID 223001, 2009.

[175] R. Raussendorf and H. J. Briegel, "A one-way quantum computer," *Physical Review Letters*, vol. 86, no. 22, pp. 5188–5191, 2001.

[176] J. Clausen, G. Bensky, and G. Kurizki, "Bath-optimized minimal-energy protection of quantum operations from decoherence," *Physical Review Letters*, vol. 104, no. 4, Article ID 040401, 2010.

[177] S. Haroche and J. M. Raimond, *Exploring the Quantum: Atoms, Cavities, and Photons*, Oxford University Press, 2006.

[178] N. Erez, G. Gordon, M. Nest, and G. Kurizki, "Thermodynamic control by frequent quantum measurements," *Nature*, vol. 452, no. 7188, pp. 724–727, 2008.

[179] G. Gordon, D. D. Bhaktavatsala Rao, and G. Kurizki, "Equilibration by quantum observation," *New Journal of Physics*, vol. 12, Article ID 053033, 2010.

[180] H. Häffner, W. Hänsel, C. F. Roos et al., "Scalable multiparticle entanglement of trapped ions," *Nature*, vol. 438, no. 7068, pp. 643–646, 2005.

[181] C. Langer, R. Ozeri, J. D. Jost et al., "Long-lived qubit memory using atomic ions," *Physical Review Letters*, vol. 95, no. 6, Article ID 060502, 2005.

[182] J. Cai, G. G. Guerreschi, and H. J. Briegel, "Quantum control and entanglement in a chemical compass," *Physical Review Letters*, vol. 104, no. 22, Article ID 220502, 2010.

[183] T. Scholak, F. De Melo, T. Wellens, F. Mintert, and A. Buchleitner, "Efficient and coherent excitation transfer across disordered molecular networks," *Physical Review E*, vol. 83, no. 2, Article ID 021912, 2011.

[184] A. N. Pechen and D. J. Tannor, "Are there traps in quantum control landscapes?" *Physical Review Letters*, vol. 106, no. 12, Article ID 120402, 2011.

[185] G. Gordon, G. Kurizki, and D. A. Lidar, "Optimal dynamical decoherence control of a qubit," *Physical Review Letters*, vol. 101, no. 1, Article ID 010403, 2008.

[186] C. Dankert, *Efficient Simulation of Random Quantum States and Operators [M.S. thesis]*, University of Waterloo, Ontario, Canada, 2005.

[187] M. J. Storcz, U. Hartmann, S. Kohler, and F. K. Wilhelm, "Intrinsic phonon decoherence and quantum gates in coupled lateral quantum-dot charge qubits," *Physical Review B*, vol. 72, no. 23, Article ID 235321, 2005.

[188] G. S. Uhrig, "Keeping a quantum bit alive by optimized π-pulse sequences," *Physical Review Letters*, vol. 98, Article ID 100504, 2007.

[189] W.-J. Kuo and D. A. Lidar, "Quadratic dynamical decoupling: universality proof and error analysis," *Physical Review A*, vol. 84, no. 4, Article ID 042329, 2011.

[190] H. P. Breuer and F. Petruccione, *The Theory of Open Quantum Systems*, Oxford University Press, Oxford, UK, 2002.

[191] N. Erez, G. Gordon, M. Nest, and G. Kurizki, "Thermodynamic control by frequent quantum measurements," *Nature*, vol. 452, no. 7188, pp. 724–727, 2008.

[192] T. Jahnke and G. Mahler, "Effective environments: preparation of stationary states with inverse temperature ranging from positive to negative values," *Physical Review E*, vol. 84, no. 1, Article ID 011129, 2011.

[193] A. E. Allahverdyan, K. V. Hovhannisyan, D. Janzing, and G. Mahler, "Thermodynamic limits of dynamic cooling," *Physical Review E*, vol. 84, no. 4, Article ID 041109, 2011.

[194] G. Gordon and G. Rigolin, "Generalized teleportation protocol," *Physical Review A*, vol. 73, no. 4, Article ID 042309, 2006.

[195] G. Gordon and G. Rigolin, "Generalized quantum-state sharing," *Physical Review A*, vol. 73, no. 6, Article ID 062316, 2006.

[196] G. Gordon and G. Rigolin, "Generalized quantum telecloning," *European Physical Journal D*, vol. 45, no. 2, pp. 347–353, 2007.

[197] I. Almog, Y. Sagi, G. Gordon, G. Bensky, G. Kurizki, and N. Davidson, "Direct measurement of the system-environment coupling as a tool for understanding decoherence and dynamical decoupling," *Journal of Physics B*, vol. 44, no. 15, Article ID 154006, 2011.

[198] G. Gordon, D. D. Bhaktavatsala Rao, and G. Kurizki, "Equilibration by quantum observation," *New Journal of Physics*, vol. 12, Article ID 053033, 2010.

[199] M. J. Biercuk, H. Uys, A. P. VanDevender, N. Shiga, W. M. Itano, and J. J. Bollinger, "Optimized dynamical decoupling in a model quantum memory," *Nature*, vol. 458, no. 7241, pp. 996–1000, 2009.

[200] G. Kurizki, A. G. Kofman, and V. Yudson, "Resonant photon exchange by atom pairs in high-Q cavities," *Physical Review A*, vol. 53, no. 1, pp. R35–R38, 1996.

[201] C. Marr, A. Beige, and G. Rempe, "Entangled-state preparation via dissipation-assisted adiabatic passages," *Physical Review A*, vol. 68, no. 3, Article ID 033817, 2003.

[202] A. Mandilara, V. M. Akulin, M. Kolar, and G. Kurizki, "Control of multiatom entanglement in a cavity," *Physical Review A*, vol. 75, no. 2, Article ID 022327, 2007.